Excerpts from

PROCESSES IN BIOLOGICAL VISION:

including,

ELECTROCHEMISTRY OF THE NEURON

This material is excerpted from the full β-version of the text. The final printed version will be more concise due to further editing and economical constraints. A Table of Contents and an index are located at the end of this paper.

James T. Fulton
Vision Concepts

jtfulton@neuronresearch.net

April 30, 2017

[xxx Very early work with a number of early conceptual figures that need to be updated]
[xxx remove zener diode symbols]

12 Primary Signal Processing--Signal Detection [1]

12.1 Introduction

This chapter will focus on the performance characteristics of the Stage 1 visual process. This Stage encompasses the operation of the photoreceptor cells in both their signal detection and signal equilibration roles. Signaling is the primary function of the photoreceptor cells. This chapter presents the first detailed description of the signaling path of the photoreceptor cell to appear in print. The description relies upon the background developed in previous chapters and the appendices. It relies on a clear understanding of four separate areas:

+ the complexity of the photoreceptor/IPM/RPE interface,

+ the complete solution to the Photoexcitation/De-excitation Equation,

+ the quantum-mechanical processes incorporated into the chromophores and the Outer Segments of vision, and

+ the role of the metabolic system in the transient performance of the complete stage.

The output signals of the photoreceptor cells are essentially fixed in peak-to-peak amplitude regardless of the absolute amplitude of the input illumination. This is achieved through the use of an adaptation amplifier controlled by a low pass filter in its power supply. The subsequent signal manipulation processes rely on the essentially fixed amplitude of the signals from the photoreceptors of Stage 1.

As late as 1973, Rodieck[2] wrote that: “The nature of the coupling mechanism between light absorption on the lamellar membrane–the photocurrent generated by the outer-segment plasma membrane–is one of the most important unsolved problems of retinal physiology.” Little has changed since then with regard to the actual mechanism involved. Only additional concepts have appeared. Both the old and the new concepts have relied primarily upon kinetic analysis to support their feasibility. Kinetic analysis in the absence of an understanding of the underlying mechanism, is a very weak tool.

The situation in the literature has not changed significantly since that time. Although considerable analysis of possible conceptual mechanisms has appeared, these have not provided a viable hypothesis. This is illustrated by the question marks in figure 13.29 of the 1999 book by Oyster[3]. A key problem has been the adoption of a proposal by Young that the Outer Segment was enclosed by a plasma membrane of the parent photoreceptor cell. Only within the last few years have images of the Outer Segment appeared at sufficient magnification to show conclusively that there is no membrane surrounding the disk stack called the Outer Segment. The disk stack is formed by secretion from the wall of the cell. It is not formed by evagination. See **Sections 4.3.5** & **4.6.2**.

There has been a large amount of intellectual capital and laboratory time invested in concepts depending on the presence of a plasma membrane surrounding the disk stack of each Outer Segment. This is unfortunate. Lacking a plasma membrane, the concepts of gates in such a membrane is untenable. Lacking gates, the various cascade theories of how a potential is generated across the membrane are untenable.

12.1.1 Glossary

Because of several differences in terminology between the conventional wisdom based on chemistry and the alternate hypotheses presented in this work, it is very important to present the following definitions here. The term transduction has a significantly different meaning when used in discussing communications via hormones and communications related to sensing the external environment. This separation has frequently been overlooked during

---

[1]Released: April 30, 2017
[2]Rodieck, R. (1973) The vertebrate retina. San Francisco, CA: W. H. Freeman pg. 328
[3]Oyster, C. (1999) The Human Eye: Structure and Function. Sunderland, MA: Sinauer Assoc. pg 582

attempts to use the hormonal concept to describe the sensory process.

Signal transduction–

1. (with respect to the hormonal system) An intracellular cascade of biochemical event that follow the interaction between extracellular growth factors and their membrane receptors, ending in the switch of nuclear mechanisms controlling the proper biological responses. (Battistini, et. al. 1993 in Papa & Tager)

2. (with respect to the sensory mechanisms of the neural system) The transfer of acoustic energy, electromagnetic energy or tactile motion by quantum-mechanical sensors into free electrons that can be further processed by the neural system.

12.1.2 Background

12.1.2.1 Relative Physics

As an example of the multi-disciplinary problem, the descriptions found in the vision literature regarding the photodetection process and mechanism are quite unlike the similar descriptions found in the realm of physics and engineering. Photodetection is usually defined in terms of one of three fundamental processes, photo-emission, photoconduction and thermally mediated conduction due to absorption of photons. Both photo-emission and photoconduction are features of solid state physics and involve well understood phenomena at the atomic level. Thermally mediated conduction is a much simpler process at the atomic level. It involves the heating of the bulk material. The change in the conductivity of the bulk material reflects this change in temperature. This process is seldom found in high performance photodetection systems, although, lacking any other uncooled technique, it has occasionally been used as a low performance detection scheme in infra-red sensors. The process exhibits an absorption spectrum that is independent of the energy, and hence the wavelength, of the incident photons.

Photoconduction is achieved by a photon impacting a crystalline lattice, of either a solid or liquid crystalline material, and creating a long life electron-hole pair. During the lifetime of this pair, multiple electron charges are able to pass through the lattice. The result is a charge current that may be significantly larger than the quantum flux of the photons. This process typically exhibits a broad absorption spectrum for photons above a specific energy level.

Photo-emission occurs in two distinct forms in physics, photo-emission from the valence band of a material into a vacuum (the historically more conventional process of external photo-emission) and photoemission from the valence band into a higher level conduction or excitation level (so-called internal photoemission). External photo-emission is characterized by a broad absorption spectrum that begins at a very precise photon energy level (described by Fermi-Dirac statistics) and extends to indefinitely higher energies. Internal photo-emission exhibits a similar, though less extended, absorption spectrum in most in-organic materials because the conduction band is quite wide. The long wavelength absorption edge is still defined by Fermi-Dirac statistics and can be described precisely by the Fermi-Dirac function. In the case of organic materials, there is normally no conduction band. The conduction band is replaced by an excitation band that is quite explicitly defined and usually narrow. In these materials, the absorption spectrum involves the difference in energy between two bounded energy levels, the valence or unexcited band and the excitation band. The absorption spectrum in this case is defined by the difference in energy between possible energy states between the two bands (while observing the Pauli Exclusion Principle. This spectrum is precisely defined by the product of two Fermi-Dirac functions. One describes the short wavelength edge of the absorption band. The second describes the long wavelength edge of the absorption band. This is the situation observed in the chromophores of vision.

It must be appreciated that the photochemistry of resonant organic molecules is basically different from that of inorganic semiconducting materials. In inorganic photodetecting materials, which typically involve the excitation of an electron from the valence band to the conduction band, the observed spectral band is a broad, generally flat, one. This is because the conduction band is generally wide and any photon with an energy greater than the valence-conduction band energy difference will cause excitation. This is not generally the case in organic photochemistry. The energy transition of interest does not usually involve a conduction band; alternately, it is a transition between one or more unexcited energy bands to an excited energy band. Both of these bands are described quantum mechanically--and their energy difference is similarly described. Thus the spectral absorption coefficient due to any individual transition is generally peaked, with a shape much like in a resonant circuit of electrical engineering (where it is also possible to combine the features of both resonant and nonresonant elements to achieve unique spectral performance) In photography, the elements of an organic molecule and an inorganic molecule are nearly always combined to achieve the desired broad overall spectral response. Moreover, the most important organic molecules in photography involve multiple auxochromes, i. e. more than three, in each chromophore to achieve wide spectral response and long stable shelf life for the product (while always abiding by the rules of liquid crystal

chemistry to insure an increase in sensitivity and not a decrease).

In developing the mechanism of the chromophoric excitation-neural de-excitation process, another embellishment will be added to the variety of excitation methodologies available. Most investigations of a neuron as a signal repeater (action potential regenerator operating in the phasic mode) do not focus on the minimal energy required for excitation of the neuron at a synapse. In the case of the photoreceptor cell (an analog, or electrotonic, amplifier creating generator waveforms), it appears that a minimum energy level is required and the neuron must be biased properly.

12.1.2.2 Common wisdom of the past

The dominant hypothesis of photodetection in vision for the last half century has been that proposed by Hubbard, and extended by Kropf based on the work of Wald. The hypothesis being that photodetection involves the photoexcitation (by internal photo-emission) of a retinene attached to a protein through a protonated Schiff base. The de-excitation of the molecule was via a physical isomerization. This method of photodetection has been carried forward as analogous to a switch that initiated the transfer of charge, between specific elements that are undefined at this time, and that a second action was necessary to terminate the transfer of charge in a timely manner. Based on this switching analogy, Baylor & Burns recently defined a set of "strong functional constraints" on any second mechanism[4].

[MERGE WITH ABOVE PARA XXX]
The primary signal detection process has been studied at a number of different times in the past but the needed tools were usually not available for adequate interpretation. In the 1930's, isomerization was one of the few chemical mechanisms known to the general scientific community that could be caused by photon effects. At that time, the photography field was beginning to introduce color photography to an ever wider range of applications. However, the technical processes of how it worked were poorly understood. The photo-chemists had just discovered that it did work and commercial pressures caused a rush to market of a basically cook-book understanding of the physics (and chemistry). The process did not involve photo-isomerization. It was quite similar to the process actually used in animal vision.

Isomerization has never been demonstrated to occur in the *in-vivo* animal as part of the vision process. It is a relatively high energy process and not well suited to achieving the near quantum limited performance of animal vision. By any standard, its proposed method of operation in the vision process is a convoluted and involved one. As the field of semiconductor physics has evolved and the field of liquid crystal chemistry has appeared, a variety of additional mechanisms have appeared that offer more satisfactory solutions to the *in-vivo* photo-detection process. Effective understanding and use of these mechanisms will once again require a multi-disciplinary approach if one is to understand the operation of the Outer Segment of the photoreceptor of animal vision.

The most recent redefinition of the above hypothesis in a theoretical context was that of Torre, et. al[5]. In that work, "a quantitative reconstruction of the *kinetics* of phototransduction was attempted." The resulting model was based primarily on proposed chemical kinetics instead of detailed descriptions of the processes involved. It included a large number of degrees of freedom as indicated by the number of arbitrary constants employed. No attempt was included to treat the quantum mechanical situation. The term phototransduction was employed, rather than photodetection, to describe the overall "process by which the absorption of a photon by a molecule of rhodopsin in a photoreceptor is transformed into an electrical signal." This description skirts the subject of how this is achieved. The next sentence says "the electrical signal is caused by the modulation of a current, usually called a photocurrent, flowing across the light-sensitive channels in the plasma membrane of the outer segments." What fundamental mechanism is used by the light-sensitive channels in the plasma membrane is not discussed. Kamiyama et. al.[6] have combined the transduction model suggested by Torre, et. al. with the excitable membrane model of Hodgkin, Huxley & Katz to create an ionic current model of the photoreceptor cell. This model is the first to delineate the outer segment from the inner segment in an electrical analog. It also recognizes the two separate polarity signals recordable from one photoreceptor cell (note the similarity of their figure 1 to Laughlin discussed below). Beyond

---

[4]Baylor, D. & Burns M. (1998) Control of rhodopsin activity in vision. Eye. Vol. 12, pp. 521-525

[5]Torre, V. Forti, S. Menini, A. & Campani, M. (1990) Model of phototransduction in retinal rods. Symposia on Quantitative Biology, vol. LV, Cold Spring Harbor, NY: The Cold Spring Harbor Laboratory Press pp.563-573

[6]Kamiyama, Y. Ogura, T. & Usui, S. (1996) Ionic current model of the vertebrate rod photoreceptor. Vision Res. vol. 36, pp. 4059-4068

those features, the model is a synthesis of a large group of individual variable resistors in series with arbitrary voltage and polarity batteries, all in parallel with a current source and a capacitor. The majority of the network is meant to represent the membrane of the inner segment of the photoreceptor cell. The model was implemented as a computer simulation program.

Leibovic has also addressed the transduction and adaptation processes[7]. However, the result does not satisfy. He notes "the processes which activate the responses to light are better understood than those which inactive them." He goes on "Whatever the details, we can imagine how thresholds and response amplitudes can be related to the biochemistry." This work suggests that "to imagine" is a scientifically weaker mechanism than that associated with intuition.

The mathematical solution to the equations of the proposed system reduce in a special case to a form explored by Fourtes & Hodgkin[8,9]. This special case involves a single processing stage as opposed to the general n-stage equation they presented. They used a circuit analog employing a pentode vacuum tube in the series arm of each of their n-stages. This analog is clearly not appropriate based on later investigations. Their n-stage solution was adopted by a variety of later investigators who defined multiple stages in order to obtain additional degrees of freedom in their mathematical manipulations. The goal was to account for the delay in output signal versus excitation that varied with stimulus level. However, Fourtes & Hodgkin were careful to note that "it must be said at once that the results do not provide real evidence for the existence of anything formally equivalent to a cascade of ten elements". Their analysis employed a variable number of elements, or stages, to accommodate a wider range of excitation levels.

The primary reason for the n-stages in their analysis was to provide sufficient delay between the onset of excitation and the response of the observed biological cells. Their equations did not include an independent delay term because they did not use complex notation in the solution of their differential equation. Additionally, their model was written in terms of voltages. For a quantum mechanical process, it is more appropriate to use a charge analog and quantify the maximum number of excitable but initially bound charges available in the photoreceptor. The limitation on the total number of charges available in the system transforms the analog into a state variable system. This is the methodology employed in this work.

12.1.2.3 Framework of this theory

This work does not support the conventional wisdom concerning the process of photosensing in vision. **It does not support:**

+ the photoconduction of rhodopsin as the excitation mechanism,

+ the isomerization of a retinene as the de-excitation mechanism within the photodetection process,

+ the switching analogy required to explain the separate excitation and de-excitation of the putative CGMP cascade,

+ the putative cGMP cascade as an explanation of the gain mechanism, nor the use of variable resistors without a means of controlling them in vision.

Neither does this work rely upon chemical kinetics as a foundation.

An alternate continuous flow process is proposed that does not require a separate and distinct terminating mechanism or any constraints on such a mechanism. It is based on an entirely electrolytic hypothesis using quantum-mechanical (internal photoemissive) detection techniques. The hypothesis relies heavily on the presence of the chromophores, membranes and specific minute volumes of water to be present in the liquid crystalline state of matter. **The success of this schism with the past is illustrated by the results; the first comprehensive, consistent and rigorous explanation of the photosensing process of vision process**.

> **From this point on, the term transduction will be used only in the electronic sense defined in Section 12.1.1.**

---

[7]Leibovic, K. (1990) Science of Vision NY: Springer-Verlag pg 44

[8]Fuortes, M. & Hodgkin, A. (1964) Changes in time scale and sensitivity in the ommatidia of *Limulus*. *J. Physiol*. vol. 172, pp. 239-263

[9]Borsellino, A. Fuortes, M. & Smith, T. (1965) Visual responses in Limulus. Cold Spring Harbor Symposia on Quantitative Biology. vol XXX, pp 429-443 This paper provides additional background re: Fuortes & Hodgkin

The proposed photodetection process is based on a simple first order physical system defined by a single first order differential equation (and a very specific set of boundary conditions). The physical model is quantum mechanical and appropriate for organic photodetectors. The transduction process (TD) is redefined into two sub-processes, transduction of photons into excitons (constrained electrons) and the process of translation (TL) of excitons into free electrons. The new transduction process is *passive*. The translation process is based on an *active* electrolytic semiconductor device (actually one of two) within the photoreceptor cell. The resulting model is much simpler and does not involve a computer simulation. It provides simple closed form mathematical equations describing all of the waveforms associated with the photoreceptor cell under all conditions of continuous and impulse illumination as well as dark adaptation in the absence of illumination. This equation is defined as the Photoexcitation/De-excitation Equation (P/D Equation). It is derived in a complete form in Appendix A as well as in a variety of simplified forms useful under certain simplifying certain conditions. One of these forms was originally postulated by Hodgkin (See previous paragraph), but without a model to explain its limited applicability.

12.1.2.3.1 Architecture & integration of the visual system

As indicated in **Section 4.5**, the photoreceptor cells of stage 1 do not stand alone. They are highly integrated into a photoreceptor/IPM/RPE complex. This complex in turn shares a highly integrated role in the overall operation of the eyes and the complete visual system. From an architectural (or system design) perspective, this integration is important to the many dynamic aspects of the system. Each system has been optimized with respect to a variety of design goals related to the environment of the animal. The resulting optimization has an impact on the performance of the photoreceptor cells of that animal.

For humans, the optimization has resulted in an adaptation function that is tailored to the diurnal illumination level defined by the earths rotation. Leibrock, et. al. have reviewed the debate in the vision literature concerning the inadequacy of the adaptation function in humans[10]. Such a discussion is parochial to the overall design tradeoff process. To achieve a significantly faster adaptation rate would compromise the rotational capabilities of the eye and seriously degrade the ability of the human to read.

The level of circuit integration found in the photoreceptor cell appears to be the highest of any neuron. This is due to the large number of discrete functions performed within the individual cell. From a system design perspective, the photoreceptor cell is a work of art. To achieve this level of integration, the signaling function of the photoreceptor cell is extremely nonlinear. The individual nonlinearities range from the simplest to the most complex, from the static to the dynamic. Analyses in the literature that have not recognized these nonlinearities have led to many unsupportable hypotheses. The concept of "dark light" is one of these xxx.

12.1.3 Definition of the cytological situation

As was developed earlier, the photoreceptor cell found in the vision process is a complex, multi-functional one. The Outer Segment is not an integral part of the cell; the Inner Segment of the cell has both a exocrine glandular function and a neural function. It appears that the neural function is not actually involved with the photodetection process; therefore, it is generally categorized as a secondary receptor in Torrey[11] and similar texts. That is to say, the dendrites of the neuron receive irritation from something other than photons; in this case, the irritation is caused by interaction with the chromophoric liquid crystal when that element is in an excited state. This situation, involving the expression, “encapsulated nerve endings”, is well illustrated by the photoreceptor case, where the outer ends of the dendrites are either enclosed in the deep fissures around the periphery of the disks or at least in intimate contact with the disks in these regions as illustrated in Chapter 5.

The complexity of the photoreceptor cell continues to present a problem for biological researchers. Because of the sizes involved and the tools available, we are still faced with a situation similar to that of sticking two probes through the outside case of a radio receiver and trying to define the type of music being received based on the signals detected. This is a particular problem with “intracellular probing” which is similar to contacting the face of a microcircuit chip with a probe large enough to contact 10-100 signal traces at one time; in this case the waveform on the probe may be a complex sum of signals and the internal circuits may be significantly damaged.

---

[10] Leibrock, C. Reuter, T. & Lamb, T. (1998) Molecular basis of dark adaptation in rod photoreceptors. Eye, vol. 12, pp 511-520

[11] Torrey, T. (1971) Morphogenesis of the Vertebrates. New York: Wiley & Sons. pg 466.

As indicated earlier, the techniques developed by the Baylor school are quite sophisticated and provide very interesting data. However, even these techniques leave several questions open. For instance, the replacement of the fluid of the IPM with a ringers solution may change the situation surrounding the OS significantly and create leakage paths to the polar ringers solution that may not exist in the real situation. It is well documented that the IPM *is* isolated from other interstitial fluids but the *reasons* for this are not documented. Secondly, although not discussed in detail by those authors, the technique used measures the net charge or current crossing an interface; it does not mean that only one conductor was involved. This is similar to placing a non-contacting current meter around a cable containing all of the wires going to a motor. The meter will read either zero or a leakage current but will not give any indication of how much current is actually passing through the motor windings; If you place the meter around only one conductor in the cable, you will get a correct reading for that individual conductor. In the Baylor case, it may be that the measured inward current is actually a leakage current to the ringer's solution Secondly, the net current measured may be due to a relatively constant inward current on one conductor subtracted from a second outward conductor on an adjacent conductor(s).

12.1.4 Derivation of the Circuit Analog

The circuit analog defined below may appear arbitrary on first viewing; however, it is able to accurately account for the performance of the visual system in considerable detail--the key criteria for a good model to meet. The equations of circuit synthesis do not lead to singular forms of a model but allow for models with different focus, i. e., in electronic modeling, it is frequently desirable to use either a voltage source model or a current source model but not both for the same source. This model has allowed many details of the mechanisms involved to be illuminated in a very useful way, specifically with regard to the mechanism of brightness adaptation. This process involves much more than the "bleaching" of a molecule. A model can never be complete, this one will surely be modified and expanded in the future, that is its basic reason for existing here.

As a starting point, no data could be found representing the measured signal output of the chromophoric material alone following excitation. Therefore, the problem was addressed as a typical 4-port black-box consisting of two internal stages, transduction of photons to excitons and then translation of the excitons into free electrons on (in) a conductor. The boundary conditions were available, particularly the output conditions as illustrated in Figure 3 of baylor & Hodgkin[12]. The challenge is to define a simple (or the simplest) circuit that can provide these characteristic in a biological context.

In the literature, transduction has generally been used to describe an overall conceptual process of converting a photon into some kind of signal useful neurologically. In this work, a much more specific description of this overall process will be given and the terminology will necessarily be further definitized. Specifically, transduction will be taken as, and limited to, the process of absorbing an incident photon and creating an excited electron in the π^* band of a chromophoric layer of the OS associated with a photoreceptor cell. Translation will be taken as, and limited to, the process whereby an excited π^* electron of the chromophoric layer is de-excited and a free electron is produced within the dendritic structure of the neuron associated with the IS of the same photoreceptor cell. These are intrinsically different kinds of processes. **Figure 12.1.1-1** describes the operation of the Outer Segment in block diagram form, except where it introduces the active device, the Activa. An Activa of type AS is used in the dendritic portion of the photoreceptor cell.

One of the most important boundary conditions illustrated in this figure is the complete electrical and quantum mechanical isolation of the chromophoric material of the disk assembly in its two critical roles represented by the two functional blocks. These blocks are labeled the liquid crystal chromophore and the "piezo-electric convertor. The later name may be poorly chosen. The function involved is the de-excitation of an exciton in the chromophore back to the ground state simultaneously with the creation of an electron-hole pair in the base region of the Activa. The only interactions with the chromophoric material are via quantum processes, either due to a photon exciting the material on the left or an exciton interacting with an electron-hole on the right. The excitation process is constrained by the limited energy acceptance range of the chromophoric material. Only photons with energy within this band can excite the bound electrons of the auxochromes of the chromophore. The material is essentially transparent to photons of other energy. A similar constraint exists at the interface between the piezo-electric convertor and the base region of the Activa on the right. The material forming the base of the Activa, believed to be a crystal of hydronium, has a minimum activation energy also. It is believed to be not more than 2.34 electron-volts at 37 degrees C based on analysis of the work of Sliney. It is probably closer to 2.0 electron-volts. Upon creation of an electron-hole pair in the base region of the active electrolytic semiconductor device, the Activa, a current is caused to flow in the collector and emitter circuits of the device. This current is no longer a quantum mechanical process. However, the amplitude of the current is very closely related to the number of quantum mechanical events occurring

---

[12]Baylor, D. & Hodgkin, A. (1973) Detection and resolution of visual stimuli by turtle photoreceptors. J. Physiol. vol. 234, pp. 163-198

between the chromophore and the base region of the Activa and the lifetime of the electrons and holes formed in that region.

12.2 Mechanism of the photodetection process

12.2.1 Electronic Characteristics of the Chromophores

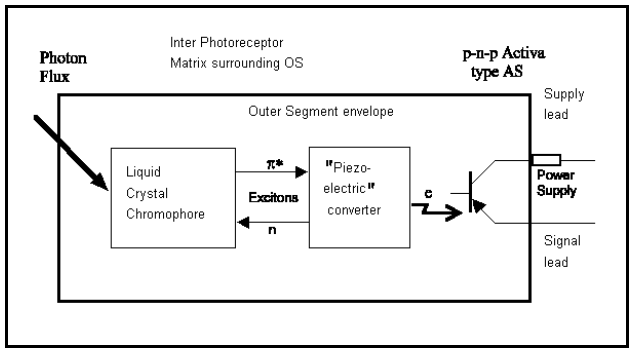

Figure 12.1.1-1 JUNK Block Diagram of Outer Segment and the translation function.

The chromophore defined in Chapter 6 as the Rhodonine family are not easily defined in their entirety because of the nearly unlimited variety of characteristics available to a molecule that contains 19-20 carbon atoms and can be defined as a member of at least 10 organic molecule families. Although the initial construction of its chromogen was undoubtedly via the isoprene chaining process. The resultant chromogen can be defined as a Vitamin, as a derivative of a lipid, as having a hydrophobic characteristic due to its hexene ring, as being hydrophilic due to its carboxyl group, or as being an alcohol due to its -OH group, etc. When converted into an actual molecule of the chromophore, the situation becomes even more complex. The molecule now exhibits both a carboxyl group and an alcohol group at the same time. A test for only one of these groups is not definitive as to what chemical class the molecule belongs. A test for the simultaneous presence of both groups would be more analytical but could be more difficult if the chromophore is in fact in an ionic state as usually proposed in the literature. In this work, it is proposed that the chromophore is not usually in the ionic state and is in fact associated to any substrate by hydrogen bonding or Van der Waal forces, a common situation found between many of the types mentioned above and various proteins. In conclusion, it should be emphasized that the Rhodonines are derivatives of the Retinene family and will generally test positive for Retinene; in fact it will test positive for both the carboxyl and alcohol members of that family simultaneously. They may also exhibit some activity similar to that of Vitamin A.

At the individual molecule level, the Rhodonines are not spectacular pigments; they are small molecules with relatively low absorption cross sections. Each molecule does exhibit a completely conjugated carbon chain connecting the two auxochromes and it is able to absorb several photons but the minimum energy requirements may rise rapidly if enough empty excited states are not available. This is particularly true for the minimum energy situation involving the excitation of a non-bonded *n*-electron into a π^* energy level. When the molecule is joined by other molecules in the spontaneous formation of a liquid crystal that is not associated with any other structure, the situation improves immensely. Under this condition the π^* bands overlap and merge, forming in effect a form of continuous conduction band, and a band which has no preferential electric field vector. The individual *n*-electrons of each molecule can now be excited into the π^* energy band without saturating that band locally and without exhibiting any polarization preference. Through this effect, the absorption cross section of the liquid crystal is expanded immensely.

While in the un-associated liquid crystalline state, the orientation of the liquid crystal is not controlled with respect to any incident photons and its absorption cross-section may vary considerably with the angle between the axis of the conjugated carbon chain and the Poynting vector of the incident light. If however, the liquid crystal is allowed to precipitate out onto a substrate, which it is very inclined to do, then the orientation of the molecules can be controlled easily and the light can be applied in the proper direction to achieve a maximum absorption cross-section.

This last situation is the culmination of the optimization process and is the same configuration used in the color photographic process, although this author is not aware that the art allows concentrating the liquid crystal on only the surfaces of the silver halide facing the incoming illumination.

12.2.1.1 The Photo-Electron Excitation Process

Based on the material in Chapter 5.1.4, the Outer Segment is seen to consist of a space frame consisting of a series of disks stacked like poker chips, each of the chips near the Inner Segment end having a crenelated edge. The notches in these disks appear to be aligned and occupied by what histologists have called microtubules but which a neurologist would call dendrites. Each disk of the space frame consists of a core disk believed to consist of a

heterogeneous structure of protein and lipid material which is coated with a mono-molecular layer of Rhodonine in a liquid crystalline structure. This structure surrounds both the surface and end pieces of the core disk. The disks are pressed together, but interestingly, the protein-lipid parts probably do not touch each other; the contact between the layers being between adjacent layers of the liquid crystals. Thus, if there is electrical, exciton or phonon (piezo-mechanical) transfer of energy between these layers, the result is a relatively large, monolithic structure of the chromophores held in parallel planes; all (except those involved in turning the corner) with their conjugate chain axes aligned with the Poynting vector of the incident light. This provides a very large area for the absorption of the photons with a number of important features:

+ the photo-electrical properties of the structure do not exhibit any polarization preference for light traveling along the length of the space frame (although illumination from the side will show a polarization preference exactly as shown by Baylor, Lamb & Yau[13]).

+ the slow wave structure of the conjugated chain of the chromophore makes the effective distance between the auxochrome layers approximately 230 times their actual spacing according to Dewar[14] resulting in an almost perfect length for causing the peak absorption band to appear in the visual spectrum at one of three locations depending on which of the Rhodonine chromophore is present in that photoreceptor.

+ the spacing between liquid crystalline layers is such that the effective index of refraction of the entire column of material is not greatly different from that of the immensely more massive protein-lipid layer and/or the interstitial fluid which is water based with an index near 1.33. This prevents the incident photons from encountering a major change in index which would cause the photons to be reflected and expelled from the entrance end of the Outer Segment.

+ the large number of chromophores present in the shared structure of the space frame provide an immense number of photo-excitable *n*-electrons and a shared π^* energy band structure which can accept them.

---

[13]Baylor, D. Lamb, T. & Yau, K-W (1979) The membrane current of single rod outer segments. J. Physiol. Vol. 288, pp. 589-611

[14] Dewar

The absorption cross-section of this structure is dependent on the number of unexcited n-electrons remaining in the unexcited state to the total number of n-electrons present prior to any excitation. Depending on this ratio, the effective absorption characteristic can vary over a very large magnitude, more than 10 to the eighth power. If the light continues to excite n-electrons faster than they are de-excited, the material will "bleach", thus reducing its absorption coefficient and resulting in the storage of a large number of electrons in the π^* energy state of the liquid crystalline structure.

> It is important to note that an Outer Segment that is separated from its Inner Segment will continue to be light sensitive initially. However, the number of available unexcited n-electrons will continually decrease with photon excitation. The unique dipolar mechanical arrangement of the auxochromes of the chromophores prevent these materials from relaxing by thermal or flourescent mechanisms. As a result the material will become transparent. Its only mechanism of relaxation is by secondary means with time constants measured in hours. Researchers usually report that any excited material, derived from separated Outer Segments and stored in the dark, has relaxed when they return to work the next day.

12.2.1.2 The Electron-Neural De-excitation Process

Building on the foundation of the previous Section; one further assumption will be made. It is known that the de-excitation of photo-electrons of the OS alone in-vitro is a very slow or non-existent process. Generally, de-excitation will occur overnight which implies a second order thermal relaxation. This fact indicates two things. The protein/lipid layer at the core of a disk does not provide an effective medium for energy transfer from the liquid crystalline structure. Further, the no longer vital dendrites of the nervous tissue remaining within the Outer Segment structure do not provide an effective de-excitation avenue either.

It is quite reasonable to assume the disk substrate materials alone do not support de-excitation of the liquid crystal. Neither the protein or the lipid classes of organic material typically exhibit any energy band differences in the range below 3 electron volts.

It is also quite reasonable to assume the no longer living nervous tissue cannot continue to interface with the liquid crystal in its normal manner. As will be seen below, a biologist would say it is only able to interact with the liquid crystal when it is in the irritable state when alive, not while it is in its refractive state or when no longer "live". The physicist would suggest an alternate explanation. Unless the Activa is properly biased, the electron-hole pairs created within the base region of the Activa will not be removed from that region. The resultant unsustainable charge distribution within the region will no longer allow acceptance of energy from the pizo-electric convertor. Therefore, the chromophore becomes increasingly excited and it is said to bleach.

It is also well established that the chromophores, at least the chromogens of the Retinene family do not fluoresce when excited, indicating that they do not spontaneously de-excite by re-radiation, at least in the anticipated and observed spectral regions

Therefore, the proposition will be made that it is a function of the living neural component of the photoreceptor cell which is responsible for de-exciting the electrons occupying the π^* energy state of the liquid crystal in the Outer Segment of that same cell.

This proposition introduces an interesting avenue of investigation. A neuron is normally a rate limited signaling device, with a maximum propagation velocity limited by the impedance of the axon sheath and a specific refractory interval before it can be caused to fire a subsequent time. A neuron exhibits a minimum input signal below which it will not fire. This level is generally in the neighborhood of 2.0 electron volts or more. For comparison, the energy threshold of silver bromide is approximately 2.6 eV. Since the energy of thermally excited electrons at the temperature of the body is approximately 25 milli-electron-volts, this provides a satisfactory margin against self induced firing. 2.6 eV is also equal to the energy of an absorbed photon with a wavelength of 0.48 microns, a very "blue" photon. 2.0 eV. corresponds to a photon at 0.61 micron, an "orange" photon.

12.3 Mechanism of the amplification process

Rodieck[15] has provided a summary of the theories of amplification in vision *circa*. 1973. He found these to fall into three categories; the proenzyme hypothesis, the photoconduction hypothesis, and the saccule hypothesis. These theories were primarily concepts at that time and they have not matured substantially. The saccule hypothesis has been advanced into the glutamate cascade hypothesis. However, this concept is also supported primarily on its ability to meet the perceived requirements based on kinetics and the use of certain chemicals found ubiquitously near neurons. As Rodieck said, "A general difficulty with all saccule hypotheses is that they fail to account for the behavior of cones whose outer-segment lamellar structure results from infolding of the outer-segment plasma membrane. . ." Concurring with another Rodieck statement, the photoconduction hypothesis, involving a change in conductivity, is not promising. Unfortunately, he also discounts the entire field of photoconduction and photovoltaic effects without further definition of the terms. The proenzyme hypothesis has not been pursued since the 1960's.

> **The primary problem with the saccule and subsequent cascade theories is the absence of any evidence of a membrane surrounding the outer segments of the photoreceptors**. To the contrary, recent electron microscopy has shown the total absence of such a membrane in a wide range of chordates. See the website, www.4colorvisioncom, for a substantial reward for any conclusive evidence for the presence of such a membrane in humans or other chordates.

MacLeod, et. al. have argued that the adaptation process is different in cold-blooded than in warm-blooded animals on purely psychophysical grounds[16]. They did not provide any rigorous model of the proposed mechanism or even quantify the gain mechanism involved. They built on a paper by Rushton in 1965 that claimed that the sensitivity of the rods (the putative achromatic detection mechanisms in vision) never changes and that the adaptation mechanism was found in a "pool" subsequent to the photoreceptor cells. These concepts are not supported here.

Based on this work, the mechanism of amplification can be clearly defined based on conventional semi-conductor electronics applied to the electrolytic environment of biology. The mechanism provides a recognized method and and achievable amount of amplification. It also explains the variation in the amplification based on the state of the applicable variables and circuits . The circuit details and results presented below contribute directly to the comprehensive understanding of the adaptation characteristics of vision presented in **Chapters 16 & 17.**

12.5 The Complete Photo Detection Process

The block diagram of a suitable network representing the photodetection function of the photoreceptor cell must contain the following elements:

1. The chromophoric transducer for which the transfer function is known and known to be nonlinear at high signal levels.
2. The exciton to electron transducer which is known to preserve the quantum nature of the signal at least at low light levels.
3. An amplifier with a passband of at least 100 hertz which is able to output approximately 3×10^4 electrons per input photon in the linear region but which exhibits a significant degree of saturation at output currents near 20 pA.
4. A power source able to provide the above number of electrons as a minimum to the amplifier when the incident flux level is measured in 100-1000's of photons per second per photoreceptor.

It must exhibit a variable time delay as a function of the input illumination. It is also necessary that some element in the network provide a level control such that the output signal excursions remain within the dynamic range of the output device, typically 0- 20 pA in the turtle but ranging up to 29 pA in both the turtle and salamander, while the input intensity varies slowly over a factor of 10^5 or more. Although this may consist of an amplifier with a logarithmic transfer characteristic, this is unlikely. The signal saturation exhibited by the data indicates that a different approach is more likely. Either;

an automatic gain control, similar to that in a radio,

a DC restoration circuit similar to that in a television receiver or

a more exotic circuit as used in early transistorized radio preamplifiers.

---

[15]Rodieck, R. (1973) Op. Cit. pg. 332-337

[16]MacLeod, D. Chen, B. & Crognale, M. (1989) Spatial organization of sensitivity regulation in rod vision. *Vision Res*. vol. 29, no. 8, pp 965-978

In fact, the automatic gain control of vision is quite different. It is associated with the bleaching of the chromophores of the retina. It involves an internal feedback mechanism (**Section xxx**). That is there is no identifiable external feedback path.

With these requirements and mechanisms in mind, the circuit of **Figure 12.5.1-1** is suggested. **(A)** shows the functional block diagram. **(B)** shows individual portions of the proposed circuit for illustrative purposes and **(C)** shows the overall circuit as proposed after assembly.

The top level functional block diagram is shown as Stage 1 in **(A).** It is accompanied by several rows of labels to orient the reader and provide a consistent relationship between the labels found in the literature. A critical point to note in the top row of labels is that the dendritic structure associated with the IS is physically located within the OS. This places the functions of transduction, translation, and adaptive amplification all within the structure of the OS. The IS is the home of the output, or distribution amplifier, of the photoreceptor cell. This amplifier uses an Activa with a different performance characteristics and therefore a different type designation. The dashed vertical line indicates the probable location of the Outer Limiting Membrane, OLM. The primary purpose of this membrane appears to be the chemical separation of the specialized metabolic processing of the IPM from the more normal metabolic processing of the INM. This membrane is, however, an electrical insulator. It plays a significant role in the signaling function of the visual system. The two arcs crossing the OLM external to the complete photoreceptor cell represent the ground bridges that play an important role in creating the conventional ERG waveform.

(B) presents the individual circuits of the photoreceptor cell for ease of discussion. The two sections on the left are laid out according to the earlier discussion. The left most diode, labeled TD for TransDuction, is the symbol used for the electronic analog of the quantum mechanical process supported by the chromophoric material during excitation. This diode is shunted by a capacitor, C_T, representing the quantum mechanical equivalent of the excited state of the chromophoric material. The diode is also shown shunted by an impedance Z_1. As discussed above, the unique character of the chromophoric molecules makes the decay time constant of the equivalent circuit, $Z_1 \times C_T$, hours long. The second diode, labeled TL for TransLation, and impedance, Z_2, constitute the de-excitation process of the chromophoric material when in contact with the properly biased Activa labeled AS. The Activa is shown in its bulk form to emphasize the energy is transferred from the chromophore material to the n-type region of the p-n-p device forming the current amplifier. The impedance, Z_2, is a pure delay circuit representing the travel time related to the travel distance between the point of creation of an excited electron, an exciton, in the chromophoric material and its point of de-excitation along the fissures of the disk stack. This delay element is a variable related to the intrinsic repulsion between likely charged particles within the conducting region of the π^* band of the liquid crystalline structure.

The impedance in the collector lead of the Type AS device is located within furrows of the disk stack and is in contact with the electrolytes of the IPM. There is no membrane separating the disk stack from the IPM. There are only the materials associated with the electrostenolytic supply. They are stored as coatings on the outside of the disk stack, including the volume within the furrows. These materials react on the outer surface of the dendrites in order to power the type AS Activas. That is why, the real impedances associated with the Activas are shown straddling the membrane wall of the photoreceptor cell. These are real impedances represented by standard electronic components. The part outside of the cell wall constitutes the battery element of the supply and the part inside the cell constitutes the diode representing the cell wall. Where appropriate, these impedances are shown shunted by a real capacitance. In the case of the type AS device employed in the variable gain adaptation amplifier circuit, this capacitance is an integral part of a low pass filter along with the electrostenolytic supply and the cell wall. As will be shown elsewhere in detail, this low pass filter has two poles. These poles determine the shape of the dark adaptation characteristic of animal vision. This same capacitor is also part of the charging circuit that controls the light adaptation characteristic of animal vision.

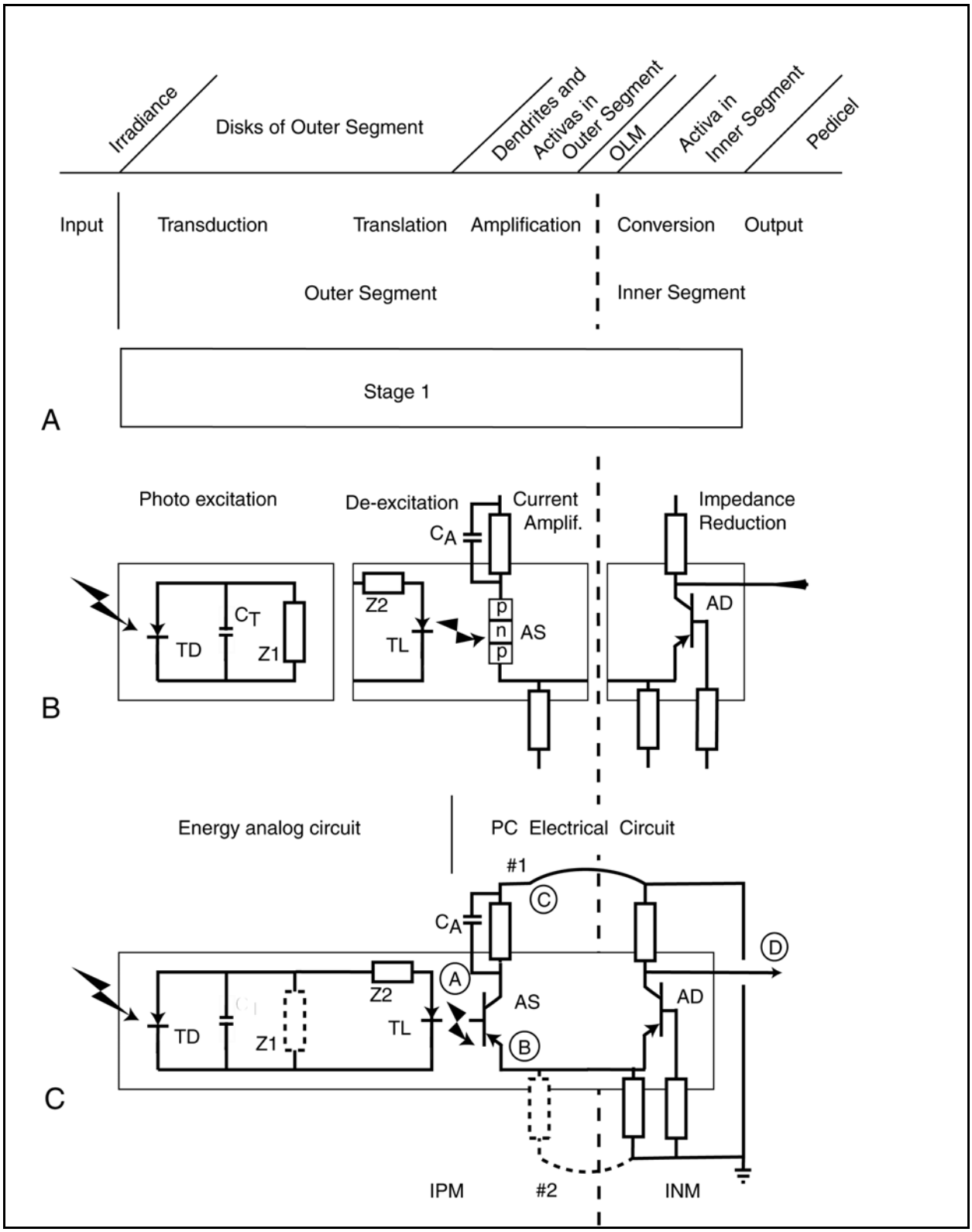

Figure 12.5.1-1 Nomenclature, block diagram and overall circuit for Stage 1, the photodetection process in vision. (A) The nomenclature in context. (B) The three basic circuit blocks and the transition from energy to electrons as the signal carrier. The Activa of the current amplifier is shown in its bulk (p-n-p) form. (C) The overall circuit diagram expressed in standard symbols.

The Activa on the right in **(B)** is located within the IS of the photoreceptor cell. It is arranged in a common base configuration. The result is that this circuit can act as a unity gain current amplifier with a much lower impedance at its output collector than at its emitter terminal. By passing this current through a suitably sized load impedance, this circuit is able to drive multiple synapses leading to other circuits. Not shown diagrammatically, but extremely important, is the fact that the diode in the collector impedance of this circuit consists of a significant area of the axolemma of this cell. This portion of the axolemma is also coated with electrostenolytic material. As a result, the voltage of the axoplasm is a logarithmic representation of the current through the type AD Activa and the load impedance. The current supply to the collector terminal of this device is clearly in contact with the INM. Similarly, the poditic supply serving the base terminal and the dendritic supply serving the emitter are also in contact with the INM.

(C) merges the circuit elements of **(B)** into a functional photoreceptor cell. The symbols representing circuit elements to the left of the solid vertical line are representations of a quantum mechanical process. The symbols to the right of the line are symbols representing real electrolytic circuit elements. This part of the diagram is not an analog of the visual process. It is ***the*** representation, using human symbols, of the actual process.

> *To the left of the vertical bar*, the description involves an **electrical analog to a physical system**, in this case, a quantum mechanical system. The current flowing in this analog will be used to describe the actual flow of excited electrons which are carrying a quanta of energy. The capacitor symbol will indicate the capability of the π^* band to store quanta of energy and the number of charges on this capacitor at any time will indicate the number of quanta of energy available for de-excitation under the proper conditions. The open block in this figure will represent a resistive impedance in the analog. This is not the impedance found in an operating photoreceptor cell. This impedance relates to a potential dissipative process leading to the de-excitatin of the chromophoric material as observed in a laboratory after separation of the OS from the IS. It need not be a resistor, it may be a photon emitting device causing flourescence of the material.
>
> *To the right of the vertical bar*, the description uses man-made symbols to represent an actual electrolytic circuit within the photoreceptor cell. It is not an analog or an equivalent circuit. **It is a real circuit of a real photoreceptor cell.**

When combined in the manner shown, the two Activas share a common emitter terminal. Only one impedance is needed to represent the connection of this terminal to the electrostenolytic supply. Based on the knowledge that the emitter lead of the type AS Activa passes through the colax of the IS to connect to the type AD Activa circuit, It will be assumed for the moment that this single impedance connects to the INM and not the IPM. Therefore, the dotted components on the right can be omitted. The resulting condition is compatible with the generation of an ERG as usually recorded in the laboratory. The impedance Z_1 has a much higher value than the combined impedance Z_2 and TL when the cell is in-vivo. Therefore, Z_1 is usually omitted from the combined figure.

This combined circuit incorporates:

1. A chromophoric photon to “exciton” transducer
2. A static gain control within the chromophoric mechansim
3. An “exciton” to electron-hole translator
4. A dynamic gain control mechanism and first Activa as an amplifier
5. An second Activa acting as a distribution amplifier
6. A current to voltage converter that also acts as a “hard” limiter

The extremely interesting fact is how all of these functions can be accomplished in such a simple combined quantum mechanical and electrolytic circuit. Another interesting fact is how the circuit elements act differently when not connected into a complete stage.

12.5.1 The Transduction Block

The transduction block consists of the disks of the OS, more specifically, the chromophoric material, rhodonine, in the liquid crystal form present as a coating over the structural protein opsin. These coated disks are stacked into a

column of thin disks. The photons that are intercepted by this column of disks, normally the column is irradiated along its cylindrical axis, are absorbed by the chromophores and cause an electron to be excited into the π^* band of the crystal. Whether a photon is absorbed or not is controlled by the absorption cross-section of the OS at the spectral wavelength of the photon. All absorbed photons generate excited electrons. These excited electrons move within the energy band of the liquid crystal until they encounter some mechanism to cause their de-excitation. Normally, this cannot occur within the crystalline structure because of the symmetrical dipole configuration of the chromophores and the inability of the protein structure to absorb energy at these energy levels, approximately 1.0 to 2.5 electron volts. Over an extended period of time, the electrons will be de-excited through second order thermal processes such as interaction with the material found in the inter-photoreceptor matrix (IPM). This secondary process involves time constants on the order of a few minutes to a few hours.

Because of its great significance in vision, the transduction process and the resultant transfer characteristic of the process is treated separately in Appendix A of this work. The complete transduction equation, presented there as the Photoexcitation/De-excitation Equation (or the P/D Equation) is found to involve a differential equation of the first order with a complex argument. This complete equation can be simplified under a number of different assumptions leading to the correct mathematical form to correlate with the work of many different investigators. The results of this treatment will be utilized beginning with section 12.5.4. [xxx]

An analog of the energy circuit for the transduction block is shown in the left portion of **(b)**. This analog consists of a radiation sensitive photoemitter, a capacitor and a resistive element. This circuit can operate without the presence of a power source (a battery). As is discussed in Appendix A, the performance of the photoemitter is a bit specialized in that this circuit analog is isolated electrically from any other source of charges and involves quantum mechanics. The total number of available charges is finite. Therefore, the number of charges generated by the photoemitter, is limited by the number already moved from the bottom of the circuit to the top and stored on the capacitor. The excess charges stored on the capacitor are eventually returned to their original location by the resistive element. The value of this resistive element will become an important consideration in the overall operation of the circuit.

12.5.1.1 The quasi-static transduction process

Figure 12.5.1-2 highlights the steady-state transfer characteristic of the transduction process. The frame on the left summarizes the functional elements involved. For simplicity, all of the chromophores of a given region of the retina will be considered en masse and (initially) to exhibit a single absorption spectrum described as that of the M–channel. The excitation photon flux is shown as F photons/sec. Each absorbed photon results in the excitation of an electron in a π–orbitals into a π^*–orbital. However, the absorption coefficient is a variable that depends on the total number of unexcited electrons in the π–orbitals. The Activa provides a de-excitation mechanism described by K de-excitons/sec. This de-excitation mechanism is represented by a current that is a fixed percentage of the collector current, I_c. The reciprocal of this percentage is defined as the amplification of the circuit. Z describes the impedance of the electrostenolytic source associated with the –150 mV supply potential. This Z plays a major role in describing the "dark adaptation characteristic" of human vision (**Section 17.6**). The output signal of the overall circuit is taken as the voltage across the resistor in the emitter circuit of the Activa.

The photon excitation process is described in detail in **Section 5.4.3**. The precise interface between the base current, K, of the Activa and the chromophore, and how it results in the de-excitation of the chromophores, is a more complex quantum-mechanical process than required to understand the overall circuit operation.

The highly sensitive chromophores are surrounded by higher energy (insulating) materials except for the active tissue of the dendrites perpendicular to the edges of each opsin disk. Further, the excitation process involves the triplet state of p*–orbitals and is peculiar to oxygen. Electrons from this level do not de-excite spontaneously (thermally). See **Section 5.3.1**. Thus, the excitation level of the chromophores is determined by the difference between the level of photon excitation, F, and the level of de-excitation via the base current of the Activa, K.

The upper right frame shows the overall situation for a constant level of de-excitation, K de-excitons/sec. As the photon flux level increases above the de-excitation level, the net excitation level, the number of π^*–orbitals, within the chromophore increases. As a result, the number of unexcited π–orbitals is drastically reduced.

The middle right frame illustrates the net absorptance of the chromophoric mass as a function of the photon flux. For fluxes below K, there is no net excitation level and the absorptance coefficient is essentially constant at its maximum value. An absorptance can be described by a relative optical density as shown by the right scale. At maximum absorptance, A_o, the optical density of the chromophore mass is high, taken here as a relative density of 2.0. As the absorptance decreases, the optical density also decreases. The chromophore mass is said to bleach as a function of the excitation level. This is caused by the failure of the de-excitation flux, K, to equal the potential photon-excited flux, $F \cdot A_o$.

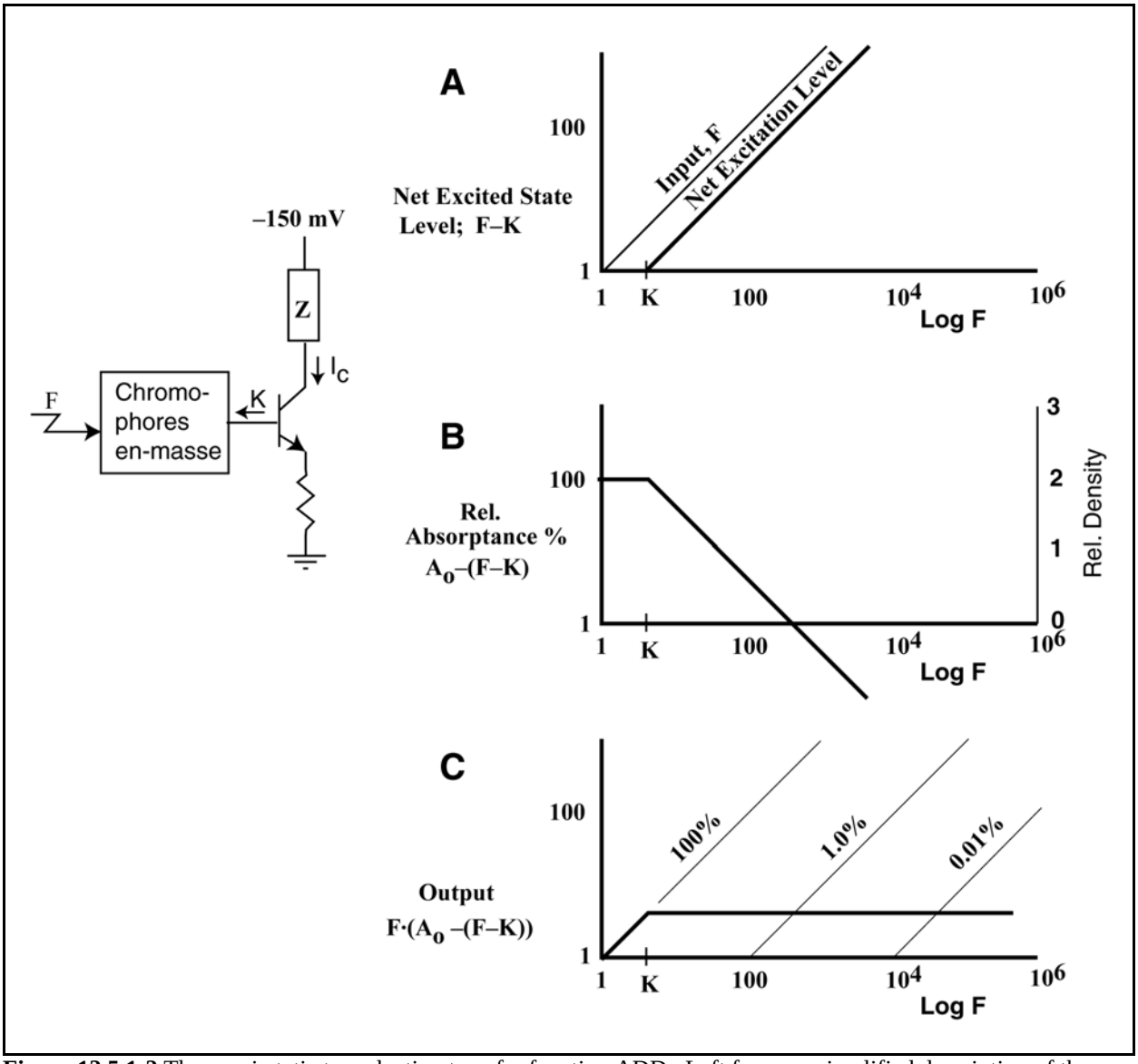

Figure 12.5.1-2 The quasi-static transduction transfer function ADD. Left frame; a simplified description of the transduction and amplification circuit associated with the adaptation amplifier of the photoreceptor cells. Right frames; descriptions of the parameters associated with the transduction process. Parametric curves at lower right indicate relative efficiency. See text.

As an aside, the unbleached chromophore mass is described as visual purple because of its high absorptance at the peak wavelength of the M–channel photoreceptors and low absorption in the blue and red regions of the spectrum. Visual purple as a color can be defined as the complement of the peak absorption wavelength of the M–channel, 532 nm. Thus visual purple is in fact a magenta as expressed by the color space of this work (and the Munsell Color Space).

Separating the reflectance from the chromophores, from the reflectance of the similarly colored substrate behind the chromophoric material, is difficult in the clinical situation.

The lower right frame shows the average (quasi-steady-state) output of the transduction process as a function of the

photon flux, resulting from the reduction in the absorptance coefficient at high photon flux levels. The value of K corresponds to the transition of the illumination level from the mesotopic region to the photopic region. The reduction in the absorptance coefficient can be described as an effective reduction in the quantum efficiency of the overall transduction process. However, note carefully, it is the effective capture cross-section of the chromophores to radiation (since there are fewer unexcited π–electrons per unit volume) that is reduced and not the efficiency of π*–electron creation as a function of photon flux. In the real case, the bulk chromophore represents a series of two-dimensional films on the surface of a finite number of opsin disks. The reduced number of π-orbitals per unit area of the film is the actual cause of the reduction in the capture cross-section.

At very high photon flux levels, the absorptance of the chromophores, and the associated optical density, becomes very low and most photons impinge upon and are absorbed by the RPE. This impingement frequently results in pain.

12.5.2 The Translation Block

[must be rewritten XXX]
The translation block consists, histologically, of the outer dendritic structure of the neuron incorporated in the photoreceptor cell. This structure consists of the cilia like structures emanating from the photoreceptor cell in the region histologically described as the cilium. These dendrites are usually labeled microtubules. They fan out into a series of contacts with the chromophoric material in the furrows aligned along the periphery of the disks. These contacts are represented in the model by a resistor and the left diode of the TL pair.

> In the following paragraph, an analogy will be made between the operation of the translation diode pair and a conventional opto-coupler used in electronic circuits. The analogy is a good one in that it involves quanta. However, it must be pointed out that the quantized energy transfer need not involve a radiative transfer; the transfer could just as well involve mechanical energy transfer with the quanta of energy involved frequently called a phonon. In that sense, the translation pair could be thought of as a kind of quantized piezo-electric transducer.

This diode is similar to a light emitting diode (LED) in an optical coupler in that it will not emit any light until it receives energy exceeding the energy of its internal bandgap. If it is supplied with more energy than that of its bandgap, the extra energy will be dissipated in the series resistor associated with it. This resistor/diode represents a relatively low impedance at its input terminals for quanta having energy exceeding the diodes bandgap, about 2.0 electron-volts.

If a photon is emitted by the left diode of the TL and received by the right diode of the TL, which also has a minimum energy requirement which is the same as that of the left diode, a free electron will be produced and it will flow around the circuit expending energy in the resistive element associated with the right diode. As in the case above, this need not be a simple resistor but it must have a dissipative element.

12.5.2.1 Polarity & Impedance

To work effectively, the TL pair must be properly biased. The left member of the pair must have the arrow end of the diode connected to a positive voltage source, i.e. it must be forward biased during emission. The right member of the pair must be reverse biased, i.e. the arrow end of the diode must be connected to a negative voltage source. In this case, a conventional current will flow into the left member in the direction of the arrow and a conventional current will flow out of the arrow in the right member.

> It is important to remember Ben Franklin's biggest mistake here. A conventional current flows from the positive to the negative terminals of a battery (in the external circuit). The actual electron flow is in the opposite direction; electrons flow from the negative terminal to the positive terminal. Care must be taken when talking of transistor devices to distinguish between the "current flow" and the "electron flow".

The left member, being forward biased, will exhibit an impedance characteristic which is that of any forward biased diode; essentially a low resistance with a negative characteristic, the current will rise exponentially with the applied voltage--the resistance decreases with voltage. In this type of circuit, there is usually an external resistance, as shown, that limits the maximum current flow.

The right member, being reverse biased, will appear like a current generator shunted by a very high impedance which is essentially constant with applied voltage until the breakdown region is encountered.

12.5.2.2 Amplification in the translation block

If the diode on the output side of the translation block is replaced by a transistor of the open base (poda) type, it is possible to obtain large current gains in this circuit under very low noise conditions. Gains of 1,000 to 10,000 are obtained in similar man made semiconductor devices.

12.5.2.3 Polarity reversal in the translation block

Notice that there is no internal connection between the input side and the output side of the translation block. The two output leads may be connected to the following amplification block without disturbing any other circuit element. Specifically, either lead may be considered the common connection and the signal can be taken from the other lead. Thus, from an electrical point of view, an output signal of either polarity is readily available from this block.

[[[(c) shows the assembled circuits where some of the conceptual elements are actually combined in the final circuit, i. e., the input of a real transistor is in fact a diode although it is not shown as such in most of the current symbology used for transistors--the transistor is not usually employed in the region where the diode characteristic is significant except in clamp circuits and logarithmic amplifiers.

> At an earlier time, the symbology for a transistor was drawn as two back to back diodes. Later there were heated discussions within the IEEE over which way the arrow should point on the emitter lead to define the type of transistor involved in the symbol finally adopted.

Figure 12.5.2-1(Figure 12.5-1(B)) includes, starting from the left, the photon/ "exciton" transducer described by the P/D equation developed earlier.

The next element is still conceptual at this time; it is an "exciton"/electron transducer that may be required to explain two phenomena:

+ the finite delay between the time of excitation and the time of de-excitation of an excited electron in the chromophoric structure of the disks related to the finite travel time from the point of excitation to the point of de-excitation.

> This delay can be addressed mathematically[17] and it is a function of the electric field created within the disks, i. e. the delay is inversely proportional to the number of excited electrons present at any given instant. The higher the excitation rate, the stronger the electric field created, the shorter the transport delay. The equation in this case involves a first order Bessel function of the first kind to describe the unit delay involved.

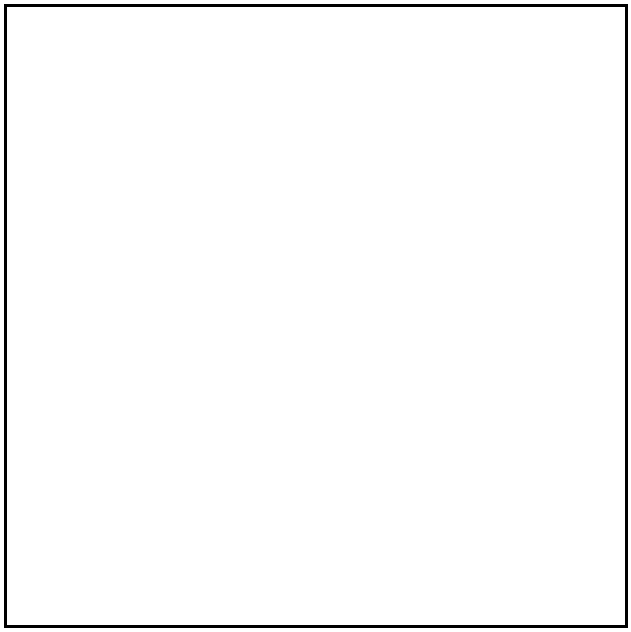

Figure 12.5.2-1 .

+ the de-excitation of electrons resulting from absorption of long wavelength photons, beyond about 0.6 microns. There may be an energy threshold related to the neuron; if so, it may require the summation of the energy from more than one excited electron in the chromophore to generate one free electron in the neuron.

For short wavelength photons and high photon fluxes, this element can be considered a network having a transfer function characterized by a constant gain, wide frequency response and zero time delay, i. e. it can be ignored.

---

[17]Goldman, xxx "Transformation Calculus, Chap. 10

The next element is a clamp circuit consisting of a series capacitance and a series combination of a diode and a "battery" in shunt with the capacitor. This circuit has two interesting functions. First, by making the voltage of the "battery", V_d, a function of the average current through the diode, the net voltage applied to the diode will be equal to the instantaneous voltage applied to the circuit minus the voltage V_d. This allows the average input level to vary over a very significant range without effecting the average output signal level, subject to the time constant of the "battery". Second, the instantaneous output voltage across the diode/ "battery" combination will be a logarithmic function of the input voltage as given by the combination of the diode internal resistance and the equivalent impedance of the source driving the circuit. This is a very key circuit element in the operation of the eye. It accounts for the large overall dynamic range of the eye, the logarithmic response of the eye over the instantaneous dynamic range of the eye, and the associated significant saturation in the data of Baylor, Torre, Lamb and others.

The last element is a current amplifier. In this case it is a living element and not just a piece of semiconductor. However, its characteristics are similar if not identical to that of a man-made semiconductor amplifier. Based again and particularly on the work of Baylor, Lamb & Yau[18], it is possible to describe this amplifier in some detail. Most importantly, it has a current gain of approximately three and one half orders of magnitude and receives its source of electrons from the electrostenolytic mechanism associated with the IS. The output lead goes directly to the IS as well. It is unusual to find this high a current gain in a single man made transistor amplifier because of the very low breakdown voltage relative to what man is used to working with.

Continuing to look at a single stage amplifier, there are two broad classes of transistors to consider for use in the amplifier; bulk effect transistors and distributed transistors.

12.5.2.4 The special case of the long wavelength visual channel(s)–a 2-exciton process

As indicated in **Section 12.5.4**, there is a special situation that is frequently found in the long wavelength chromophoric channel of the visual system. It is virtually identical to the phenomena found in modern silver halide photography where a "dye" similar to the rhodonine family is used to coat the silver halide crystals. By coating the crystal in this way, the spectral sensitivity of the silver halide emulsion is extended to wavelengths beyond the band gap limit of the crystal itself.

Specifically, the dye is deposited as a liquid crystal on at least a portion of the surface of the silver halide crystal. The incident photon excites the chromophore and an electron is transferred to the π^* band of the chromophore just as described earlier. However, this excited electron does not have sufficient excess energy to cause the release of a free electron at the interface with the silver halide crystal.

Here again, the process is a quantum one and the correct method to handle this problem is a probabilistic one. The question becomes; what is the probability that one or more excited electrons, acting in consort at the interface, can cause a free electron to be created in the silver halide crystal. This action would involve the summing of the energy of individual excited electrons. The equation could be written as follows: $P(free) = P(1) + P(2|1)*P(1)$: i.e., what is the probability that a free electron will be released as a result of the action of one excited electron acting alone, P(1), plus (or) the action of a second excited electron P(2|1) acting essentially simultaneously with the first, or another excited electron, P(1). In photography this logic can actually be carried to the third and fourth terms in a similar equation and positive results are obtained in practice at wavelengths out to about 4 times the band gap of silver halide. Moreover, the same silver halide crystal retains its inherent spectral sensitivity as well. Thus, the coated crystal exhibits two distinctly different spectral absorption bands, not unlike the three distinctly different spectral bands of vision.

In the above equation, we have already seen that the value of P(1) is virtually zero. However, the value of the term $P(2|1)*P(1)$ is relatively high, and the process is useful. The effect is to generate a square law relationship, $Y = X^{½}$ between the number of free electrons produced and the number of excited electrons producing them. This relationship is illustrated in **Figure 12.5.2-2(Figure 12.6** [-1 needs to be added])

[18]Baylor, D. Lamb, T. & Yau, K.-W. (1979) Responses of retinal rods to single photons. J. Physiol. 288 pg 613-634

Note that this "Square Law" process is not what is commonly referred to as a "2-photon" process. In this case, it is two excited electrons, or excitons, that are involved. These quanta are not moving at the speed of light, have a relatively long life expectancy at one location and are subject to the affects of electrical fields. Thus, the chance of interaction between, or joint action by, two excitons is considerably higher than for two photons.

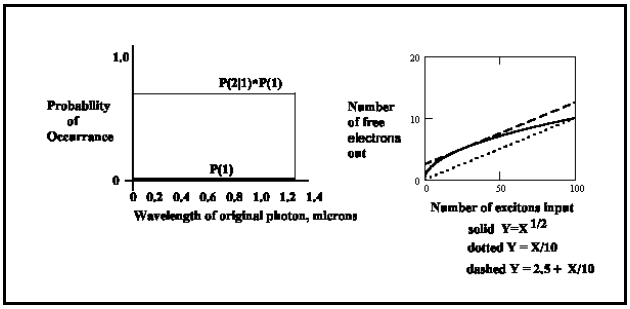

Figure 12.5.2-2 NEEDS WORK Transfer characteristic of translation block . # of free electrons "out for diode" in base region of adaptation Activa. **label curves for L- and both M- & S- channels. Curve line applies prior to adaptation amplifier action

Sliney, et. al.[19] have provided data on the spectral absorption of the L-channel in human vision extending out to 1,060 nm. The photon energy at this wavelength is only 1.17 electron-volts. This would indicate that the energy threshold of the neural system of vision at body temperature is not more than twice this number, 2.34 electron-volts, or a three exciton process would necessarily be required in human vision.

2-exciton and 3-exciton mechanisms are currently being found in the field of dye lasers[20] and have been known in photography since the 1940's (See Mees & James, 1966). Prasad used a 1.3 micron photon to generate a 0.43 micron laser radiation at very high efficiency. Interestingly, Naka & Rushton[21] made the comment in one of their 1966 papers that they would not find it surprising if this process, from the photographic field, should be found in vision as well. [***]

Arkhipov & Bassler have recently discussed the multiple-exciton event in the context of conjugated polymers similar to those of the visual chromophores[22]. While valuable, their discussion did not proceed to a definitive conclusion. They describe a sequential, quasi-instantaneous process. This process may involve excitation to a higher π-level on the excitation side of the barrier, or the accumulation of energy in the coarse of transfer across the barrier.

As in the photographic process, the characteristics of the process in vision is a function of the energy of the excitons relative to the n-electron ground state and the minimum energy threshold of the translation block. In the human visual system, the process involves the L-channel excitons, energy of approximately XXX and the translation block threshold at a temperature of 37 degrees Celsius. This effect is reported at a number of places in the literature. It is more clearly reported[23] in the case of the median ocellus of the *Limulus*. This eye incorporates two photoreceptors, one with peak sensitivity at 360 nm. in the ultraviolet and a second with peak sensitivity at 530-535 nm, corresponding to the M-channel. There is no reported photoreceptor sensitive to the intervening region normally occupied by the S-channel at 425 nm. Because of this "space" between the channels, it is much easier to distinguish the basic difference in sensitivity between the channels. Not only is the UV channel more than 200 times more sensitive to light than the M-channel, the M-channel exhibits a "gamma" of one half that of the UV channel. This is illustrated in **Figure 12.5.2-3(Figure 12.6-2).** The inset illustrates the fact that the sensitivity in the M-channel changes faster than in the UV-channel. The effect becomes important at a shorter wavelength in the *Limulus* than in man because of its lower operating temperature. This lower temperature causes the threshold energy, or energy gap, of the translation block in *Limulus* to be higher[24] than in man.

---

[19]Sliney, D. Wangemann, R. Franks, J. & Wolbarsht, M. Visual sensitivity of the eye to infrared laser radiation. J.O.S.A. vol.66 No. 4 April 1976

[20]Prasad, P. (2002) xxx NY: University of New York at Buffalo. In Photonics Spectra, April 2002, pg 22

[21]Naka & Rushton (1966) XXX

[22]Arkhipov, V. & Bassler, H. (2003) Exciton dissociation in conjugated polymers *In* Nalwa, H. & Rohwer, L. *eds*. Handbook of Luminescence, Display Materials and Devices, Volume 1: Organic Light-Emitting Diodes. NY: American Scientific Publishers Chapter 5

[23]Chapman, R. & Lall, A. (1967) Electroretinogram characteristics and the spectral mechanisms of the median ocellus and the lateral eye in Limulus polyphemus. J. Gen. Physiol. vol. 50, pp. 2267-2287

[24]Millman, J. & Halkias, C. (1972) Integrated electronics: analog and digital circuits and systems. NY: McGraw-Hill pg. 29

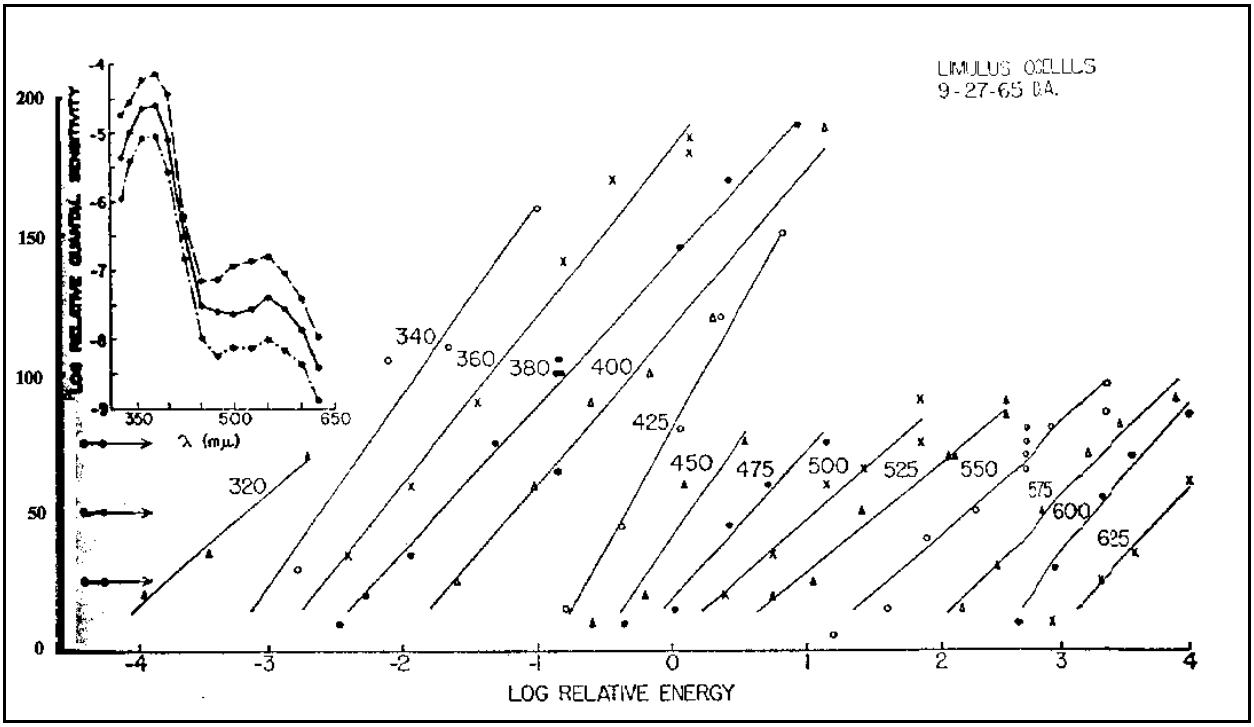

Figure 12.5.2-3 From Chapman & Hall (1967) . Note the change in slope with wavelength. The slope in the long wavelength region is one half the slope in the short wavelength region. The slopes in the 320 nm and in the midwavelength region are distorted by averaging.

When this new relationship for the transfer characteristic of the translation block is introduced for the long wavelength chromophoric channel, the results are significant in at least three ways. These ways will be discussed exhaustively in **Section 13.5.3**. Briefly, they result in

1. Gamma Differences within the spectra

2. Decrease in long wavelength channel sensitivity relative to the other channels to broadband illumination

3. Loss in spectral discrimination in the region between the M- & L- channel with lowered broadband illumination [not M- & L- in case of Limulus]

[move all or most of the following to 13.5.3

1. Gamma Differences within the spectra

The L channel now exhibits an overall square law response relative to the input irradiance. For comparison purposes, **Figure 12.5.2-4(Figure 12.6** [-1]) also shows the linear relationships; Y = X/10 and Y = 2.5 + X/10. These relationships help to illustrate that the response of this block can track a linear function over significant amplitude ranges. The important feature that will be significant in Chapter 13 is that the square law curve falls below the dashed, offset, curve at both high and low input levels.

In photography, this same manifestation is recognized by the variation of "gamma" with wavelength, where gamma is the slope of the output density versus irradiance. It is typically 1.0, linear, in undyed emulsions and the short wavelength region of dyed emulsions; and 2.0 in dyed emulsions (or in a single dyed crystal of silver halide). In practice, most emulsions utilize a mixture of silver bromide and silver iodide which have different bandgaps, and hence, different cutoff wavelengths. Because of this difference, the transition from a gamma of 1.0 to 2.0 does not occur abruptly at a given wavelength.

Flicker intensity threshold (FIT) experiments have demonstrated this 2:1 relationship between the flicker sensitivity of the L- and M- channel many times.[25]

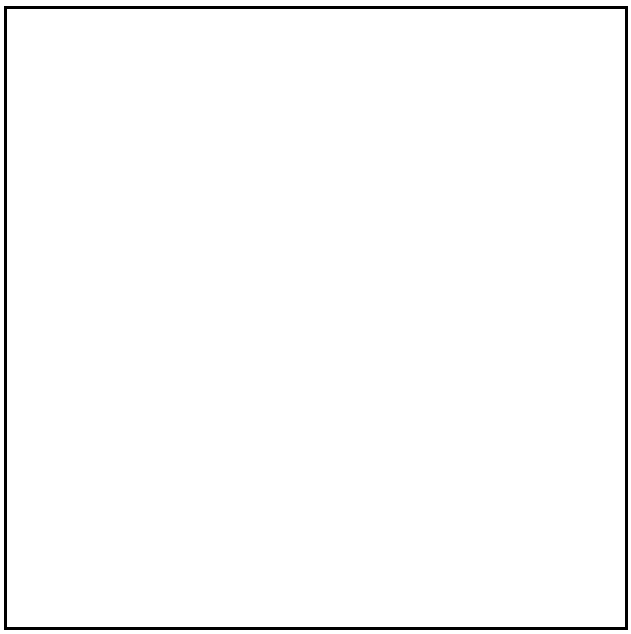

Figure 12.5.2-4 .

2. Decrease in L-channel sensitivity

When this relationship is processed in the secondary signal processing circuitry, the characteristics known as the photopic and scotopic spectral responses are seen to be manifestations of a common signal processing algorithm which utilizes slightly different chromophoric input signals. The primary difference is that the level of the L-signal drops more rapidly with irradiance than do the other channels (2 channels in trichromats and 3 channels in tetrachromats). This rapid decrease in the L-signal at the output of the translation stage causes the observed overall photopic spectral response to change to the scotopic response as the response due to the L-signal is lost. Figure XXX shows this phenomena with considerable clarity (from my earlier papers)

3. Loss in spectral discrimination

With the decrease of the L-channel signal level relative to the other channels, there is a consequent loss in spectral discrimination in the region between the M- and L- channels, accompanied by a Purkinje Shift. Although little data is available for humans in this regime, there is good data available for the turtle[26]. Pluvinage & Green have provided detailed data for the L–channel photoreceptors of the reptilian red-eared turtle, *pseudemys scripta elegans*[27]. They show a very straight square-law response over two orders of magnitude in incident intensity at 680 nm (pp 678-9) and also document the logarithmic rolloff at higher intensity levels (pg 685). They also provide very good P/D responses on page 677.]

12.6.1 The Large Signal Model ??LOCATION

[these two subsections probably apply to the entire translation block xxx]

The large signal model must be evaluated in terms of the temporal characteristics of the input signal. If the signal is at a constant level with respect to time, there will be an initial transient during which V_d is established. After that has occurred, the output signal level will be a constant level equal to the input level minus the equivalent level represented by the voltage V_d**.**

If a large signal is applied for a short period relative to the time constant of the circuit, R_v*C_v but a long time relative to the time constant in the P/D and U(t); following a brief transient, the output amplitude will be the logarithm of the

---

[25]Kalloniatis, M. & Pianta, M. (1997) L and M cone input into spectral sensitivity functions: A reanalysis. *Vision Res*. vol. 37, no. 6, 799-811

[26]Neumeyer, C. & Arnold, K. (1987) Tetrachromatic colour vision in goldfish and turtle. in Seeing Contour & Color WW 105 N874 1987

[27]Pluvinage, V. & Green, D. (1990) Evidence for a power law intensity code in the coupled cones of the turtle *Vision Res* vol 30(5), pp 673-682 & 683-691

input minus the initial equivalent level represented by the voltage V_d. This output will begin to decay immediately as V_d changes until a new steady state value is reached based on Rs, Rd and R_v*C_v. Upon the removal of the applied signal, there will be a transient similar to the starting transient after which the output will begin to decay back to the level present prior to the short pulse according to the time constant of R_v*C_v.

Based on the observed characteristics in the referenced test data and the literature, the large signal dynamic range of the photoreceptor is quite enormous. It is a photon counter at low irradiances and its maximum signal level is limited, according to the P/D, by the availability of n-electrons in the chromophoric liquid crystal of the OS (the total of all disks which are in electronic communications within a single OS). The maximum sustained signal level, i_o, may also be limited metabolically by the ability of the IS to support the necessary supply current under long term conditions; this would introduce another time constant into the overall "Adaptation Equation".

The instantaneous dynamic range of the photoreceptor is much smaller. As shown by the test data, the maximum output current available from most photoreceptors is in the 20-30 pA range and it clearly exhibits the logarithmic characteristic of the diode at the input to the amplifier stage. Whether it is appropriate to describe the diode circuit as a clamp depends on the values of the resistors involved. But clearly, for large instantaneous signal changes, the signal level is clamped to $i_o=i_s$.

It should be noted that the overall dynamic range of the eye is essentially linear until the number of available n-electrons is depleted. However, the instantaneous dynamic range is effectively limited to a range on the order of 100:1 and the output is a very accurate logarithmic function of the input.

12.6.2 The Small Signal Model ?? LOCATION & COUNTER

The small signal model of the photoreceptor is straight forward based on the complete equation. This equation is differentiable and an exact output can be obtained for any input condition. The P/D remains a linear equation under all signal conditions.

Furthermore, the diode characteristic will remain constant under any small signal conditions, and V_d will not change significantly. Therefore, the output characteristic will be a true representation of the input after any transient due to the time constants of the circuits; P/D, U(t) and (Rs, Rd and R_v*C_v).

12.5.3 The amplification block REWRITE

Eddington, writing in Gennis[28], has attempted to describe the operation of the signal transduction process in terms of a cytoplasmic cascade. His conclusion as of 1989 was that "the details are somewhat murky or unknown." The following and later sections will clarify most of these details. However, the clarification is not compatible with a cytoplasmic cascade.

The amplifier block within the photoreceptor cell is very sophisticated compared to most man-made circuits. The basic functional circuit is known as a differential pair. However, it has been optimized in a number of ways. Notice the circuit is not symmetrical in circuitry or in Activa. The first Activa associated with the translation block is operated in the open base configuration. It is also an Activa with a very thin base region. This thin base region makes the Activa subject to electrical breakdown within the base region. This leads to a special form of amplification. The base-to-emitter region is also extremely thin. This leads to a large base-to-emitter capacitance that appears to play a special role in the overall circuit.

The Activa associated with the output to the pedicle is operated in a fixed base bias mode. It is a more robust Activa used as an "impedance amplifier" and to provide the function of a distribution amplifier. This distribution amplifier can support a large number of orthodromic circuits without introducing cross-talk between them.

The topological and functional characteristics of the combined adaptation and distribution amplifiers forms a circuit well known in communications. It is the cascode circuit; it is known for its high sensitivity and low noise performance.

12.5.3.1 The Adaptation Amplifier

[xxx rewrite]
The adaptation amplifier plays two primary roles involving a variety of individual circuit techniques. These techniques have not been discussed in the vision literature previously. The first technique is probably the least

[28]Gennis, R. (1989) Biomembranes: molecular structure and function. NY: Springer-Verlag pg. 354

known. It involves the negative internal feedback within the chromophores of the outer segments (**Section xxx**). This mechanism is usually associated with the observed "bleaching" of the retina. This mechanism provides a variation in initial sensitivity of at least 10^5:1. The second technique is related to the role of the emitter impedance in both the output circuit and the input circuit. This couples a sample of the output signal back to the input circuit. The third technique is associated with the internal capacitances and leakages between Activa elements. Because of the limited experimental data concerning this circuit, it is difficult to determine which of these techniques is most important.

A fourth technique of potential interest involves a bipolar photoreceptor device (as proposed here based on the Activa) in series with a diode connected active load. Mead has described the performance of this circuit formed from conventional integrated circuit elements[29]. **Figure 12.5.3-1** shows that dynamic ranges of four orders of magnitude or more can be obtained by a very simple circuit.

The combination of bleaching within the chromophores and the availability of a diode load in the collector circuit of the adaptation amplifier appears to provide all of the automatic gain control needed in vision.

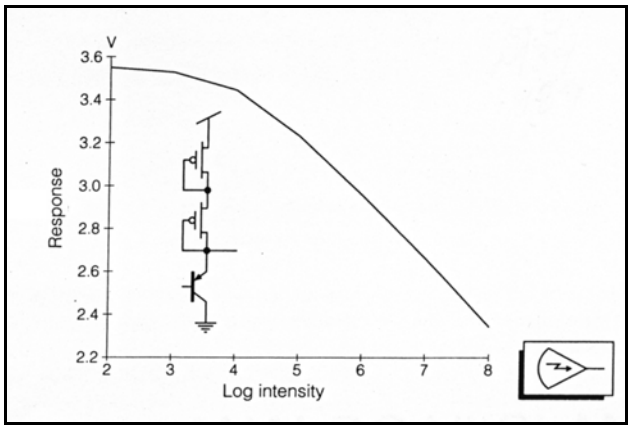

Figure 12.5.3-1 Measured response of a logarithmic photoreceptor circuit. From Mead, 1989.

12.5.3.1.1 Internal negative feedback via the poorly regulated electrolytic supply EMPTY

12.5.3.1.2 EMPTY

12.5.3.1.3 Internal negative feedback via the emitter impedance

In most man-made differential amplifier circuits, the two transistors are matched. However, in vision, matching the Activas does not accommodate the different requirements placed on the two devices. With matched devices the common emitter terminal acts as a "virtual ground." The potential of this terminal remains constant even though the current in the two paths to the emitters may change. However, if the devices are not matched, the common emitter terminal may vary in potential with respect to the current from the first Activa. This variation in potential appears as a negative feedback signal at the base terminal of the first Activa. If the potential at this terminal does vary and the capacitance between this terminal and circuit ground is significant in size, the circuit will provide more negative feedback at low frequencies than at higher frequencies. This will cause the output signal of the overall circuit to appear to have been passed through a high pass filter.

12.5.3.1.4 Internal negative feedback via internal capacitances and leakage currents

The fact that the base terminal is not physically connected to any other circuit element in the adaptation circuit leads to several potential variations in the operation of the circuit. The most significant is if there is a resistive path between the collector and the base and a significant shunt capacitance between the base and emitter terminal. Such a path introduces a significant frequency selective negative internal feedback path to the circuit. The effect is the same as described above. The low pass character of the feedback path results in an apparent high pass filter in the forward signal path of the overall amplifier.

12.5.3.1.5 Net effect of negative internal feedback in the inner feedback path

The transfer function of the photoreceptor cell is known to exhibit a falling response at frequencies below one Hertz. Whether, this response is due to a zero in the transfer function of the circuit or a combination of a zero and a pole providing a response typical of a lead-lag network is unknown. However, each of the above negative internal feedback techniques can provide such performance. Additional experimentation will be required to further quantify the performance of the adaptation amplifier and the photoreceptor cell at frequencies below one-tenth Hertz. It should be noted that nearly all data in the literature shows a decrease in signal with decreasing frequency below one

[29]Mead, C. (1989) Analog VLSE and Neural Systems. NY: Addison-Wesley pg 261

Hertz. However, during the analysis, the investigators invariably present solid lines suggestive of a flat response at lower frequencies. Since it easy to demonstrate that the human visual system has zero response at zero frequency, there is no finite low frequency asymptote in the human visual system. There is a zero in the overall transfer function somewhere. It appears to be in the adaptation amplifier and be due to one or more of the above mechanisms.

12.5.3.2 Circuit analogs of the adaptation amplifiers EMPTY

The complexity of the adaptation amplifier circuit makes a simple exposition of its performance difficult.

12.5.3.2.1 An operational amplifier analog of the adaptation amplifiers

It is the hydraulic and nutritional properties of the eye and optic nerve that control the adaptation characteristics of the visual system. **Figure 12.5.3-2** illustrates the relevant elements of the system for pedagogical purposes. The illustration is not sufficiently precise for research purposes. It does not treat light adaptation properly. The amplifiers shown in symbolic form are the adaptation amplifiers of the individual photoreceptor cells. They receive excitation from their respective spectrally selective Outer Segments. They deliver their output to their respective distribution amplifiers also contained within the photoreceptor cells. The amplifiers normally employ internal negative feedback. However, they are drawn as if they used negative external feedback to highlight this function. The capacitances C_A are actually shunted across the nodes shown by the black dots and there is no external path back to the input of the amplifiers.

As shown the circuit consisting of C_A and R_{eq} form a 3 Hz low-pass filter. The effect of this filter in a feedback circuit is to decrease the DC gain of the overall circuit below 3 HZ. This has the effect of removing the DC component of the irradiance in each channel. As a result, the visual system is essentially blind to slow changes in illumination. In some animals, tremor and other motions are introduced into the line of sight to overcome this feature and allow imaging of a scene at constant irradiance.

The crosshatched blocks are the electrostenolytic supplies to each amplifier. These supplies are connected in parallel to the vascular system as shown at the top of the figure. The vascular system is shown by an electrical analog where the capacitors represent hydraulic reservoirs and the resistances represent the impedances of the vascular channels. The symbols V_x represent the energy potential of the vascular system at a given point. The relative values of these elements are not currently known. However, the multistage character of this network is the source of the dark adaptation characteristic of the visual system. The differential equation describing this situation is third order. Its solution results in the exponential-sinewave function that is characteristic of the dark adaptation function.

The output impedance of the operational amplifier shown is not symmetrical.

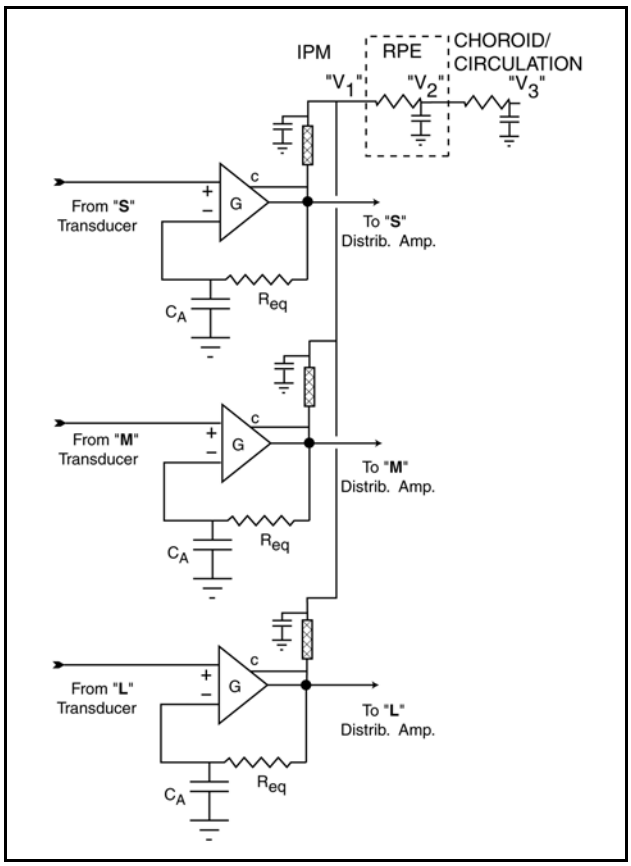

Figure 12.5.3-2 A pedagogical description of the adaptation amplifier block. The description is not appropriate for considering light adaptation. The adaptation amplifier share a common power supply. The adaptation amplifiers are shown symbolically to highlight what is normally an internal feedback mechanism (C_A & R_{eq}). The gain of each amplifier is controlled by the voltage applied to the collector terminal, c.

12.5.3.2.2 A discrete component analog of an adaptation amplifier EMPTY

The adaptation amplifier is so beautifully tailored to its requirements that it becomes difficult to create a simple discrete component analog with similar performance. Such an analog must emulate not only the electrolytic components but also the hydraulic components.

12.5.3.3 The overall performance of the adaptation amplifiers

Figure 12.5.3-3 shows the fundamental performance of the individual adaptation amplifiers as a function of the intensity of the irradiance and the short term gain of the circuit. The output is shown at the pedicle of the photoreceptor cell. The output follows the dotted line. When completely dark adapted and without external excitation, the potential of the pedicle is nominally -22.5 mV relative to the INM. xxx At that point, the AC and CDC signal amplitude begin to rise until saturation occurs within the amplifier circuit. As a result, the typical cutoff potential of -70 mV is reached.

12.5.3.1.1 The uniformity of the output of the adaptation amplifiers

One of the advantages of feedback in amplifier design is that it transfers the uniformity of the output from being a function of the individual active device to a function of the feedback device. In this case, at high signal levels, the output gain of the photoreceptors is actually a function of the diffusion parameters of the bio-energetic supplies serving the adaptation amplifiers, via the inter photoreceptor matrix (IPM), and the width of the space charge regions of the activas. The latter are controlled by the rules of stereo chemistry and the former are shared between all of the photoreceptors within a significant zone of the retina. The result is a very high degree of output signal uniformity within that zone, much higher than would otherwise be expected. This sharing also accounts for some of the halo effects (edge effects) observed near high contrast transitions.

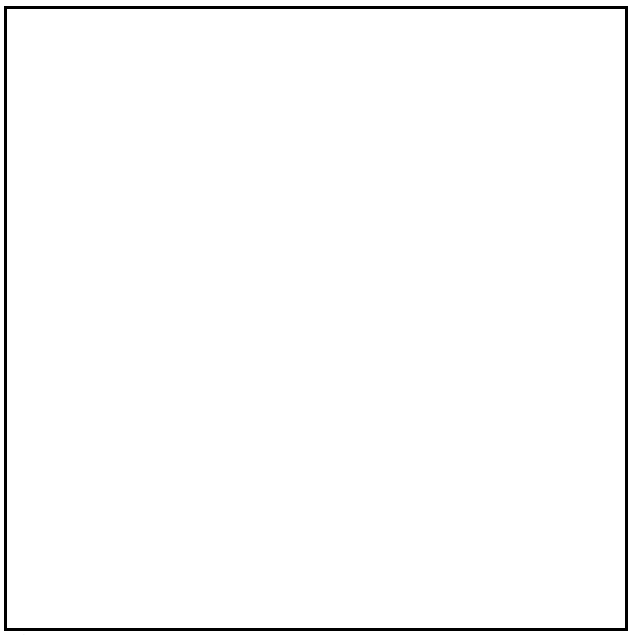

Figure 12.5.3-3 Empty

12.5.x Automatic gain control in the excitation-de-excitation mechanism–"bleaching"

[xxx see energy diagram figure in 12.9]
The following presentation provides the first detailed explanation found in the literature of how the visual system achieves its remarkably large dynamic range. This range is estimated as 10^5:1 to 10^7:1, from the bottom of the scotopic region to the beginning of the hypertopic range. The phenomenon of bleaching of the retina observed by the ophthamologist, and the mechanism of automatic gain control resulting in this phenomenon require accepting the quantum-mechanical character of the photo-excitation process as well as the electrolytic operation of the neuron containing an Activa. It is not compatible with the more conceptual chemical theory of the neuron and its reliance on simple concepts such as the role of the G-proteins in vision.

The photo-excitation/de-excitation mechanism associated with each of the photoreceptors of the retina incorporate a uniquely effective automatic gain control mechanism. The mechanism is straight forward. It entails a limited capability of the dendrites contacting the chromophore lattice associated with the disks of the outer segment. As a result of this limited capability, the de-excitation of the electrons excited into the excitation band of the energy diagram is also limited in rate. As a result, the number of available unexcited electrons in the liquid crystalline matrix decreases after the light level exceeds a minimum value. This causes a decrease in absorption cross section with higher light level. As a result the absorption efficiency decreases as a direct function of the illumination level after the level exceeds a minimum value.

The quantum physics of the actual process is developed in **Sections 5.4** & **5.5** of this work. A simple analogy is shown in **Figure 12.5.3-4**.

Consider a laboratory still designed to be energized by a high intensity light fed through a narrowband optical filter. Consider a low-boiling point solute with a narrowband absorption coefficient matched to the light from the narrowband source. The solvent is assumed to be transparent at the wavelength of the excitation. Consider a condenser with a return path controlled by a small opening at the valve shown. Arrange a gauge to measure the amount of recovered solute in the standpipe shown.

The dark adapted state exists when all of the solute is in the beaker. Under this condition, the absorption coefficient of the solution is maximum and the light is most effective in evaporating the solute.

As the intensity of the light is raised, more solute is initially evaporated from the beaker. However, the amount returning to the beaker is restricted by the valve. Hence, the molarity of the solute/solvent mixture decreases. As a result, the absorption cross section of the solution decreases and the rate of evaporation is decreased. The overall result is that once a threshold level of light intensity is reached, the efficiency of the process (evaporating solute from the pool) goes down as the light intensity goes up. Under very high intensity, the efficiency can approach zero, as it does in vision. In the case of vision, the process automatically modifies the absorption cross section of the chromophores over 5-7 orders of magnitude.

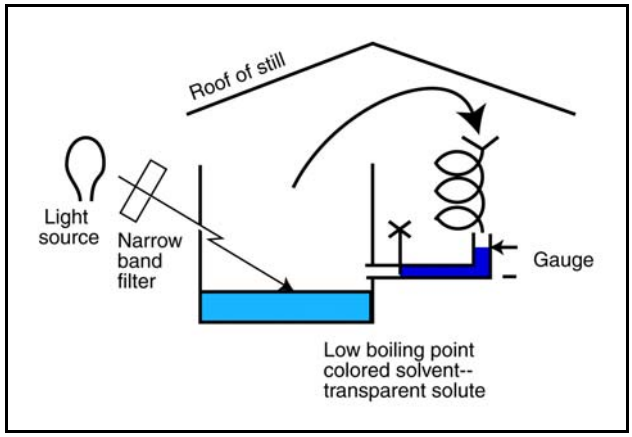

Figure 12.5.3-4 An analog of the automatic signal amplitude control employed in vision. Each individual photoreceptor of vision employs the equivalent mechanism. See text.

In the analog, the evaporated molecules of solute correspond to the excited (previously neutral) electrons of oxygen atoms attached to the conjugated backbone of the Rhodonine molecules. The excited electrons are returned to their unexcited state within the lattice of the chromophores by the limited capacity of the dendrites to de-excite them.

The entire process occurs within the outer segments of the photoreceptors (and the dendrites in contact with the individual disks of the outer segments). There is no requirement for the chromophores, or the ligands of retinal, to disassociate from the lattice structure of the outer segments and be transported to the RPE layer of the retina to be regenerated as suggested by previous theories of photoreceptor operation.

The gauge shown should be interpreted as a differential gauge. It measures the difference in height between the start and the end of a unit of time.

Above the threshold value, the product of the rising stimulus level and the inversely proportional absorption cross section results in a nearly constant output signal, except for the small differences measured at the “gauge.” This differential voltage is applied between the base terminal of the adaptation amplifier Activa and the surrounding ground potential of the IPM.

The fading of the color of the solution in the beaker of the analog is equivalent to the bleaching of the chromophores observed by the ophthalmologist when viewing the retina.

Functionally, the operation of the chromophores in the presence of a dendritic structure of limited average current capability explains the gross operation of the visual system as a function of illumination intensity. **Figure 12.5.3-5** describes this operation.

In this figure, the expression “chromophores en masse” can refer to the group of chromophores in the liquid-crystalline state associated with and appropriately oriented within a single outer segment of a photoreceptor. Alternately, it can refer to the larger group associated with multiple outer segments exhibiting the same spectral sensitivity within a given unit area of the retinal surface. The Activa shown can consist of a single Activa within a single photoreceptor or it can represent a group of Activas associated with a group of outer segments as defined above. In either case, the single base connection to the chromophores en masse consists of multiple neurites contacting the chromophore material at the edges of the disk stack(s). These neurites have frequently been described as dendrites. However, they are more appropriately described as podites when examined in terms of their electrical function.

The Activa is shown with a load impedance labeled Z. For the present discussion, this impedance is a simple one consisting of only one discrete electrical element. When discussing the "dark adaptation" characteristic of vision, it will be shown to consist of a network of two or more filter stage. As in the first amplifiers of all photoreceptors, the output signal is described by the current passing through the emitter of the Activa as shown.

In the steady state situation, the stimulus flux, F, is described in photons per second per unit area applied to the outer segments. The equivalent de-excitation mechanism is described by K in units of current, electrons per second per unit area of the outer segments.

Under dark adapted conditions, the multilayer arrangement of the chromophores coating the disks in the disk stack represent a very efficient absorption mechanism. For purposes of discussion, the absorption efficiency, or the quantum efficiency, of this process will be considered 100%. For stimulus flux levels below a specific value, the de-excitation effectiveness of the current K is more than adequate and there is no buildup of excited electrons within the chromophore masse. However, for higher values of flux, the current K does not provide adequate de-excitation and a net excitation level (frame A) is observed in the energy diagram of this quantum-mechanical process (**Section xxx**). As a result of this excess of excited electrons in the excitation band and resultant shortage of neutral electrons in the valance band of the chromophore material, the material exhibits a reduced absorption coefficient and appears bleached to the observer (frame B).

As a result of this bleaching under increasing stimulus conditions, the rate of excited electron generation in the valance band is greatly reduced. As a result, the absorption coefficient is inversely proportional to the incident flux and the product of these two terms results in a constant signal output (frame C). This feature exhibits the automatic gain control mechanism of the retina recognized by an observer as bleaching. Functionally, it causes both the steady state and dynamic components of the output current to remain virtually constant above a fixed level. This level generally corresponds to the transition between mesotopic and photopic illumination regions. The reduction in absorption coefficient can be described as a reduction in the quantum efficiency of the photo-excitation process in vision.

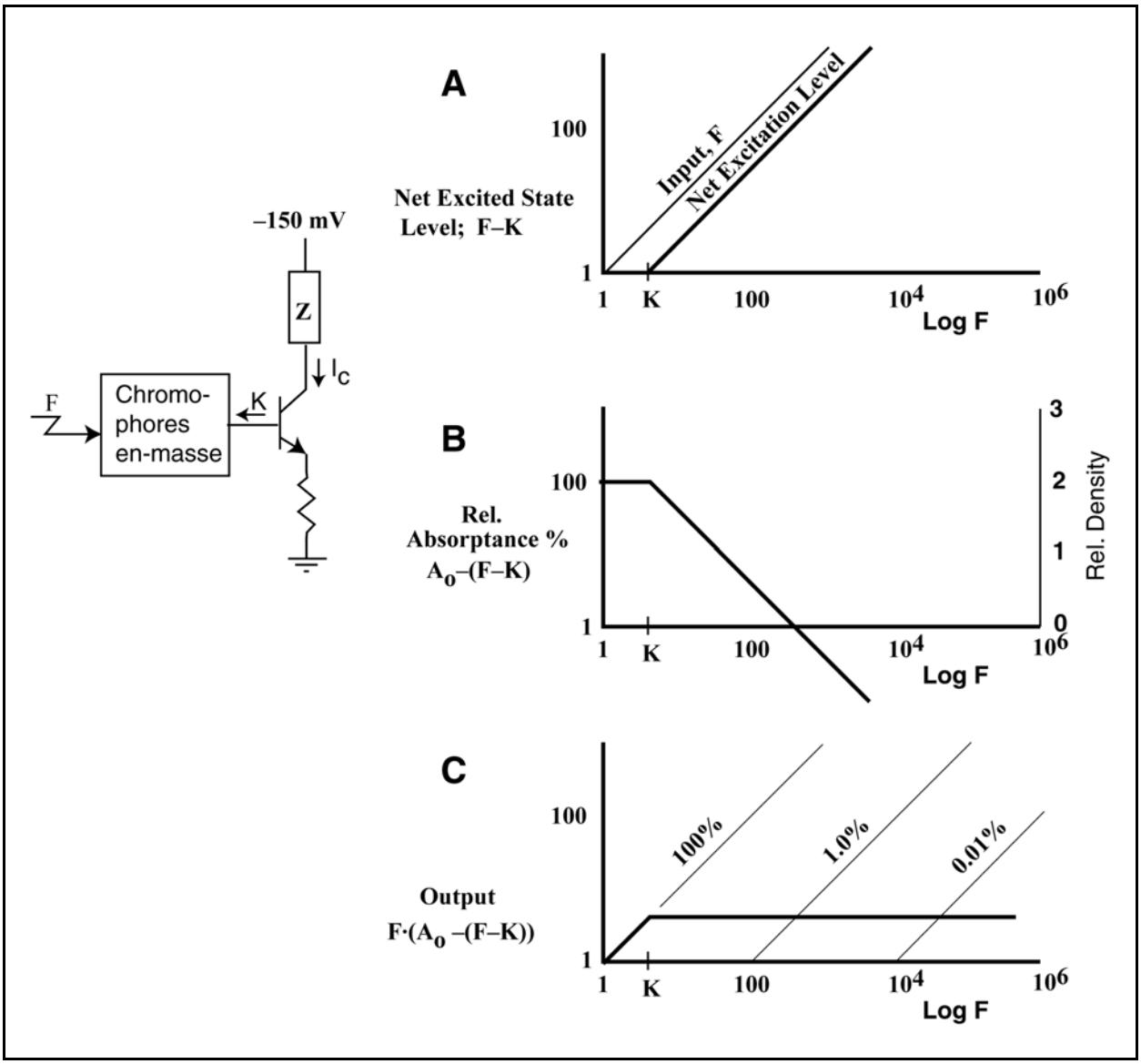

Figure 12.5.3-5 The transfer function of the outer segment chromophores and the dendrites of the first Activa. The simplified circuit is shown on the left. Frame A; the stimulus intensity and the level of photo-excitation. Frame B; The relative absorptance (left scale) of the process as a function of stimulus intensity. The optical density of the chromophores of the outer segments as a function of the stimulus intensity (right scale). Frame C; the AC output level measured as the current passing through the emitter terminal of the Activa with an overlay showing the effective quantum efficiency of the overall process.

12.5.3.2 The Axon Drive Amplifier

The right hand portion of **(b)** describes, in the simplest form, the amplifier portion of the photoreceptor cell. This amplifier is almost surely located to the right of where the dendritic cilia combine near the cilium. However, this amplifier element, labeled the activa in this work, may not actually be contained within the cell nucleus as implied

by the location in the Outer Nuclear Layer. It may be located within the Inner Segment but physically separate from the nucleus.

As will be shown in Appendix B, this amplifier block contains a biological system that exhibits all of the characteristics of a biological transistor circuit. In its simplest form, this amplifier consists of biological transistor exhibiting a linear gain mechanism with a complex input impedance as shown. The input impedance consists of a theoretically perfect diode (DL) in series with a resistive element representing the actual resistance of a real diode, and a battery. The battery is used to forward bias the biological transistor. It is polarized such that the diode is forward biased. Because of this forward bias, the diode exhibits a small resistive impedance with a negative characteristic--the resistance decreased with voltage.

12.5.3.2 An analogous circuit with external feedback

[show a figure based on operational amplifiers. Have draft]

12.5.4 Individual response functions

Figure 12.5.4-1(Figure 12.5.4 from old work xxx) describes the relevant transfer characteristics for the blocks making up Stage 1 of this model; the disk structure of the OS (transduction), the disk to dendrite interface (translation)**,** and the activa (amplification). For the purposes of this section, only the impulse response

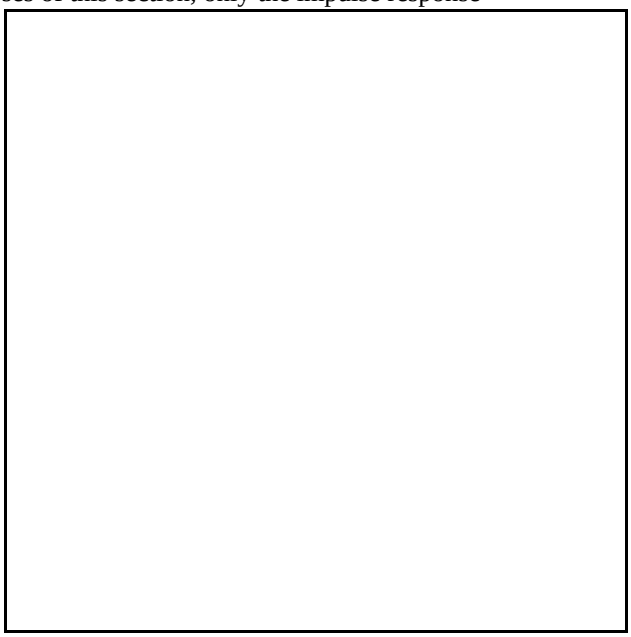

Figure 12.5.4-1 The transfer function of Stage 1, the photodetection stage of this model.

In (a) of this figure, the transduction response taken from Appendix A is shown. For the purposes of this section, only a simplified version of the P/D equation is used, i.e. the amplitude response to an impulse function without regard to the transport delay portion of the equation. In this case, the amplitude corresponds to the number of excited electrons in the π^* band of the liquid crystal. If the impedance shunting the capacitor is purely resistive, the amplitude will also correspond to the flow of charges through the impedance. A simplified version of the P/D equation is shown for several values of the resistive impedance in the circuit.

In (b) of this figure, the transfer function of the translation block is shown. Since the input to this block is a quantum phenomena, it is most appropriate to speak of the probability that a given quanta will generate a free electron upon encountering the TL block. As shown on the left, for any radiant photon which is absorbed by the UV, S or L chromophore, the probability of generating a free electron is 1.0. All of these excited electrons will possess at least 2.0 electron-volts more energy than there unexcited state. They can give up this energy upon de-excitation. The graph on the right is therefore a straight line at 45 degrees. Every excited electron created by absorption in the UV, S and L chromophoric bands will generate a free electron upon de-excitation. There is a special case which applies to the L channel which will be discussed in section 12.6.[xxx]

In (c) of this figure, the input impedance of the amplification block is shown. As is discussed elsewhere in this work, the amplification function in most of the visual system involves a specialized form of that term. When in the common podium configuration, as found in the photoreceptor cell, the biological transistor does not exhibit a voltage gain. It is operating in a current mode, and the amplification involves a change in impedance level which results in a power gain but not a voltage or current gain. In many respects, the amplifier in the photoreceptor cell is acting as an isolation circuit and not as an amplifier in the normal sense. However, it does exhibit a special relationship between the voltage and the current at its terminals. This is primarily due to its use in a large signal circuit operating near the zero bias point. This characteristic, known as the input static characteristic, is shown for the condition where there is near zero resistance in the podium to neutral connection.[[**** Is this the input diode or the

transistor itself?]]
This characteristic is frequently represented by a simpler characteristic also illustrated in the figure. This characteristic looks like two resistors in series with the high impedance shunted by a perfect diode with a turn-on characteristic at a voltage of V_x, which is a multiple of V_T--the voltage equivalent of kT/Q. Below V_x, the circuit exhibits a very high impedance, higher than the output impedance of the translation circuit. Above V_x, the circuit exhibits a very low impedance, lower than that of the translation circuit.

[[Because of the extremely large difference in the impedances described above, it is mathematically convenient to use a simplified mathematical expression for this characteristic. The curve of X/c+X, where c is any constant value, is also shown in this figure.]]

12.5.5 Assembly of the overall circuit

When the blocks described above are interconnected, and it is a direct connection where a direct current path exists throughout except at the TL diode interface, several important changes occur in the operation of the circuits.

Interconnection of transduction and translation blocks

As discussed briefly above, the P/D process involves a photoexcitation and a de-excitation process. The photoexcitation process is not changed as a result of interconnection. The de-excitation process is changed significantly. Whereas, without interconnection the process is controlled by a parasitic process involving the edges of the disks contacting surrounding materials; the time constant of this parasitic process is in the region of minutes to hours and is controlled by the effective resistance of the process.
With interconnection, the high parasitic resistance is shunted by a relatively low resistive path represented by a forward biased diode and possibly a series resistor. This shunt resistance becomes the dominant current path in the de-excitation process with a time constant on the order of 1.5 seconds. The interconnection has no impact on the output of the translation block. For completeness, the output of the transduction block is shown in **Figure 12.5.5-1**(**Figure 12.5.5(a)**) for the case where the translation block is connected to it. **Figure 12.5.5-1**(**Figure 12.5.5(b))** illustrates the current output for the translation block when these two blocks are interconnected.

Interconnection of translation and amplification blocks

[[***Prior to interconnection, the output circuit of the translation block exhibits a high shunt impedance across a current source. In operation, any charge generated at the diode essentially reverse biases the diode, maintaining or raising the effective impedance. Upon interconnection, the amplifier block causes several changes. As drawn, the amplifier block includes a battery. In the interconnected circuit, this battery forward biases the diode, DL, and creates or increases the reverse bias on the output diode of the coupler, TL. The resistive component of the DL is very low relative to the TL whenever, the DL is forward biased. This resistive component is also non linear, exhibiting the conventional exponential relationship between current and voltage. The result is that the current delivered by the TL to the input of the amplifier transistor is impacted by the condition of the diode, DL. When DL is forward biased, its impedance is low and much of the current will be shunted through the DL. Under this condition, the voltage at the input node of the amplifier will be related exponentially to the current generated by the TL. If DL should become reverse biased, its impedance becomes very large, probably higher than that of the TL, and all of the current generated by the TL will be presented to the input of the transistor. The voltage at the input node is then directly related to the current by the resistive value of the two reverse biased diodes, TL and DL. ***]]

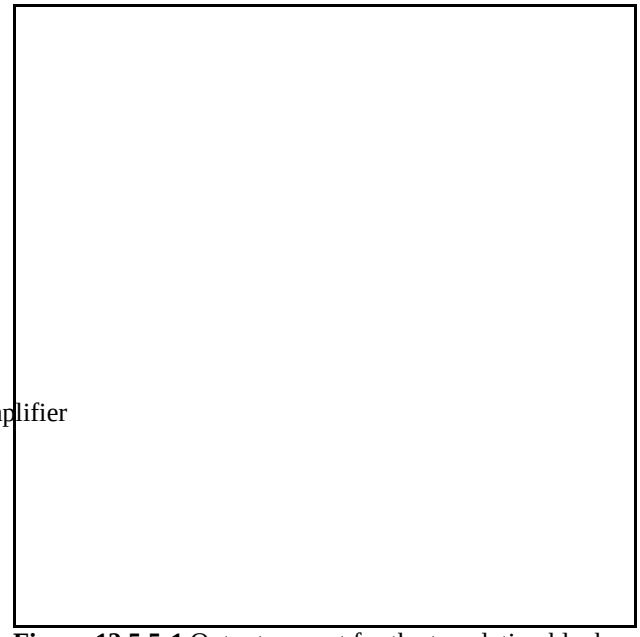

Figure 12.5.5-1 Output current for the translation block .

Figure 12.5.5-2(Figure 12.5.5(c)) illustrates the current injected into the transistor for the typical bias situation. For low irradiance, the current waveform is the same as in **Figure 12.5.5-2(Figure 12.5.5(b)) .** At higher irradiance, the input current is limited as part of the current is shunted through the diode, DL.

12.5.5.1 Output of the amplification block

The amplifier transistor is connected in the common podium configuration and is thus operating in a mode exhibiting a current gain of 1.0 +0 -0.01. Thus the voltage presented across the output resistor will be equal to the input current times the output resistors impedance. In the absence of any irradiance, the output voltage level will be established by the current going into the transistor at the dendritic input. With an increase in irradiance, the current going into the transistor will increase in a complex relationship to the current generated at the TL as indicated above. Basically, the output will be linearly related to the T current until the diode DL becomes conductive. When that occurs, the output voltage will no longer increase linearly with the current from TL but will increase more slowly. The result is an amplitude limiting process. **Figure 12.5.5-3(Figure 12.5.5(d))** illustrates the current output of the transistor. Assuming the load resister is linear, the voltage output would have the identical shape as in **Figure 12.5.5-3(Figure 12.5.5(d))**. If however, the input impedance of the next neuron is represented by a non-linear resistive element, the voltage waveform would be reshaped, to exhibit the product of the output current and the non-linear impedance.

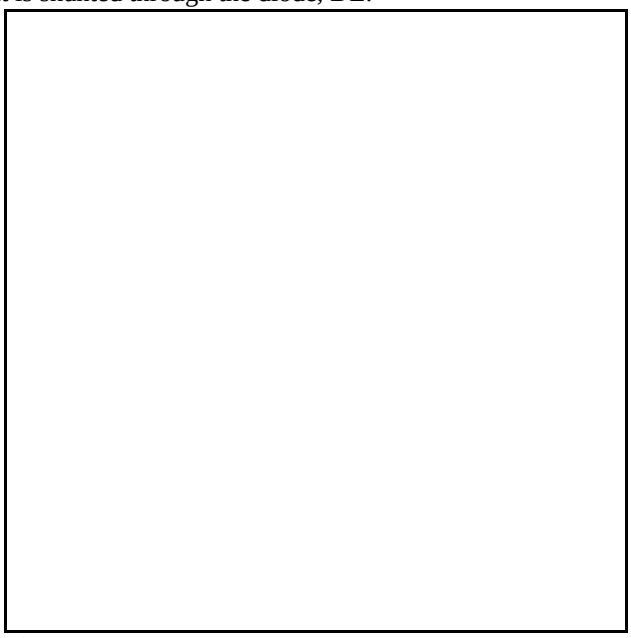

Figure 12.5.5-2 .

12.5.6 The electrical topology of the photoreceptor cell

[use fig. 12.9 and 12.9.2 in this section

With an appreciation of the individual blocks in Stage 1, it is now possible to present a more complete description of the circuits necessary to accomplish the performance achieved. **Figure 12.5.6-1(Figure 12.5.6-1(a))** is an attempt to describe a complete circuit representing the performance of both the transduction and translation functions; the transduction function only because of the intimate relationship between the two blocks. As explained earlier, the upper part of the figure is an analog of the physical circuit of transduction since the actual function is a quantized process in the energy domain. The lower part of the figure is an equivalent circuit capable of being implemented using man made components to achieve essentially the

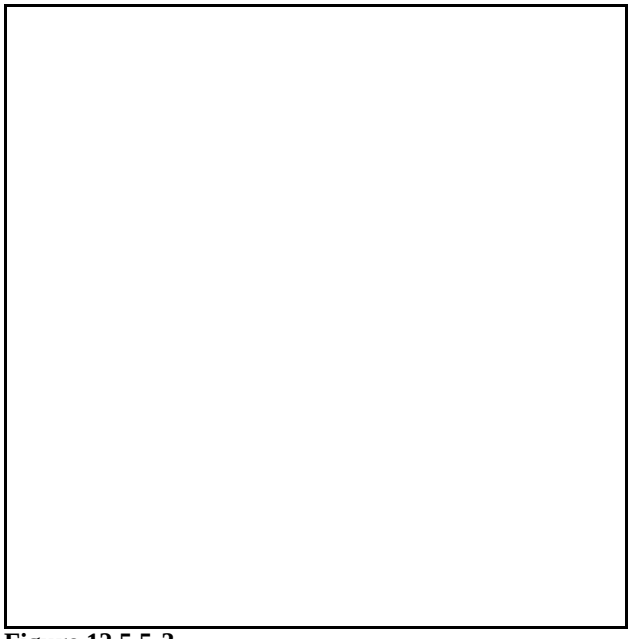

Figure 12.5.5-3 .

same results as in the biological counterpart.

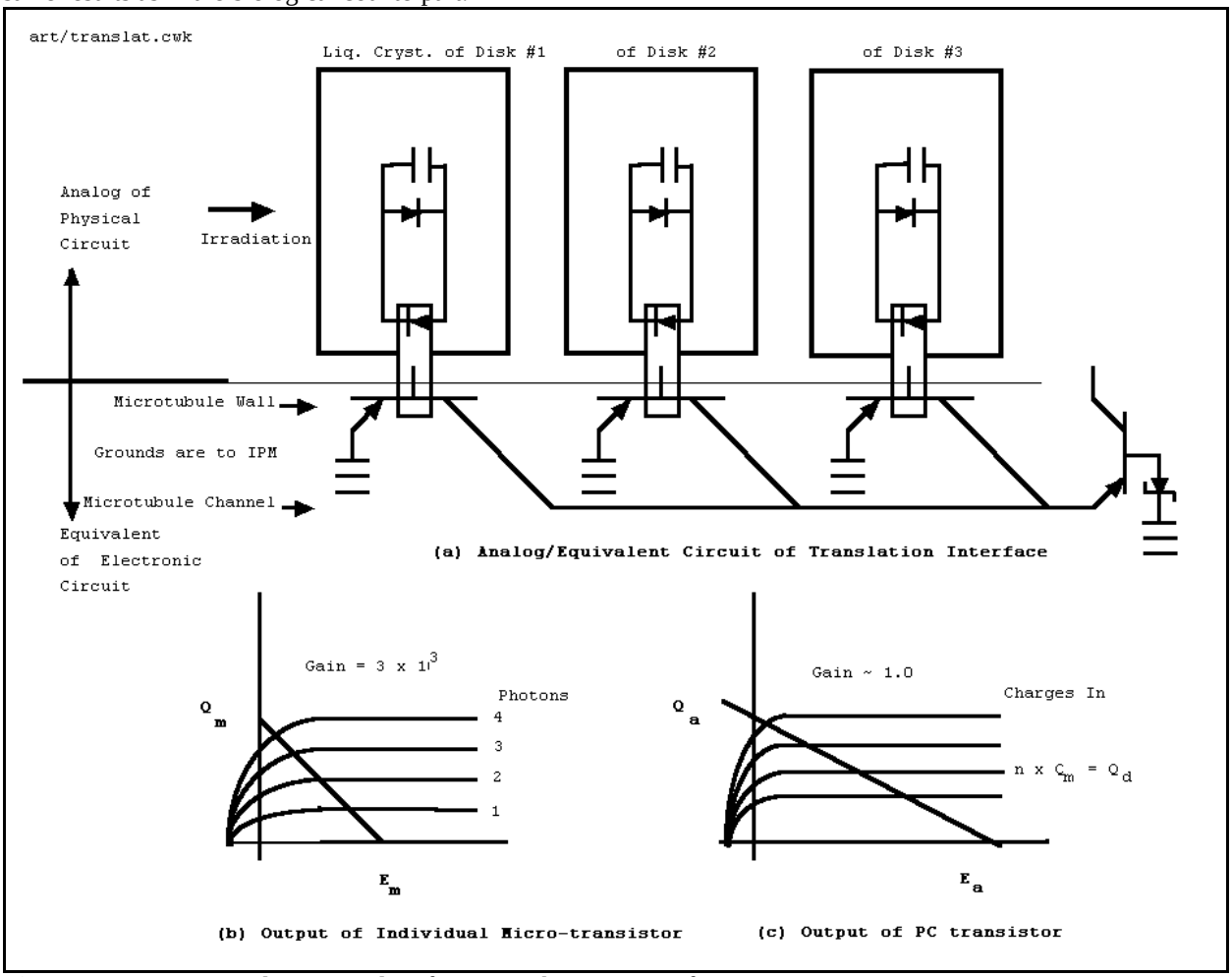

Figure 12.5.6-1 Circuit diagram and performance characteristics for Stage 1 .

In the upper part of the **(a)** portion of the figure, each large rectangular box is meant to represent the liquid crystalline material of a single disk, with three of approximately 1000 shown. Within each box is an isolated energy circuit as developed in Appendix A and described by the P/D equation. This circuit creates excited electrons in the π^* band of the chromophore which are stored in the analog of a capacitor and are returned to the ground state by interacting by the diode in the lower part of the box which operates in a mode similar to a light emitting diode but in the mechanical instead of the radiative regime. The mechanical impulse generated by this diode for each electron de-excited is coupled, as indicated by the small rectangular boxes, to the open podium lead of the micro-transistors making up the wall of the microtubules in intimate contact with the disks.

The lower part of the **(a)** portion of the figure, illustrates the equivalent circuit related to the microtubules in the OS and the larger transistor located in the IS of the photoreceptor cell. The biological circuit has evolved in this fashion for reasons of optimization. As in the semiconductor world, a microtransistor of very small dimension can achieve very high current (charge) gains but it will have a very low breakdown voltage between the emitter and the collector. In addition, because of the proximity of the collector potential to the voltage due to the photovoltaic effect, the micro-transistors will have a very limited linear dynamic range, only a few electrons per second per disk/microtubule interface (of which there are some 6-12 per disk in various animals).

The labels on the left of the lower part of the diagram are meant to give a sense of where the individual components are located. The micro-transistors essentially form a continuum along the wall of the individual microtubules with

the output signal being transported along the inside of the microtubule, either on the surface or in the interior medium. The emitter lead of each microtransistor is in contact with the IPM, surrounding each OS, which provides the electrical return for the circuit.

To prevent voltage breakdown in the micro-transistors of the translation block, the micro-transistors are all supplied power from the transistor in the IS. This transistor incorporates a Zener diode element in its podium lead which effectively limits the voltage applied to the micro-transistors under any and all conditions. The configuration of a single microtransistor connected as shown to the IS transistor is called a cascode circuit in semiconductor and vacuum tube technology and it is known for its excellent low noise performance. As far as this author is concerned, multiple input circuits in a single cascode circuit is unknown in the world of man-made circuits. However, it should provide the same quality of noise performance. The beauty of this arrangement is that;

+ it offers a very high electron gain in each microtransistor, on the order of 3000:1
+ the charge from each microtransistor is accumulated on one conductor
+ the total charge accumulated is applied to the input of the IS transistor which acts as an isolation amplifier with a current (charge) gain of slightly less than 1.0 (although it may provide power gain due to the lower output impedance of the circuit compared to that of the micro-transistors)

It should be noted that the Zener Diode is structurally identical to the other diodes used, except it has a slightly thinner active region which causes it to go into breakdown at a slightly lower voltage than the other reverse biased diodes. This slightly lower voltage and the small emitter to base voltage of the IS transistor insures that the micro-transistors of the translation block never go into breakdown.
The total current (charge) supplied to the entire structure is limited by the impedance in the collector, or axon, lead of the IS transistor (which is not shown in the figure).

It should also be noted that this overall arrangement does not require significant power from outside sources. The P/D function within the disks is completely self-powered and consumes nothing. The micro-transistors all draw their power from the IS which in turn is powered by the voltage provided to the collector lead through the load impedance. This voltage source may be in either of two places; it can be in the IS (and probably associated with the cell soma) or it can be in a cell in a more basel location in the signal processing chain.

Although this model is compatible with the composition of the membrane associated with the micro-transistors having a high content of Ca^{++}, Na^{+} or K^{+} ions, it does not require the physical movement of any atoms or ions, physical movement is limited to “holes” and electrons. Any physical movement of atoms or ions would effectively destroy the utility of the microtransistor until the ionic structure could be rebuilt.

Figure 12.5.6-2(Figure 12.5.6-1(b)) provides additional detail with regards to the transfer characteristic of each microtransistor. As developed elsewhere, the difference in voltage between the collector potential, E_m and the photovoltaic potential is quite small, less than 100 millivolts in most species**,** resulting in considerable curvature and compression in the transfer characteristic for even very small signals. However, the gain achieved is quite large. The device is literally reacting to the input of individual electrons and generating a significant output current; Q_m is on the order of 3000 electrons for each electron generated on the open input lead.

Figure 12.5.6-2(Figure 12.5.6-1(c)), on the other hand, operates in a significantly different regime. It accumulates the charges from each microtubule in the OS via non-algebraic arithmetic--no charge is able to escape back through a conductive path to ground. This total charge can be considerable considering the size of the circuit elements. There are typically 1000 disks in an OS and 8 microtubules per OS. Giving a signal level increase on the order of 8,000 through non-algebraic arithmetic. It then amplifies the resultant signal through trans-impedance amplification, lowering the impedance of the output signal considerably relative to the input signal. Although the current gain of this circuit is less than or equal to 1.0, it is able to output a current of up to 20-30 pA under steady state conditions. The total signal gain, n, is on the order of 3000 times 8000 or 24 million to 1 (about 130 Db) which is quite impressive for any similar circuit.

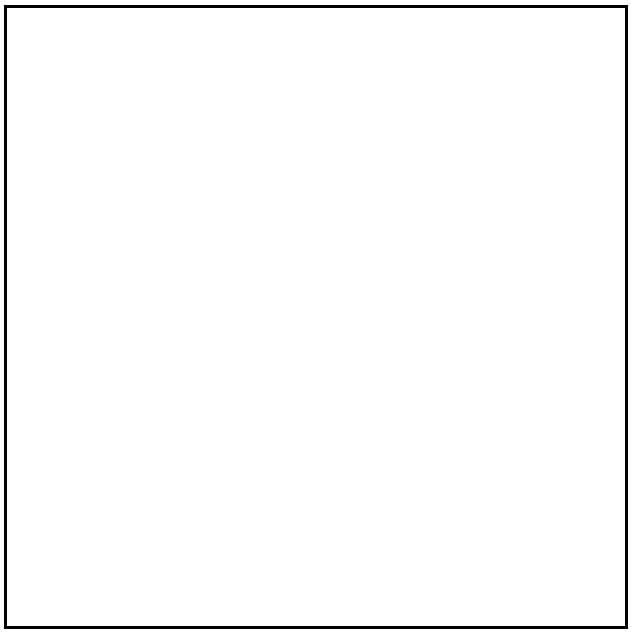

Figure 12.5.6-2 .

12.5.7 Effect of dis-assembly in the laboratory

It is very instructive to take a moment to examine the characteristics of the overall photodetection process, Stage 1, in the visual process developed here and to examine the observable characteristics of the various components in the laboratory.

12.5.7.1 Probing

As indicated elsewhere, the process of probing the photoreceptor cell in the laboratory is an awkward process, although useful information can be and is obtained. The size of typical probes is 10-25 microns, much larger than the 0.1 to 2 micron structures involved in the activities related to vision. Therefore, attempting to obtain electronic signals that are not contaminated by the probing process is difficult and time consuming, essentially a probabilistic process in itself.

12.5.7.2 Dissection

If the "battery" powering the neural portion of the photoreceptor cell is disconnected from the neuron, the resting potential and the output waveforms associated with the cell will be grossly affected. Even penetrating the cell membrane has the potential of changing the resting potential and hence the overall performance of the cell.

As shown in the pipette isolation technique, the total current into and out of the OS can be measured during irradiation by sucking the OS of an otherwise complete cell into a pipette which is connected into an electrical measuring set. Breaking the connection between the OS and the IS immediately terminates the electrical response to irradiation. The OS can still be bleached but it will not return to the unbleached condition except after an extended period of time. The OS is not a stand-alone photoreceptor. It must be attached to the IS for proper operation.

Similarly, the output of the IS, as measured at the pedicel, does not respond to irradiation in the absence of a proper connection to the OS via the dendrites passing through the cilium.

12.5.7.3 Extraction

The conventional process for extracting the visual chromophores in the laboratory does not lead to the extraction of the original material nor does it preserve the necessary and specific configuration of the chemical material that gives it its unique properties. The normal procedure is to separate the matrix of the OS from the matrix of the IS by tearing or slicing. This process effectively separates the OS electrically from its associated dendritic structures. After this, the OS is usually separated from the RPE, also by physical means. This destroys the environment in and around the OS, including the chromogen material awaiting utilization in the formation of new disks coated with chromophore in the form of a liquid crystalline layer.

As seen in (a) of **Figure 12.5.7-1 Figure 12.5.4,** when the dendritic material is removed from the disk material in the process of extracting the "pure chromophore", the remaining material is no longer shunted by the conductive element represented by the translation block. Therefore, while the disks, and the associated chromophoric material, are still sensitive to irradiance, the relaxation time is extended considerably; i.e. the material will still bleach rapidly as called for by the P/D equation but it will now relax under the control of a much longer time constant. This is exactly what is observed, the material bleaches but takes hours to return to the unbleached, photosensitive, condition.

If the disks extracted above are examined carefully, it will be found they still exhibit their normal spectral characteristics as long as the chromophore remains in the liquid crystalline state. If the chromophoric material is diluted in order to continue extracting it from the protein material of the disks, the ordered and shared state of the π band is disturbed. This has two effects; the individual molecules of the chromophoric material now exhibit very narrow absorption bands at visual wavelengths, measured in angstroms, as appropriate to such molecules at room temperature. Secondly, the absorption coefficient of these materials drop by several orders of magnitude since the slow structure associated with liquid crystalline materials no longer exists and the molecules are no longer electrically resonant at visual wavelengths.

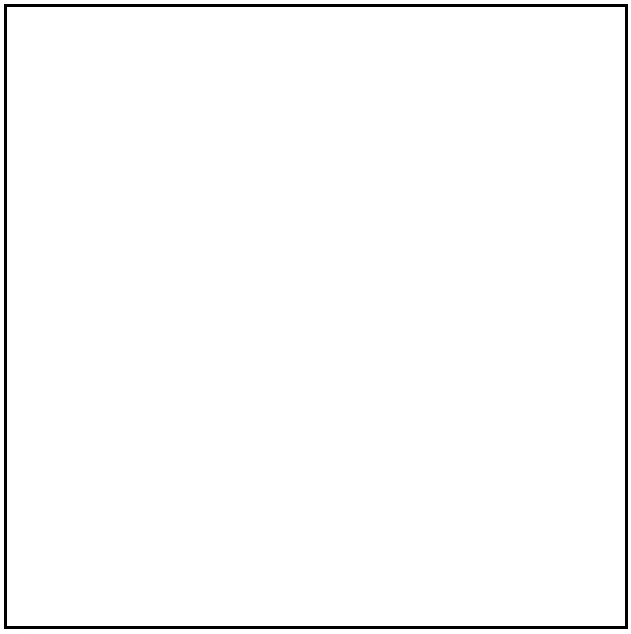

Figure 12.5.7-1 .

If the chromophoric molecules extracted by dilution above are now treated with an oxidizing agent, which most detergents are, in order to speed up the extraction process, another significant change takes place; the delicate chromophoric molecules are now oxidized by the detergent and they lose one or both of their heavy atom terminal groups--to be replaced typically by a hydrogen or a methyl group. The effect of this action is to transform the Rhodonines into a retinene or a similar fragment that is no longer a chromophore in the visual spectrum. The remaining material can no longer by characterized as a visual chromophore but only as a chromogen.

12.7 The Transfer Functions of Stage 1

12.7.1 The steady state transfer function

12.7.2 The transient state transfer function

[Work in Devoe 1966 including the circuit diagram shown in Armington 1974]

Note also Crone page 190 and the mathematical problem with this description

12.7.3 The “Overdriven” transient state transfer function

The overall small signal transfer function of the photoreceptor is also well behaved.
P/D will describe the frequency response of the transduction portion of the circuit. U(t) is a function of the average signal level or background and will properly describe the time delay exhibited by the output signal. And the resistances and capacitances of the diode stage will also contribute a roll-off to the frequency response. And again, it needs to be pointed out that the metabolic supply in the IS may contribute a time constant to the overall response but this should be negligible under small signal conditions.

12.8 Comparison with data in the Literature

This section may appear superfluous since much of the most important literature has been utilized in the development and justification of the overall model. However, there are more comparisons to be made.

It is necessary to show how the model developed here applies to all types of animal vision. Thus, it must be shown to apply to *Arthropoda* and *Mollusca* (basically all invertebrates with vision) and to *Chordata* (the vertebrates and some of their ancestors) and possibly a few unusual cases such as *Limulus* (which may have a unique photoreceptor cell, known as the eccentric cell) and *Annelida*.

Reference will be made to the Photoexcitation/De-excitation Equation (P/D Equation) developed in **Section 16.3**. It describes the electrical waveforms generated within the outer and inner segments of the photoreceptor cells. After some modification, the P/D Equation appears as the "generator waveform" at the pedicle of a photoreceptor cell. Reference will also be made to **Section 11.1.5** where a variety of waveforms were defined by Class. **Figure 12.7.1-1** offers a modified diagram annotating the relationship of these waveforms to the photoreceptor cell. The electrostenolytic supply for the adaptation amplifier (on the left) has been shown explicitly because of its importance to the discussion of **Section 12.8.1. 2** & **3**. The details of this circuit, its relation to the vascular supply of the retina and its impact on adaptation mechanism will be detailed in **Sections 12.5.3.2.1** & **16.4.2.1**. The Class A waveform path is shown dashed because there is no known technique for contacting the open connection to the base region of the Activa within the adaptation amplifier. The other Classes of waveform have all been recorded in the laboratory as will be discussed below.

The area between the RPE and the inner segments of the photoreceptors is chemically unique. It is an area free of oxygen and dopamine and filled with the disks of the outer segments. Oxygen must be excluded to avoid oxidation of the chromophore material on the disks in liquid crystalline form. The disks are immersed in a solution of chromophores and chromophore carriers, IRBP's. The solution also contains glutamate as the neural system fuel and GABA as a waste product of electrostenolytics. Bruck's membrane is well documented as the outer surface of the RPE closest to the pupil of the eye. Verhoeff;s membrane is less well documented and may not be a physical membrane. It is potentially the reflective region occupied by some of the stored chromophore material or some other functional element.

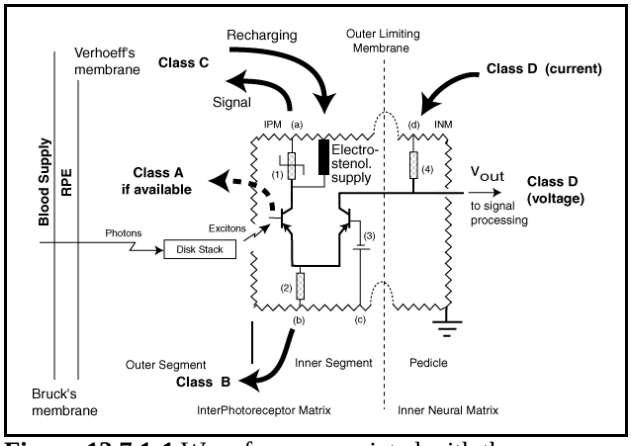

Figure 12.7.1-1 Waveforms associated with the photoreceptor cell. The electrostenolytic supply to the collector of the adaptation amplifier Activa has been shown explicitly. See text.

12.8.1 The outer segment and the suction pipette technique

The Baylor school has been studying the photoreceptor cell for many years using a technique where a single operational OS is sucked into a Faraday cage in the form of a micropipette. In the more recent experiments, this pipette has had a thermocouple mounted near the tip of the pipette to provide precise temperature information. By moving the OS into the Faraday cage gradually, it is possible to determine the source of the current emanating from the OS. The current is very uniform as a function of the length of the OS. This technique essentially isolates the selected OS from the IPM. Therefore, the collected current is returned to the system through the ground connection provided by the experimenter. In this way, a Class C waveform is obtained but the return path is not via the ground bridge between the IPM and the INM. The waveform is usually measured as a current because of the extremely high impedance level.

If measured as a voltage, the Class C waveform can be considered the result of a second order physical system if the capacitance associated with the collector is significant. Therefore, the waveform is not discontinuous, as in the Class B waveforms, where the amplitude departs abruptly from the baseline. It would depart with a small amount of curvature after the intrinsic delay of the P/D Equation. Other considerations may apply, see **Section 16.4.1.1.8**.

The circuit under test will remain functional for some time. It can continue to operate because of the electrostenolytic materials stored within the furrows of the disk stack and surrounding the OS.

Baylor provides some interesting data when applied to this model[30]. Under totally dark conditions, the adaptation amplifier Activa is essentially cutoff except for the noise current due to both the chromophore and the Activa itself. Under this condition, the Class C waveform is dominated by the impedance of the electrostenolytic supply and the capacitor, C_A. Because of this, the waveform is band limited to approximately 3 Hz at the half power point in monkey. In the dark, the RMS noise floor for this same waveform had a variance of about 0.03 pA^2. This waveform is not associated directly with the signal path in vision which is generally regarded to have a bandwidth of at least 50 Hz. However, its noise spectrum does define the first time constant of the dark adaptation portion of the light adaptation function in monkey. This 3 Hz low pass filter in the feedback path of the adaptation amplifier becomes the lower frequency limit of the high pass network contributing to the actual signal path bandwidth of 3 to >50 Hz.

In spectral experiments, the same school has provided data they did not expect using the micropipette approach. During the 1970's they worked with turtles at 20C[31]. They isolated photoreceptors with spectral peaks reported as 460, 550 and 630 nm. (accuracy limited by the 15-20 nm. width of the spectral filters) using axial illumination. They also reported two cells with a peak response near 515 nm. During the 1980's they attempted similar experiments with turtles using the new technique. Based on their experience, they attempted to measure the spectral response of a variety of "cones," both red and green. In these micropipette experiments, they illuminated the OS in the transverse direction. As a result, they recorded spectrums, they interpreted as red cones, with a peak spectral response in the region of 498 +/-2 nm. They have not offered an explanation of why they have been unable to record the expected chromatic spectrum. By illuminating the OS from the side instead of from along its axis, they have recorded the isotropic (non-operational) spectrum of the chromophore material instead of its anisotropic (operational) spectrum. It is assumed here that the two cells reported to have a peak near 515 nm. in the 1970's experiments were misalligned relative to the incident illumination. The result was a spectrum representing a mixture of the isotropic and anisotropic spectrums.

Beginning in 1990, the Baylor school began applying the stimulus axially with regard to the outer segment. As a result, the operational spectra of photoreceptors were recorded. In one of the the L-channel chromophore was recorded. They reported its peak near 640 nm instead of the 625 nm used in this work.

12.8.1.1 The Class C voltage waveform at the outer segment

Theoretically both the potential change related to, and the current flow from, the confines of an individual outer segment should be measurable and compared to that predicted by the P/D Equation. However, the potentials related to the dendrites of the outer segment are difficult to probe. Baylor & Hodgkin presented voltage data on what they believed was a single photoreceptor of the turtle. **Figure 12.8.1-1** shows their data overlaid with the predicted P/D Equation. They discussed their results in terms of a peak near 644 nm (the discussion was based on their measurements at a wavelength of 644 nm as well as 400 and 805 nm). Note the range bars. Eleven responses were averaged at 644 nm, 14 at 805 nm and 11 at 405 nm. The vertical scale does not reflect the voltage measured at a common excitation. It has been scaled to estimate the voltage generated per photon absorbed (not applied) at three different wavelengths. This required the intensity of the stimulus to vary. They did report a resting potential of -43 mV and a maximum response to light of -23 mV at 22.2 Celsius. The stimuli were applied axially to the outer segment and the resulting spectrum is that of the anisotropic absorption of a L–channel photoreceptor. The expected peak absorption would be at a wavelength of 625 nm. It was not possible to define the exact location of the probe relative to the cell in that era. The diameter of the probes frequently exceeded the diameter of an individual cell. These values suggest the probe was contacting the interior plasma associated with the common emitter terminal of the inner segment of the photoreceptor rather than the axoplasm. If true, the response represents a Class B waveform. The time response did not vary significantly between the wavelengths used because the product of absorption and stimulus intensity, $\sigma \cdot F$ was held constant.

---

[30]Baylor, D. Nunn, B. & Schnapf, J. (1984) The photocurrent, noise and spectral sensitivity of rods of the monkey, *Macaca fascicularis*. J. Physiol. vol. 357, pp. 575-607

[31]Baylor, D. & Hodgkin, A. (1973) Detection and resolution of visual stimuli by turtle photoreceptors. J. Physiol. vol. 234, pp. 163-198

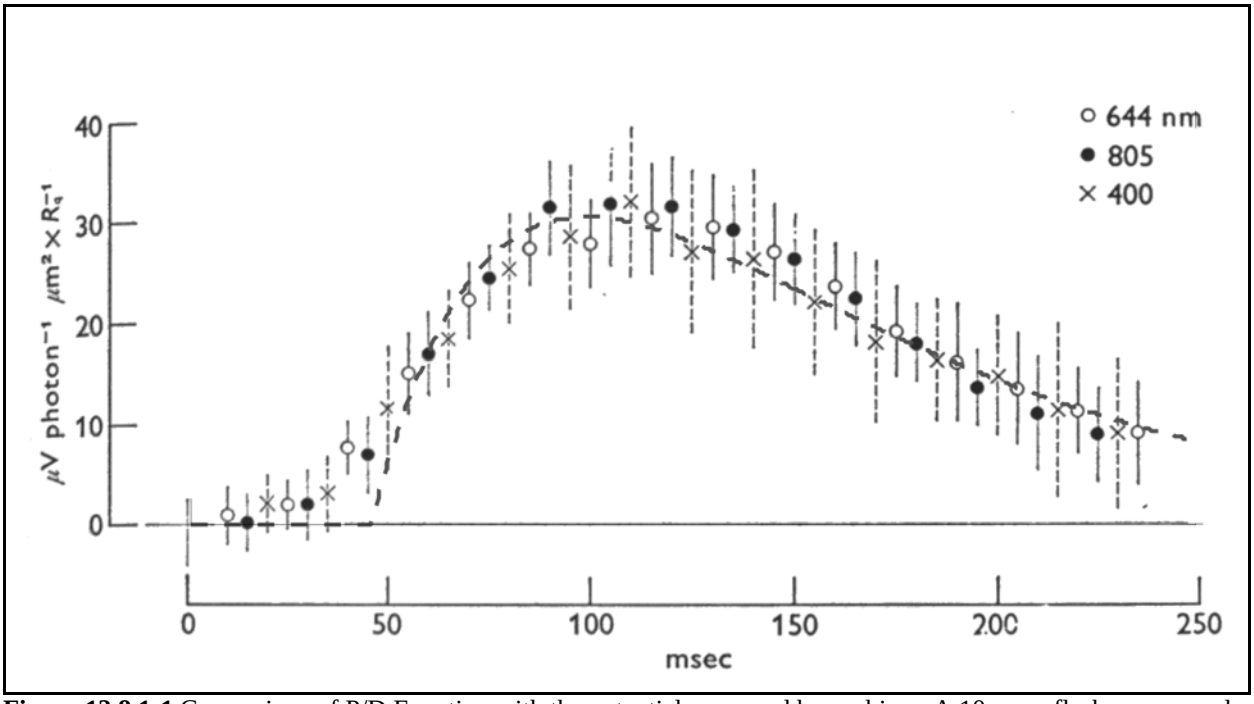

Figure 12.8.1-1 Comparison of P/D Equation with the potential measured by probing. A 10 msec flash was passed through a narrow band filter. The impulse form of the P/D Equation is shown as the dashed line for a $\sigma \cdot F$ value of 175. An absolute delay of 46 msec is shown. The data is from Baylor & Hodgkin, 1973.

Using the overlay, the peak in the amplitude of the data can be equated to $0.55 \cdot \sigma \cdot F = 96.25$/msec based on a time constant of 80 msec at 22.2 Celsius. $\sigma \cdot F \cdot \tau = 2.2$. When referenced to 37 Celsius, the effective time constant of the P/D mechanism of turtle is 12.5 msec. Since this is the same time constant as man, this suggests that the identical mechanism is employed.

Neither the theory or the measured data suggest any crossing of the horizontal axis (an undershoot) at this point in the signaling path of turtle. The absolute delay of 46 msec. was not analyzed as to the portion due to the intrinsic delay in turtle, the delay in the adaptation amplifier and any instrumentation delay.

12.8.1.2 The Class C current waveform at the outer segment

Collecting the total current from within the confines of a single outer segment provides the best opportunity to measure a waveform directly related to the Photoexcitation/de-excitation mechanism. The Baylor team demonstrated the collection of the current from a single outer segment using a Faraday cage as a collection device. Their initial focus was to obtain the response at very low stimulus levels (seeking the response from a single photon). **Figure 12.8.1-2** shows their data overlaid with the performance predicted by the P/D Equation.

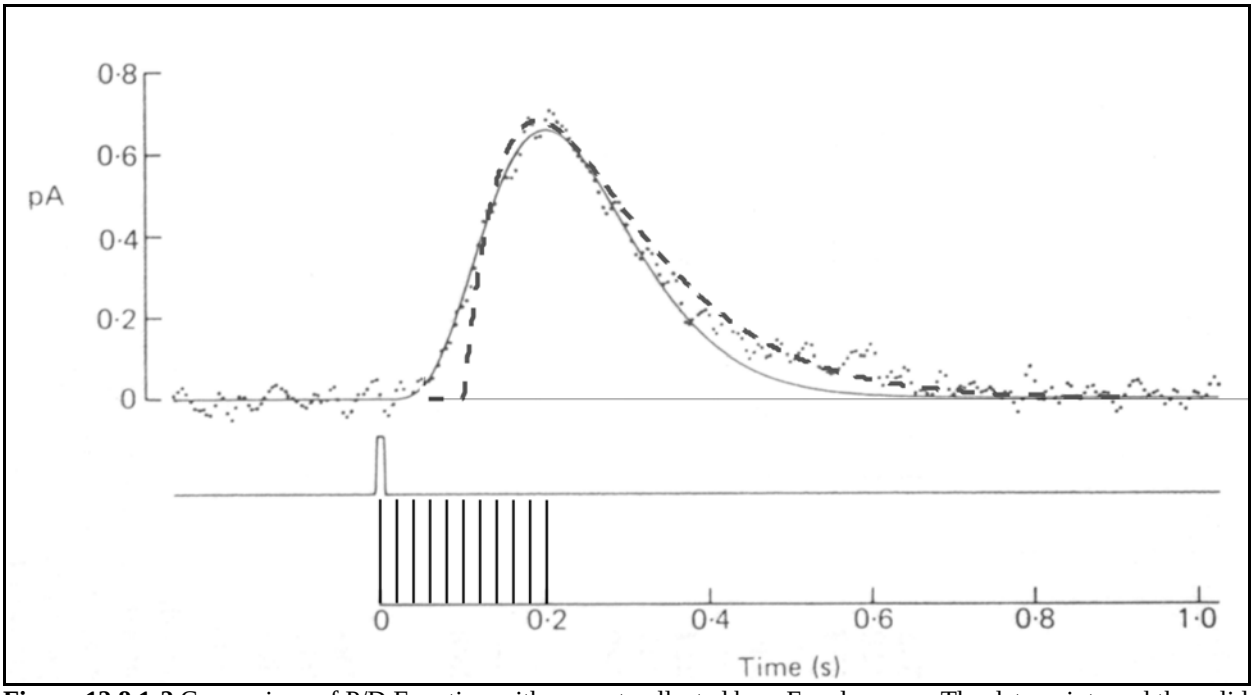

Figure 12.8.1-2 Comparison of P/D Equation with current collected by a Faraday cage. The data points and the solid line are from Baylor, Nunn & Schnapf, 1984. They used a six stage filter to create the solid line. They noted the response did not match the data points adequately near 0.2 seconds and between 0.4 and 0.7 seconds. The heavy dashed line is the P/E Equation for $\sigma \cdot F \cdot \tau = 0.60$. The fit is better in both regions. The light dashed line shows an alternate value of $\sigma \cdot F \cdot \tau = 0.56$. See Text.

Baylor et. al used six identical low pass filters in series (but presumably isolated from each other–see Fourtes & Hodgkin, 1964) to emulate their data. The noted that the resulting curve was not as narrow as desired near 0.25 seconds and did not fit the data well between 0.4 and 0.7 seconds. They also noted that the data from other cells deviated even further from their proposed curve.

The P/D Equation provides a better fit to the data set presented in the figure. The Equation was drawn for $\sigma \cdot F \cdot \tau = 0.56$, $\tau = 0.70$ seconds and $\sigma \cdot F = 8$ (heavy dashed line). At these values, an intrinsic delay, following the start of the impulse, of 5.2 ms is predicted. It provides an excellent fit to the data after time = 0.1 seconds (See **Section 16.4.1.1.8** for a discussion of the deviation in this area for low values of $\sigma \cdot F$). A second curve is provided to indicate the sensitivity of the P/D Equation to the above values. The light dashed line is drawn for $\sigma \cdot F \cdot \tau = 0.60$, $\tau = 0.60$ seconds and $\sigma \cdot F = 10$. The predicted intrinsic delay for these values is 5.0 ms. By increasing $\sigma \cdot F$ slightly, the P/D Equation can fit data sets with a longer tail as described by Baylor, et. al. Neither the data as measured or the P/D Equation exhibits any negative component under the above conditions.

Bearing the subject of **Section 16.4.1.1.8** in mind, the long time constant of 60-70 ms in the eye of monkey may be significant. If this value was confirmed for higher levels of sF, it would suggest a significant difference between humans and the Macaca family. Such a long time constant compared to the 12.5 ms of humans would suggest much less capability in analyzing fine detail quickly. This capability is critical in reading (other than for the large block

characters usually used in learning experiments with monkeys).

More experimentation is needed in this area to further refine the instrumentation and separate the data into additional classes if necessary. Establishing mean values and range bars for each class of data would allow further perfection of the theoretical model.

The data of figure 3 of Baylor, Lamb & Yau (1979a) provides very important data concerning the class C current waveform. **Figure 12.8.1-3** reproduces their data for the Class C current of the toad, *Bufo marinus*, using the suction pipette technique and transverse stimulation of a "red rod." Temperature was poorly controlled to the range of 18-25° Celsius. The peak absorption was at 500 nm as expected for the intrinsic absorption of the Rhodonines when the outer segment is subject to transverse stimulation. Frame A shows the data as collected, including significant saturation at 20 pA output current. Below 20 pA output current, the waveform faithfully reproduces the theoretical P/D response. Frame B shows the expected performance of the first Activa under these operating conditions. A nominal electrostenolytic supply voltage of -154 mV is assumed. A nominal electrostenolytic supply impedance of 7 megohms is also assumed. Under these conditions, the instantaneous output current, i_c, is proportional to the excitation current, i_b, for output current levels below 20 pA. The output current is outgoing from the cell to the pipette wall. As the excitation current increases, the output current increases proportionately in accordance with the load line, until the load line, R_L, intersects the saturation line. At this point, the Activa stops exhibiting "transistor action" since the collector potential is below the saturation potential. This is the reason for the hard saturation in frame A.

It is clear from frame A that the maximum output current is 20 pA regardless of the particular impedance of the assumed load line. The load line shown was chosen to give a 25 mV saturation voltage in accordance with other available data.

12.8.1.3 The Class C waveform at the outer segment with recharging

When the excitation discussed above is increased, either in intensity or duration, the total charge flowing in the collector circuit of the adaptation amplifier becomes significant. This causes a change in the potential of the collector relative to the electrostenolytic potential supply circuit. This circuit will begin to supply charge to the collector circuit to restore the quiescent condition.

May need to use σ_{eff} at low $\sigma \cdot F \cdot t$ product. Address meaning of red and green when excitation is transverse]]

The current waveforms presented in Figure 1 of Schnapf, Kraft & Baylor[32] for the human and Figure 1

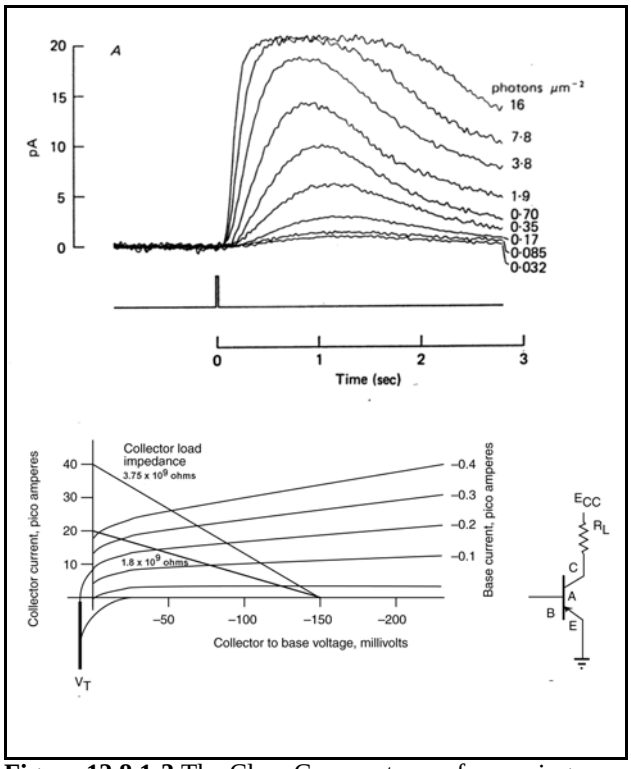

Figure 12.8.1-3 The Class C current waveform using suction pipette techniques. A; The collected Class C current showing saturation. From Baylor et al., 1979a. B; the current-voltage characteristic of the associated first Activa. See text.

[32]Schnapf, J. Kraft, T. & Baylor, D. (1987) Spectral sensitivity of human cone photoreceptors. *Nature*, vol. 325, pp 439-441

of Baylor, Nunn & Schnapf[33] for the monkey appear to represent the Class C current waveform measured using the micro-pipette technique. This waveform is at the collector terminal of the Activa within the dendrites associated with the outer segment. The waveforms can be analyzed in terms of a forward current due to the application of the Class A waveform to the base of the Activa. and a reverse current due to the recharging of the capacitor associated with the collector of the Activa after the end of the Class A waveform. It is the recharging current that causes the "undershoot" noted in the measurements of Schnapf, et. al. In the first paper, the labeling of the putative types of photoreceptors should be studied carefully.

Part of the data in the first paper and the P/D Equation are compared in **Figure 12.8.1-4**. The measurements were *in-vitro* at 37 Celsius using transverse illumination. The data was band-limited to 50 Hertz. Only the data for the "green" photoreceptor is shown. The other data involves a higher degree of saturation and complicates the analyses. It is presumed that the adaptation amplifier is operating at maximum gain in the figure. By collecting data at 500 nm, they also show the difference in spectral absorption between the two photoreceptors documented. In the first case, the traces are the average of eleven individual traces. In the second case ("Green"), the number of traces averaged was a variable. Neither case provides range bars on the data sets.

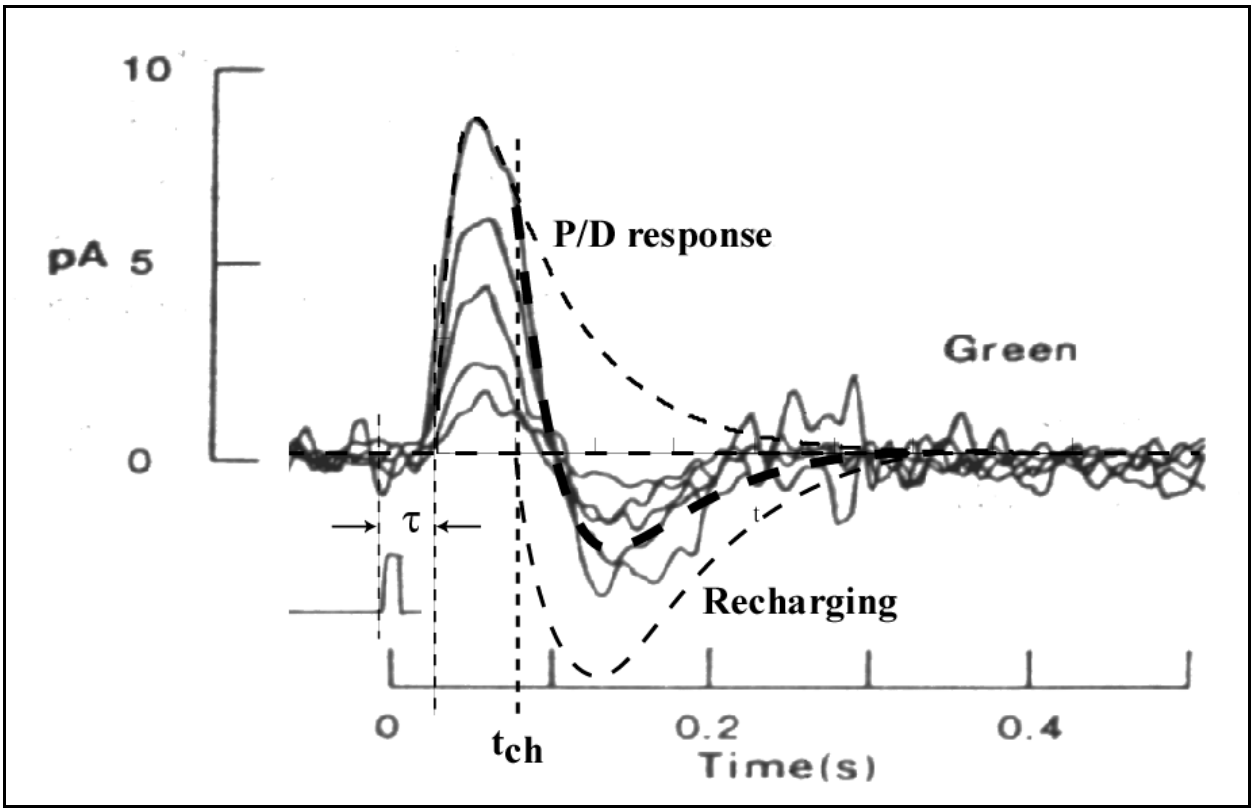

Figure 12.8.1-4 Comparison of the P/D Equation and recharging with published measurements at the collector of the adaptation amplifier Activa. P/D Equation plotted for $\sigma \cdot F=18$, $\sigma \cdot F \cdot \tau = 0.25$, $\tau = 12.5$ ms. See Text. Measurements by micropipette *in-vitro* at 37 Celsius. Data points from Schnapf, Kraft & Baylor, 1987.

The P/D Equation is plotted for an absorbed photon flux, $s \cdot F = 18$, a temperature of 37 Celsius and a time constant of 12.5 ms. The resulting function predicted an intrinsic time delay of $\tau = 4.6$ ms, as shown. This is slightly longer than the 3.0 ms measured relative to zero on the graph of the original publication. The difference, 1.6 ms, may be due to the (unspecified) width of the pulse used. Tau is measured from the beginning of the stimulus.

The P/D function (upper thin dashed line) overlays the upper curve so well, it is difficult to see the features in the

[33]Baylor, D. Nunn, B. & Schnapf, J. (1987) Spectral sensitivity of cones of the monkey *Macaca fascicularis*, *J. Physiol*. vol. 390, pp 145-160

data curve. Both curves rise, peak and begin to descend along identical loci. At the time marked t_{ch}, there is a distinct discontinuity in the measured curve. It is at this time that the recharging mechanism becomes significant. The time course of the recharging circuit is estimated. The net area under the P/D Equation and the net area between the recharging curve and the axis should be equal if charging is the proposed mechanism. The instantaneous difference between the P/D response and the recharging function is shown by the heavy dashed line through the data set. This line, when combined with the P/D Equation prior to t_{ch}, traces the expected path for a noise free response to the stimulus as measured made by the investigators.

12.8.2 Probe and ERG data of the photoreceptor output

12.8.2.xxx Polarity of the photoreceptor output

There is an open question that keeps reappearing in the literature. Is the photoreceptor output of *Chordata* of opposite polarity to that of either *Arthropoda* or *Mollusca*? The confusion is compounded by the variety of data acquisition techniques used, the presentation convention used, and frequently the presence of a b-wave that is larger and of opposite polarity than the a-wave.

12.8.2.1 ERG data

Many records are ERG based with one electrode contacting the outside of the eye and the second contacting an "indifferent location". Frequently in ERG work, the investigator will be talking about the b-wave since it is much larger than the a-wave (and of course of the opposite polarity). Therefore, it is necessary to be sure that the comparison is carefully made. **Figure 12.8.2-1(Figure 12.7-0)** illustrates the ERG data available from a number of sources. Whereas Devoe[34] plotted his data for the wolf spider with the initial edge going upward on the paper, his caption to the figure says "Negativity of the cornea of the illuminated eye with respect to the indifferent electrode is upwards". The data is for a long pulse of irradiance. Hamasaki[35] provides a variety of ERG recordings for the Octopus due to pulse irradiation, all of which show an initial response proceeding in the negative direction. There is a lot of this data available and the general conclusion is that in the protostomic animal, the ERG begins with a negative going waveform called the a-wave (which is followed by a larger positive going b-wave in many protostomic animals).

Because of the importance of the *Limulus* in vision research, it is important to determine if this ancient animals visual system conforms to the above finding. Chapman & Hall[36] provide very compelling data in this regard. They show ERG waveforms for both the compound lateral eyes and the simple median eyes of *Limulus*. Whereas the data for both eyes is plotted as upward going waveforms in their Figure 1, they indicate in the text that "the corneal surface became negative with respect to a reference elsewhere". It is concluded that *Limulus* conforms to the protostomic norm.

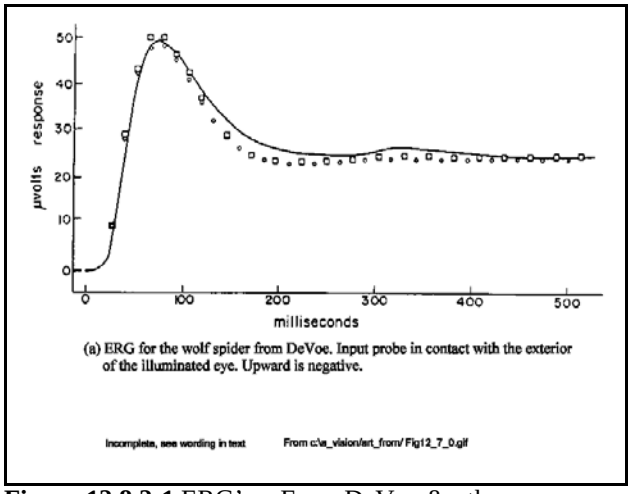

Figure 12.8.2-1 ERG's From DeVoe & others .

[34]Devoe, R. (1965) A non-linear model of sensory adaptation in the eye of the wolf spider. In The functional organization of the compound eye, Bernard, C. editor. NY: Pergamon

[35]Hamasaki, D. (1968) The ERG-determined spectral sensitivity of the Octopus. Vision. Res. vol 8, pp 1013-1021

[36]Chapman, R. & Lall, A. (1967) Spectral mechanisms of Limulus eye. J. Gen. Physiol. vol. 50, pp. 2267-2287

Breton et. al.[37] provide a large volume of ERG's for humans, concentrating on the a-wave but showing the b-wave clearly. They used a contact lens with a metallic ring to contact the eyeball and the "indifferent electrode" was contacting the temple area. All of the recordings show an initial rising waveform which is negative going. Rubin & Walls[38] discuss the historical aspects of the human ERG extensively with respect to the a-wave and waves b through d. Their examples all show a negative going a-wave. Dowling & Wald[39] show a wide variety of ERG's recorded during their investigations of vitamin A deficiency in rats. They take pains to show an enlarged view of one of the ERG's to emphasize that the initial response is the negative going a-wave followed by a larger positive going b-wave.

Smith & Lamb present a human ERG based on a well characterized experiment using only "blue" light (peak wavelength of 450 nm, Lee # 195, but no definition of the cutoff wavelength).

The literature clearly indicates that the leading edge of the a-wave in *Chordata* is negative going.

Based on the available data, with the input electrode contacting the eye surface, the **ERG's of *Chordata* and both *Arthropoda* and *Mollusca* begin with a negative going a-wave.** Therefore, all animals generate an initial electrical response to light that is of the same polarity as measured by an ERG.

12.8.2.2 Probe data for *Chordata*

When probe data is examined, the same confusion is found as in the ERG data. However, another variable associated with technique appears; during the period prior to the 1970's, the probes used to measure waveforms in the retina were grossly larger than the individual cells. This led to confusion between extracellular and intracellular waveforms and also confusion as to whether the cell contacted was in the Outer Nuclear Layer (a true photoreceptor cell) or the Inner Nuclear Layer (most likely a horizontal or amercine cell). In more recent time, the probes have become much smaller and the technique of sucking a single photoreceptor cell into a pipette has raised the precision of the experiments immensely.

In 1962, Hagins provided some excellent data concerning the P/D process in squid for a temperature of 5-10C. He measured the potential of the inter-photoreceptor matrix at different locations relative to a very small illuminated area. The results were complimentary to the suction technique of Baylor at a later time. However, Hagins' figure 8 used a very poor scaling technique. By ignoring the variable delay and variable slope of the P/D process as a function of illumination, and re-scaling the measured waveforms individually to align their rising phases, the figure suggests that lower illumination levels produce higher sustained output voltages. Re-plotting this data, or reviewing the original data shows that the squid photoreceptor cell employs the same P/D process as do chordates and other animals.

In 1983, Ottoson attempted to put the question of polarity at the electrical probe level to rest by publishing side by side figures attributed to an invertebrate and a vertebrate. Unfortunately, this presentation is not satisfying for a number of reasons;

+ he attributes the left hand figure to the horseshoe crab which can be confusing to the student since the waveform is not from the crab family of zoology but from *Limulus*, a member of a virtually extinct and separate family, *Xiphosura polyphemus* of *Arthropoda, Chelicerata*.

+ the left hand figure is not in the paper to which it is attributed. The right hand figure is a highly stylized version of the original, apparently for the purposes of a textbook.

+ the left hand figure has been redrawn from the original with the voltage scale changed implying that the pulses crossed the zero level. In the original, the baseline was labeled zero and there was no guarantee by the original author that the baseline was at -50 mV.

+ the figure on the left is the response to a pulse and on the right is the response to an impulse.

+ the use of probe data from the unusual eccentric cell from *Limulus* to represent all invertebrates

---

[37]Breton, M. Schueller, A. Lamb, T. & Pugh, E. (1994) Analysis of ERG a-wave amplification and kinetics in terms of the G-protein cascade of phototransduction. Inves. Ophthalm. & Vis. Res. vol. 35, no. 1

[38]Rubin, M. & Walls, G. (1969) Fundamentals of visual science. Springfield IL: CHARLES C. Thomas

[39]Dowling, J. & Wald, G. (1958) Vitamin A deficiency and night blindness. Proc. Nat. Acad. Sci. vol. 44, pp.648-661

is open to question. It leaves the impression that the photoreceptor cell in *Arthropoda* generates pulses, a function usually found in the ganglion cells of *Chordata*. A better interpretation would be that the left figure represents a ganglion cell of the type found in *Limulus*.

+ other authors report electrotonic waveforms in eyes of *Arthropoda* distal to the eccentric cell which more likely relate to the invertebrate photoreceptor cell.

Schneeweis & Schnapf provided good data on the photoreceptor responses of macaque monkey[40]. Some of their photoreceptor outer segments were illuminated axially. Others were illuminated transversely. They provided both voltage and current waveforms under patch clamp conditions. Their figure 1 stresses the difference in the waveforms to be expected under these different conditions. In their discussion of figure 1, they appear unaware that the voltage waveform represents the derivative of the current waveform. Both waveforms show the same delay following the stimulus. However, the voltage waveform, being a derivative, necessarily reaches its peak before the current waveform. Saturation plays a major role in their current waveforms as a function of stimulus level. Comparing their voltage waveforms of figure 2 with the current waveforms of figure 4 is quite instructive. Note their responses were recorded using amplifiers with passbands extending down to DC. They did not describe their criteria when they noted, "Responses of red and green cones were indistinguishable." It would be expected that the responses would be different in amplitude for the same stimulus level in accordance with the absorption characteristic of each photoreceptor. The sentence appears in a paragraph unrelated to their chromatic tests.

12.8.2.3 Probe data for non-chordates

Looking at more general data for the protostomic group of animals, Shaw[41] indicates the scope of the difficulty in specifying the nature of the initial response. His Figure 10 for the Locust, shows initially positive going waveforms from a retinula on the left and initially negative going waveforms from a lamina cell on the right; both responding to a pulse over roughly 5 orders of magnitude. The left hand figure shows definite signs of temporal band limiting by the impedances involved--and may not represent a true intracellular signal. His Figure 15 provides a similar dual picture for the same animal and without any obvious bandlimiting. Which structure corresponds to the photoreceptor cell of the deuterostomic eye?

Zuker in 1996 **[[check his ref 21** before adding this reference. he was working in chemistry]]shows initially downward going *current* waveforms in his Figure 3 for the "photoreceptor cells" of the compound eye of *Drosophila*. These waveforms are very clean and correspond in shape very well to the P/D Equation of this work. However, in the text, he says "(Drosophila photoreceptors, like most invertebrates, depolarize as opposed to hyperpolarize in response to light)" Whether his drawings conform to the normal convention of negativity being indicated in the lower portion of a graph and his words are a cop-out **OR** Vice Versa is hard to confirm. He does not specifically indicate the polarity of his data.

Trujillo-Cenoz[42] shows a different set of circumstances and uses different notation in examining the unicorneal (simple) eye of the spider, *Lycosa*, and the compound eyes of two flies, *Sarcophaga* and *Lucilia*. Meinertzhagen[43] provides a further description of the visual pathways of the insect as does Laughlin[44].

By combining their notation and pictures, from both conventional and electron microscopes to develop a closer parallel to the deuterostomic eye. From his discussion, it is possible to draw up a correlation list;

Arthropoda	*Chordata*
Rhabdom	Retina

[40]Schneeweis, D. & Schnapf, J. (1999) The photovoltage of macaque cone photoreceptors: adaptation, noise and kinetics *J Neurosci* vol. 19(4), pp 1203-1216

[41]Shaw, S. (1968) Organization of the locust retina. *in* Invertebrate receptors. Carthy, J. & Newell, G. editors. London: The Zoological Society of London by Academic Press pg. 149

[42]Trujillo-Cenoz, O. (1965) Some aspects of the structural organization of the arthropod eye. Cold Spring Harbor, NY:Cold Spring Harbor Biological Laboratory vol. 30, pp. 371-382

[43]Meinertzhagen, J. (1977) Development of neuronal circuitry in the insect optic lob. *in* Soc. for Neurosci. Symp. II. (Cowan, W. & Ferrendilli, J. eds.) Bethesda, MD: Soc. for Neurosci., pp. 92-119

[44]Laughlin, S. (1981) Neural principles in the visual system. *In* Handbook of Sensory Physiology, Vol. 7/6B, (Autrum, H. ed.) NY: Springer-Verlag. pp. 133-280; pg 262

Rhabdomere	Outer Segment
Microvilli	Disks
Photoreceptor Cell (Retinula)	Photoreceptor Cell (Inner Segment in this work)
Monopolar Cell	Bipolar Cell
Eccentric Cell	Horizontal (or Amercine) Cell
Lamina	
Medulla (retinula #1-6)	Magnocellular region (luminance signals)
Medulla (other levels for retinula #7-8)	parvocellular (chrominance signals)

[[can I add Mollusca to the above table?]]

According to Trujillo-Cenoz, the Rhabdom consists of a group of Rhabdomere behind a single lens in both the unicorneal and multiple corneal arthropod eye. It contains a number of individual photoreceptor channels, frequently arranged like segments of an orange (frequently 7--sometimes with a few of different spectral response relative to the rest of the group) and corresponds morphologically to the more extensive retina of the deuterostomic eye. His Figure 2 clearly shows the similarity between his term Microvilli and the Disks of the chordate eye (the longitudinal cross section of a cylinder and any cross section of a disk appear identical, even to the loops on the end of the cross section due to lack of adequate resolution at 110,000 X magnification). He describes these microvilli as being 0.5 μ long and 500 A wide; since they are cylinders, it would be better to say 0.5 m long and 500 A in diameter. The microvilli are laid down in perpendicular layers as shown in **Figure 12.8.2-2(Figure 12.7.2.-XXX)**. [**XXX might be his fig 1**]This feature provides a capability not available in the eye of *Chordata*, the detection of the optical polarity of the incident light. It is likely that this capability explains the need for the multiple and separate retinula in the individual ommatidia and/or ocelli. Different photodetector cells are arranged to sense different layers of the microvilli and to send their output to different regions of the lamina of the eye/brain. The eccentric cell appears to exhibit many of the characteristics of a cell used to collect data from a group of vertebrate photoreceptors, for either spatial or chrominance integration purposes.

Although Trujillo-Cenoz did not use the term, it appears that other authors are using the term retinula cell to refer to his photoreceptor cell. This would complete the comparison between the simile between the two visual systems; the combination of the Rhabdomere and the Retinula cell would be the equivalent of the Outer Segment and the Inner Segment of this work. In both of these contexts, the Rhabdomere and the Outer Segment are extracellular. Using this list, there is a close simile between the two types of eyes at the morphology and cytology level. The only unique twist is that the eccentric cell has penetrated up into the Rhabdom so far in order to contact a group of photoreceptor cells.

In the above simile, there is no distinction between a monopolar cell and a bipolar cell with regard to the signal pathway-these are morphological or cytological designations.

With the minute distances involved in the insect visual pathway, it has been difficult to define and categorize all of the structures involved. Further, it is not clear that the encoding and decoding function related to the ganglion cells in the higher vertebrates at least, is needed. This function is performed to provide fast, low loss signal transmission over relatively long distances. It may be that only the R7 & R8 cells require encoders to transmit their signals to more distant sections of the medulla.

Some authors speak of a laminal cell in the protostomic eye, others appear to consider it part of the brain. The distinction is trivial for the purpose at hand. In several cases, they speak of laminal cells as of opposite polarity to more distal cells which would indicate they involve signal inversion as in the case of horizontal and amercine cells. Whether inversion is involved brings us to the crucial question, is the output of the retinula cell of opposite polarity to that of the photoreceptor of the deuterostomic eye?

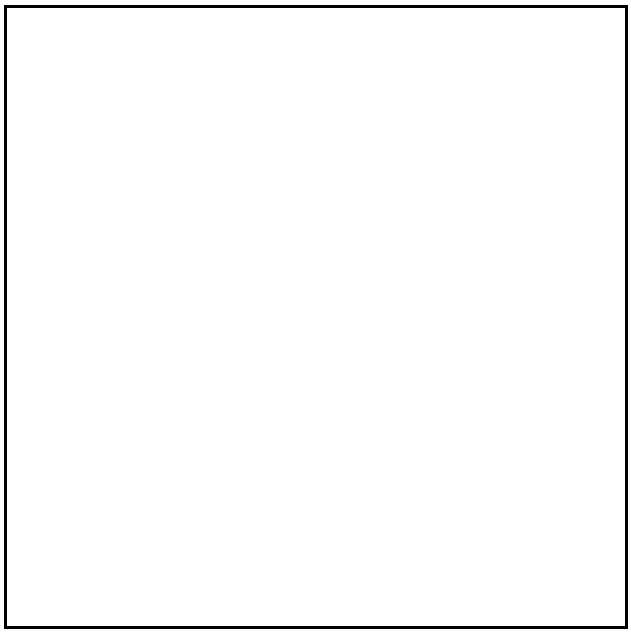

Figure 12.8.2-2 From Trujillo-Cenoz (1965).

It is absolutely mandatory to go back to primary sources to answer this question. Many authors of secondary

material, textbooks, reviews and articles in related disciplines, generally quote material at hand on this question--and without attribution. Furthermore, many of these secondary authors speak of a signal as depolarizing synonymously with a positive going leading edge. It is important to note that in all cases reviewed, there was no quiescent value given for the waveform that would indicate a negative resting potential.

Figure 12.8.2-3(Figure 12.7-0) from Laughlin , with modification, provides the answer to the question of polarity. Frames (b) and (c) are taken directly from his paper except for the dotted line in the upper probe of (b). As indicated below, it can be argued that the probe tip was actually extracellular when the waveforms were recorded. It is proposed here that the probe tip was extracellular in (b) and further, the waveform recorded from a retinula depends on where it is probed. The cartoon in frame (a) has been added to provide another perspective. In this case, the probe is shown near the proximal end of the retinula and the recorded waveform is shown with a negative going leading edge. There is significant laboratory work reported in the literature that says the output waveform from the insect eye is hyperpolarizing and the resting potential is given. Goldsmith[45], working with the compound eye of the worker honeybee presents his data with the summarizing statement: "When light strikes the compound eye of a worker bee, an electrode in the superficial layers of the retinula records a monophasic, negative retinal action potential." In the caption to Figure 4 of his paper, he specifies for both the compound eye and the ocelli: "an upward deflection signifies negativity of the electrode in the illuminated eye."

[45]Goldsmith, T. (1959) Wavelength discrimination in eye of honeybee. in Sensory Communication, Rosenblith, W. ed. Cambridge, MA: MIT Press pg. 366 (similarly in many other papers)

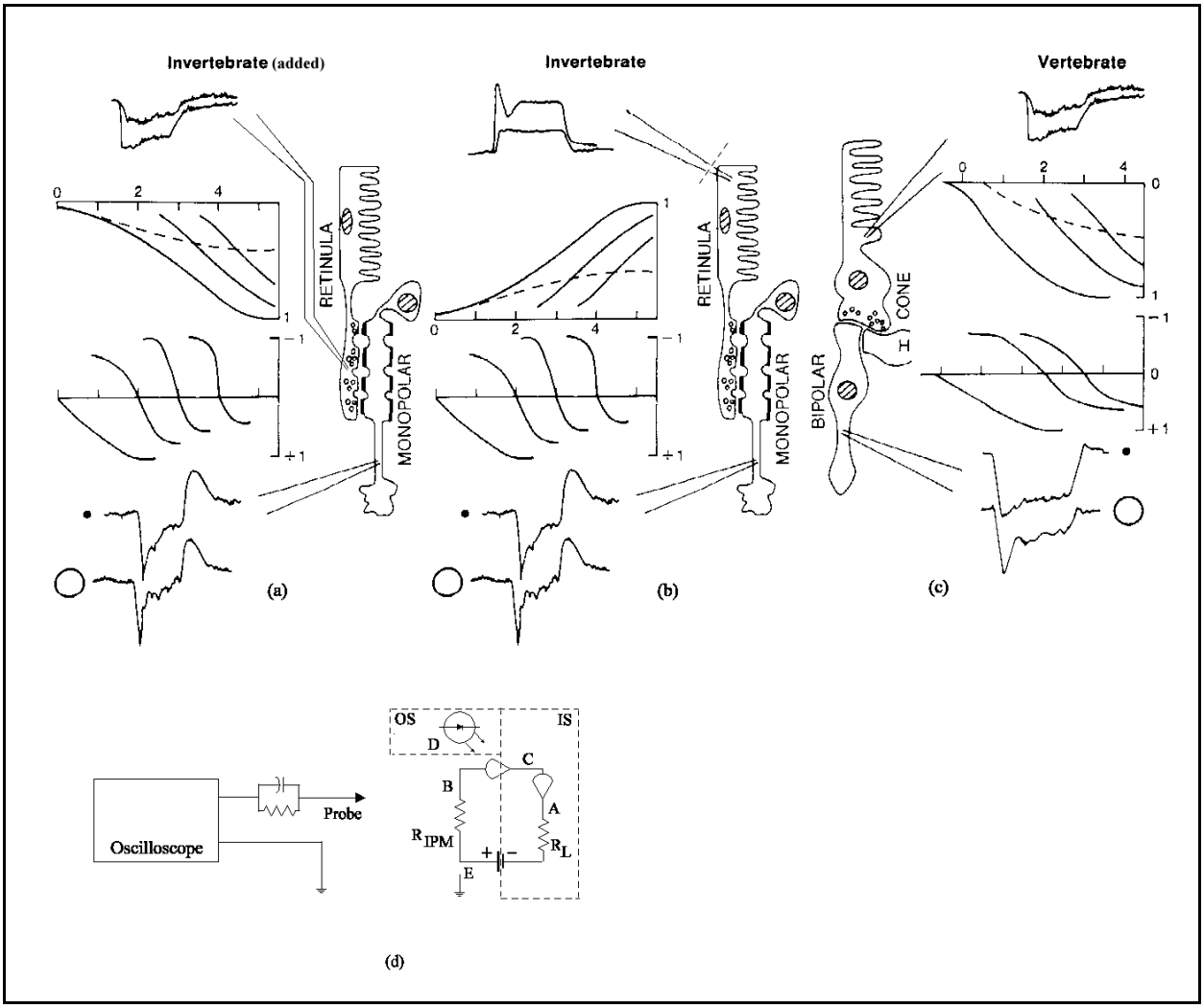

Figure 12.8.2-3 Photodetection waveforms for Invertebrates & Vertebates. From Laughlin (1981) .

Upon reviewing much of the literature, it appears safe to conclude that it is possible to obtain two different action potentials from the retinula of the invertebrate eye, depending on where you probe. The waveform measured extracelluarly near the distal end of the retinula does not generally exhibit a quiescent level consistent with the interior of a retinula cell and the leading edge is positive going. *In the absence of a non-zero quiescent value, it is not appropriate to speak of depolarization.* The waveform measured intracellularly near the proximal end of the retinula does exhibit a quiescent level of typically -50 mV and does exhibit a negative going leading edge (hyperpolarization).

If one looks at the electrical situation in the region of the retinula, it is possible to rationalize the various primary reports in the literature. Looking at (d), which is based on both the data reported in the literature and the model defined in this work, the basic circuitry found in both retinula of protostomic animals and photoreceptors of deuterostomic animals is shown. As shown above the table correlating the terms used for the different eyes, the stack of disks correspond to rhabdomeres, the disks correspond to microvilli, and in both cases the dendritic structures are too small to be recognized and labeled (except in the case of the deuterostomic eye where they can be seen in the region of the cilliar collar and are described in that region as the cilia. (d) presents a simplified version of the detailed circuitry developed earlier in Chapter 12. However, it shows that there are three main regions from the electronic point of view;

+ the OS contains two important structures, the disk stack and the (8 or 9)dendritic structures that surround and are laid into the grooves in the disk stack

+ the IS contains the rest of the circuitry associated with the photoreceptor

The disk stack consists of basically organic material which is non-conductive of conventional electrical currents and is extracellular with respect to the photoreceptor cell. The dendritic structures are intracellular but of extremely small dimensions, on the order of 50-100 Å in diameter (or less in the grooves). They do contain a conducting channel, the inside of a microtubule, and their exterior wall is basically a continuous energy sensitive transistor (although shown here as a discrete device for simplicity). The IS contains, in its neural portion, the activa. This is the active device, one or more of which are found in every neuron. It provides the amplification associated with the nerve, this amplification can result in either electrotonic amplification or switching which generates the action potentials. The activa is in communications with the dendritic structure, the surrounding medium (the Inter-Photoreceptor-Matrix or [IPM] similar designation) and the axon of the nerve. It also obtains prime power and maintenance from the housekeeping portion of the cell surrounding it.

If one attempts to use a probe and recording device to obtain waveforms from this photoreceptor, it is possible to probe a variety of different environments within the overall structure. If one attempts to record a signal at D, the environment is basically non-conductive and the signal will be minimal and mostly consist of capacitive pickup from surrounding structures. If one attempts to record a signal from C, the mechanical difficulties are large because the structures are so small--unless it is accomplished near or within the cilia collar. The impedance is also very high in this area. The easiest places to acquire a signal are at B and A.

The signal at B is quite diffuse over an area surrounding the disk stack. Because it is diffuse along each dendrite surrounding the disk stack, it is difficult to capture a significant portion of the current unless the micro-pipette suction technique is used. However, it can be probed successfully, although the extremely high impedance level frequently limits the obtained waveform to the low frequency components. The signal at B does not involve a intracellular resting potential. Therefore, *the waveform at B cannot be described as depolarizing*. It can be described as having a positive going leading edge. If the observed signal waveform does contain a DC level, it is more likely to be due to the voltage at the location of the reference lead compared to the IPM.

The signal at A is at a much lower impedance than at B. It also involves a larger and more accessible structure. Since the electronic system in vision is typically DC coupled, this waveform does exhibit a quiescent or resting potential at any point where it is encountered (a variable with temperature but typically -50 mV). The signal associated with this point in the circuit has a leading edge which is negative going and typically saturates at a level of about -70 mV. -70 mV is the nominal supply voltage provided by the cell wall of the photoreceptor cell. *The waveform at A is the true and typical electrotonic output waveform of the photoreceptor* which is frequently called the generator potential. It is generally described in this work as a result of the P/D process and described by the P/D Equation (frequently without regard to the DC bias associated with it.

The features of the circuitry associated with the photoreceptor cell are be addressed fully elsewhere in Chapter 12 and the Appendices. The answer to our question is straightforward: The output signal (A) from all photoreceptor cells in the animal kingdom consists of a signal waveform exhibiting a negative going leading edge (the so-called generator potential) and associated with a -50 mV bias level. There is available in the proximity of the OS or Rhabdomere an alternate signal (B) that has a 1:1 amplitude relation to the output waveform. However, it is inverted and does not exhibit a resting potential indicative of a intracellular recording. This signal exhibits a positive going leading edge.

This model is completely compatible with the suction micro-pipette technique developed by Baylor et. al.[46] even with regard to their breaking of the cell at the cilia collar. Specifically;

+ they were able to collect all of the diffuse current surrounding the OS at B. The waveform of the current collected can be described very well using the P/D Equation.

+ the “Light flashes evoked transient outward currents.” in the region surrounding the OS.

+ they were able to show that under saturating conditions the maximum current was about 27 pA.

+ they were able to show that if the OS was separated from the IS at the cilia collar, the current

---

[46]Baylor, D. Lamb, T. & Yau, K.-W. (1979) The membrane current of single rod outer segments. J. Physiol. vol. 288, pp. 589-611

obtained was the same as the saturation current above, demonstrating that the maximum current available was given by the fraction, E_D/R_D, in the model (by collecting essentially all of the current at C, the impedance of the IPM was not involved).

+ they also showed that the peak current went up in a linear manner as more of the OS was moved into the micro-pipette, indicating the combined optical absorption (photoexcitation) and de-excitation profile was quite uniform over the length of the OS.

+ they showed that the current profile decreased uniformly with distance after the cilia collar was moved into the micro-pipette--indicating that the current passing through the battery E_D and the resistor R_D was obtained over a continuous region of the IS cell wall.

They also calculated the current emanating from a one micron circular ring of the OS of 0.75 pA/μ. Thus a probe in this area with a 1.0 μ collecting area would only pick up a small fraction of this total current around the ring. This is why the measurements at point B are usually low pass limited. The impedance is extremely high and the current is extremely low. The overall probe circuit exhibits a low pass characteristic under these conditions. The impedance of the IPM in series with the capacitance shunting the probe contact (or compensation circuit) limits the frequency sensed to below
$1/(C * R_{IPM})$ hertz. It is difficult to observe system noise under these conditions and the reported waveforms are usually smooth as in Laughlin's figure for the waveform at B in the invertebrate.

In this case, as in the ERG case, *Limulus* represents a special case. Davson[47] indicates that the retinula cells each have a fiber emanating from them but these fibers do not exhibit action potentials and they may or may not be nerve fibers in fact. He indicates that the eccentric cell may be regarded as the true neural pathway from the ommatidium and that the structure passing up through the central axle of the rhabdom is the dendrite of this eccentric cell. The axon of this eccentric cell does exhibit action potential impulses. {His words clearly reflect the time period of their original preparation, when electrotonic signals were not recognized as true signal waveforms in the retina.} No lamina cell is indicated in his discussion of the *Limulus*. Behrens & Wulff[48] obtained electrical signals from both retinula and eccentric cells in Limulus. **[[need this paper]]** They report a electrotonic wave with small spikes associated with the retinula cells and a slow wave with large spikes associated with the eccentric cell. This would appear to define the retinula output as that of the photoreceptor and the eccentric cell as a (nearly) conventional ganglion cell. If this is correct, the initial output of the photoreceptor cell upon irradiance in *Limulus* is { +/- }going .

The data related to the electrical response of the photoreceptors in deuterostomic animals is immense and quite compelling, especially the data of the last 20 years. It invariably shows an initially negative going voltage response at the output of the photoreceptor cell; and this applies to both warm blooded and cold blooded members of this group. See any of the papers in this time period from Hodgkin, Baylor, Fuortes, Lamb, Etc.

12.8.2.3 Conclusion

With the above discussion and simile in mind, it is now possible to provide the answer to the question of the polarity of the initial electrical signal emanating from the photoreceptor cell (or retinula where appropriate) of all animal eyes. *The output waveform generated in the photoreceptor cell of any animal eye and passed to the next level of signal processing always exhibits a negative going leading edge upon irradiance.* This signal waveform is accompanied by a DC resting potential indicative of the cell interior and is a function of cell temperature. This negative going waveform is due to the creation of free electrons in the dendritic structure of the IS (located within the OS) and the movement of these electrons to the input of the Activa located inside the IS.

[[continuation of 12.7

Whereas, Baylor et. al. and others attempt to explain the delay in the output characteristic of the eye relative to the input by introducing explicitly multiple additional time constants and implicitly multiple additional circuits; this model introduces a single time delay related to a physical transport mechanism which is easily explained and justified This delay, U(t), is electric field intensity related and matches the measured data very well. The other models have a difficulty explaining why various assumed time constants would be changing in order to account for

---

[47]Davson, H. (1990) Physiology of the eye, 5th ed. NY: Pergamon Press pg. 280
[48]Behrens, & Wulff (1965)

the measured delay. Adopting the P/D (with delay) equation as the replacement for their "Independence" equation (4) allows their data to be fit almost perfectly to this model. Each of the curves in their Text-fig. 11 is now matched to an individual theoretical curve instead of merely residing inside of an overall envelope. The theoretical curves are shown in **Figure 12.8.2-4(Figure 12.7-1).**

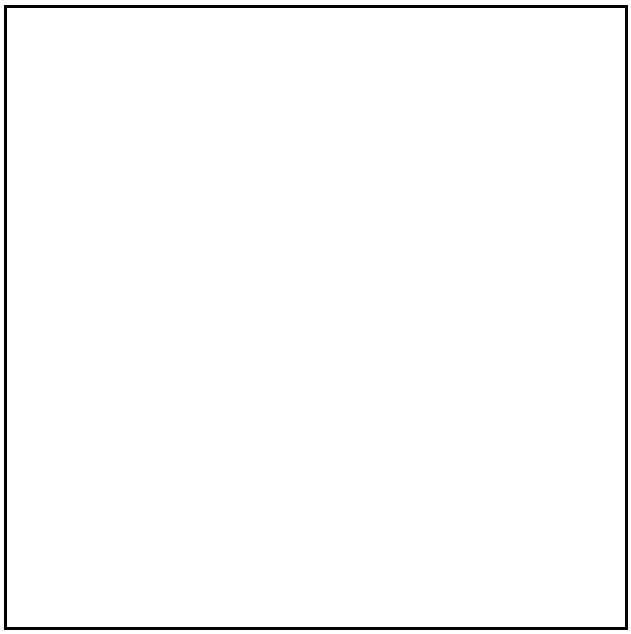

Figure 12.8.2-4 My theoretical curves .

The recent work of Breton et. al.[49] deserves special attention in light of the model proposed here for several reasons.

First, with the model shown to describe the total waveshape measured at the IS/OS interface as a function of irradiance, including both the rising response and the trailing response; it is possible to subtract an appropriate set of these waveforms from their figure 3 and thereby obtain a new set of waveforms related to the rest of the signaling system subsequent to this interface**. Figure 12.8.2-5(Figure 12.7-2)** shows their original Figure 3(A) and the same figure after the portion of the waveforms occurring at the OS/IS have been removed. Further analysis of the resulting waveforms will be undertaken in Chapter 13.

Second, it should be noted that the data of Breton et. al. is not taken from a single photoreceptor in a suction pipette; the waveforms shown in **Figure 12.8.2-5**(**Figure 12.7-2(A))** are the cumulative waveforms obtained when a single flash of light is applied to virtually all of the photoreceptors in the eye simultaneously. To obtain a plot as they do that still faithfully follows the predicted response of a single photoreceptor, even after averaging the result of two to four flashes, strongly infers that all of the active photoreceptors in a given retina are basically identical under threshold conditions--identical in sensitivity, amplification, bias potentials, etc.

[49]Breton, M. Scheuller, A. Lamb, T. & Pugh, E. (1994) Analysis of ERG a-wave amplification and kinetics in terms of the G-protein cascade of phototransduction. *Invest. Ophthalm. & Vision Sci*. vol 35 #1 pg 295-309

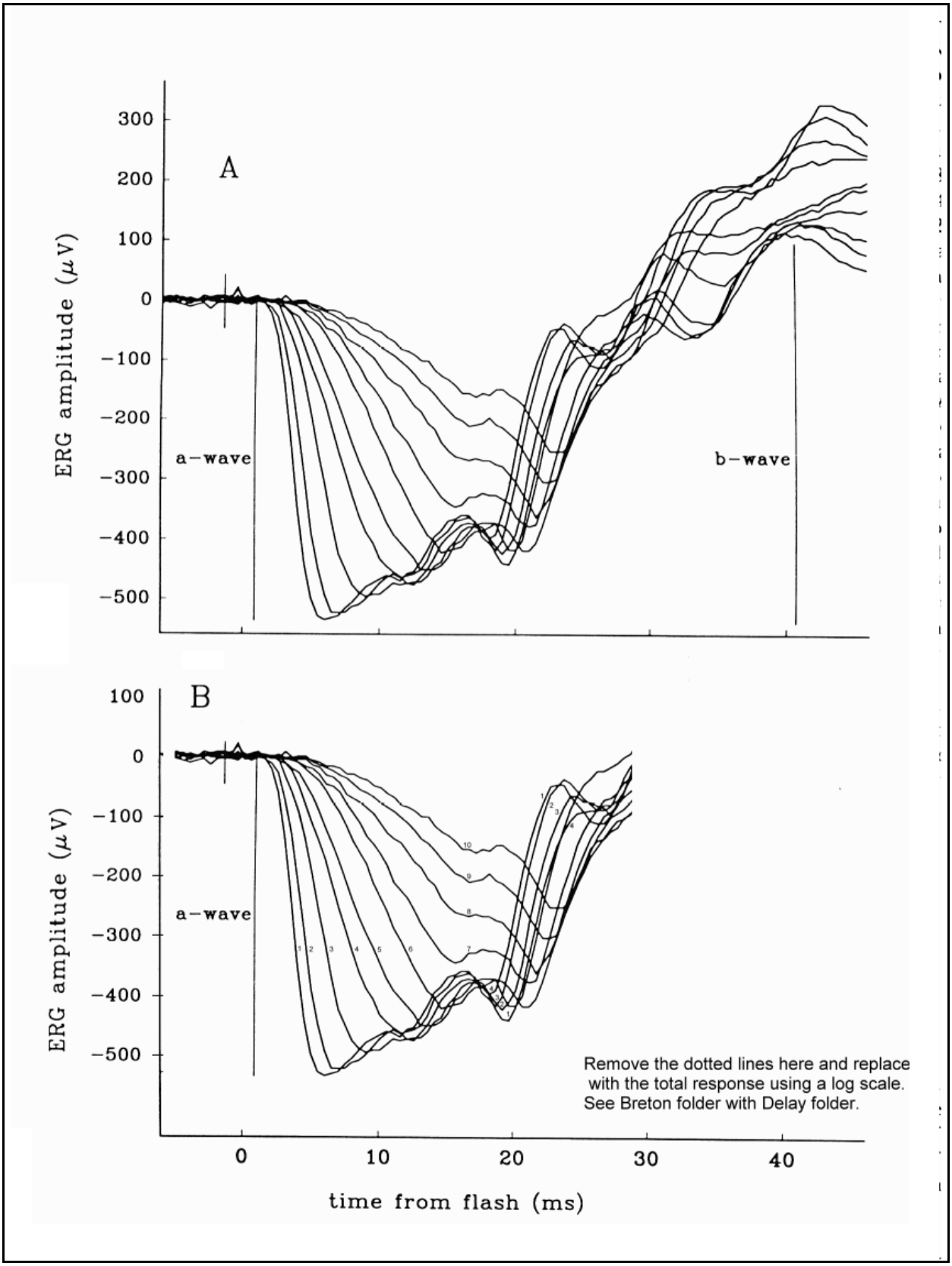

Figure 12.8.2-5 Human ERG. From Breton (1994).

A particularly interesting situation involves the sometimes large time delays presented in the literature under small signal conditions. **Figure 12.8.2-6(Figure 12.7-3)** illustrates this situation. Note the large delay between the output waveform and the incident modulated irradiance. The delay is a significant fraction of a cycle of the modulation. In the absence of this model, it is difficult to explain how such a large amount of delay could be introduced into this situation. However, as seen here, the delay is a property of the average flux level and not the modulation itself. At higher average irradiance levels, the delay in the modulated waveform will be reduced. in accordance with the function U(t) even though the modulating waveform is not changed. Since the actual small signal delay is a direct function of U(t) and U(t) is a reciprocal function of the average input radiance level, it is absolutely imperative to state the input radiance level when presenting the small signal transfer characteristics of the eye. Otherwise, the large phase delays can not be accounted for.

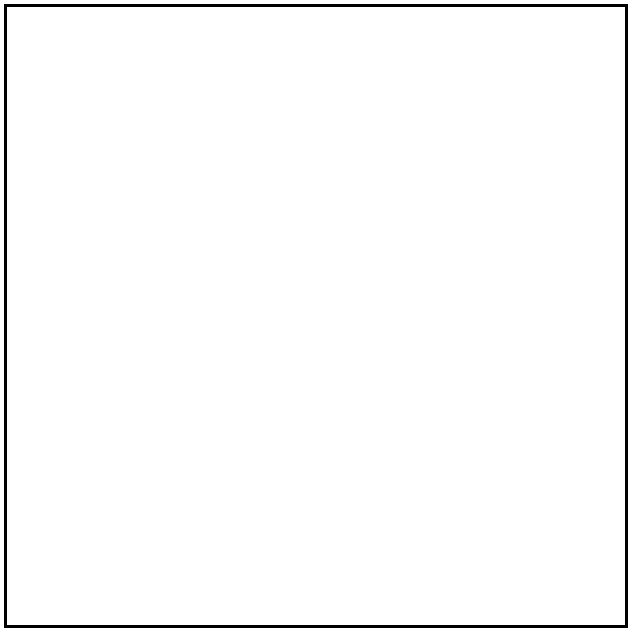

Figure 12.8.2-6 .

12.8.3 Dynamics of photoreceptor cells

Hagins CSH pg410 for Squid.

12.9 Summary

The success of the P/D equation and the overall model of the photodetection function of the photoreceptor cell in describing the measured performance of the eye in a variety of animals is remarkable. It's ability to predict completely the details of the test data of Baylor, Torre and Breton demonstrates its correctness. More will be said concerning the data of Breton in the next chapter. Briefly, this model allows one to explain the difference between the a-wave and the b-wave of the ERG. As will be seen later, it does even more than this; it suggests and helps prove that the b-wave consists of more than one signal--quite possibly an early b-wave related to the circuitry in the Inner Nuclear Layer (IN) and a later b-wave related to subsequent circuitry; which may also be in the IN or may consist of the low passed signals related to the ganglion cells in the Outer Nuclear Layer (ONL).

This success clearly indicates it ranks ahead of other models of the photoreception process. It indicates the "photo-electronic" detection theory is far superior and more accurate than the "photo-isomerization" theory in describing the vision process. Specifically, it is compatible with the excitation/de-excitation process restoring the individual chromophoric molecules to their original state in less than 1 milli-second under most radiance conditions and requires no transport of a species to the RPE for reconstitution. It also eliminates any need for "dark processes" as usually inferred to satisfy the photo-isomerization theory.

The model does not require the physical transport of any ions through a cell wall surrounding the disks; in fact, it does not require any cell wall to surround the disks.

The model does not require any flow of chromophoric molecules in or out of the OS except for normal growth at the end near the IS. For those that do flow into the disks, there is no need to pass through a cell membrane to reach the disks; and it appears there may be openings in the collar of the IS to facilitate the flow of chromophoric molecules in that area.

[xxx The model is completely compatible with the following currents within the photoreceptor cell membrane (which need not contain the disks); a real current traveling into the OS from the IS and a real current traveling back to the IS and onto the pedicel of the cell. The current traveling into the OS is basically the power supply to the neuron amplifier. The current traveling out of the OS is the signal carrying current. The algebraic sum of these two currents is the exact current measured with the suction pipette technique.

Actually, there may not be any "free electron" as opposed to "bound electron" current involved within the disks of the OS depending on the further analysis of the "exciton" to electron transducer, if any. It may be that the output

current associated with the OS is actually generated in the dendritic structure interdigitated with what is usually thought of as the OS. Similarly, the current passing out of the IS may remain inside the dendritic structure associated with the neural function and never actually flow into the disks. In such a case, only "bound electrons" would be moving within the disks, essentially along the surfaces of the disks in response to the creation of a space charge due to the photoexcitation of the electrons themselves. This space charge would constitute the electric field required to push the bound electrons to the periphery of the disks and into proximity with the dendritic structures.]

The explanation of the "hyperpolarization" of the photoreceptor cell due to photoexcitation is completely explained by this theory. The output signal consists of a quantity of electrons which is numerically related to the photon flux and there is no inversion in the neural amplifier. Furthermore, the reason for the net current, measured at the IS/OS junction, going to zero is obvious. The signal current cannot exceed the supply current in a non-resonant amplifier circuit.

The description of a biological transistor as described above may be a bit difficult for some biologists to accept, and its detailed elucidation may require considerable analysis. However, the structures available in a biological membrane are very comparable with the "back to back diode" description of a semiconductor transistor of a non-biological type. While not realistic at a detailed physiological level, it is possible to describe the operation of these devices using an analogy involving the opening and closing of gates in a membrane wall. No such gates have been identified in electron micrographs of real neurological lemma.

Employment of an ion transport related mechanism to generate a current in a biological transistor located on the OS side of the OS/IS interface would require transport of ions from the IS to the OS (or the dendritic structure) in large numbers, at high rates and high ion current densities to accommodate a 30 pA current within a very small diameter structure. This appears unlikely at first glance. It is more likely that the walls of the dendritic structure (possibly in conjunction with the membranes of the disks) are acting as a biological transistor based entirely on electron charge transport--the only ionic motion would be that of a standing wave type, as in ocean waves.

It appears that the microtubules known to occur in the proposed dendritic structures of the IS and in the region of the pedicel(s) of the photoreceptor may be filled with a conducting medium and constitute the electronic conductors of the photoreceptors. They are known to consist of biological material with hydrophobic and hydrophilic components formed into a tube. Whether a single microtubule can be shown to extend all the way from the OS to the pedicel is an interesting area of study.

It would be extremely interesting to see the results of Baylor's and Lamb's work repeated for light in the vicinity of 0.64 microns. Such data would determine the characteristic of the "exciton" to electron transducer if it is in fact related to the energy of the incident photons. **[See Kraft, et. al. 1990]**

It should be noted that so far, no distinction has been made in this chapter between the different types of photoreceptors. Whether they were sensitive in the long, medium, short or UV spectrum has not been of concern. Up to this point, they all operate alike. Each photoreceptor operates in a quantum mode and can detect and report the absorption of a single photon at a signal level that can be processed by the follow-on signaling stages. Their overall response characteristic is linear up to very high levels where the percentage of the total number of available n-electrons is reduced significantly. Their instantaneous dynamic range is logarithmic and controlled by the input characteristic of the dendritic tissue of the photoreceptor neuron.

First, the total signal current entering the PC does so through the poda bias source (the broad arrow). This current is independent of the state of illumination.

Second, the total signal current emanating from the OS is a function of the incident light level. In the absence of illumination, no current travels from the OS into the IPM. Under illumination, the current emanating from the OS is a state variable highly dependent on the amplification factor of the adaptation amplifier in the dendrite. This current level is strongly dependent on the level of the current illumination and the illumination history of the OS. The current leaves the OS in a distributed manner based on where the light was absorbed and where the excitons encounter the dendrite. It is proposed that the light is normally absorbed uniformly over the length of the OS. This results in the current leaving the OS with a constant current density over the length of the OS.

Third, the total signal current leaving the PC at the axon connection is equal to the poda bias current minus the total signal current leaving the OS. This current is maximum when the PC is not illuminated.

Since these currents are difficult to measure, it has been conventional to measure the voltages in the regions in or

near the various circuit elements. Even this is difficult. Frequently, the voltage representing the current flow in multiple PC's is actually measured. A probe placed in the IPM adjacent to a number of PC's will show no signal related voltage in the absence of illumination. Upon illumination, the voltage sensed by this probe will become positive.

If a second probe is placed in contact with the axon conduit of a PC, it will show a resting potential for the axon, in the absence of illumination, which is lower than the resting potential of the axon membrane. This lower reading is due to the potential drop represented by the impedance of the power source multiplied by the current flowing through the power source. Upon illumination of the PC, the axon voltage will actually rise toward the axon membrane resting potential as the current passing through the axon power source decreases. This is normally described in the literature as a hyperpolarization of the axon voltage.

The light impinging on the proximal end of the Outer Segment encounters a uniformly absorbing material of relatively low and relatively constant index of refraction. The absorption characteristic depends on which of four chromophores occurs in that photoreceptor. As the light is absorbed, it causes the excitation of electrons within the liquid crystalline structure of the absorber. The absorbers have the structure of a resonant retinoid absorber. These materials have very long excitation lifetimes and are known not to fluoresce. However, the material is in intimate contact with the dendrites, located in the furrows of the disks, of the neural portion of the photoreceptor cell. These dendrites are occasionally labeled microtubules in the literature. This intimate contact supports the transfer of energy between the absorber and an active semiconductor device, an Activa, in the dendrite. In this way, the "exciton" of the absorber is de-energized and returns to the valence band of the liquid crystal. Simultaneously, a free electron is created within the base region of the semiconductor device. The Activa is incorporated in an overall circuit located within the neural portion of the photoreceptor that consists of two Activa arranged in a differential circuit. These devices are electrically biased by the metabolic materials coating the external surface of the cell. There are a number of different Activa used in the nervous system of animals and they can be described by their parameters just as solid state semiconductors are. Alternately, they can be described by their purpose or application. Chapter 9 will describe these devices individually in detail. The first Activa in the photoreceptor cell will be called the adaptation amplifier because of its unique characteristics and role. The second Activa will be called the output amplifier.

The signal generated by the adaptation amplifier is passed to the output amplifier of the differential pair through a common emitter connection. The output amplifier of the differential pair is biased through connections to other areas of the photoreceptor cell wall to provide an output current of about 20 pA (pico-amperes) under zero input signal conditions. The gain of this amplifier is equal to minus one (-1). Thus, the output current decreases with increasing signal at the input of the adaptation amplifier. The result is an output signal that varies between 20 pA under zero input illumination to the Outer Segment of the photoreceptor cell to an output current of 0.00 (zero) pA at maximum input illumination tolerated by the input transducer.

The above output current of the differential amplifier is passed along the axon lead of the photoreceptor cell to the synapse with the following bipolar cell, and possibly other cells. The synapses of the retina are all gap junctions. At the synapse, the signal current is passed to the dendrite of the bipolar cell. Note that the signal consists of a change in signal current of up to 20 pA in a direction opposite to the quiescent D.C. current of the output amplifier. The dendrite passes this total signal current to the input terminal of the bipolar Activa. This input terminal appears as a perfect diode to the incoming current.

Since it is difficult for the experimentallist to interrupt a circuit to measure a current, he normally measures the voltage at a node of an overall circuit. In this case, the node is the output voltage at the axon of the output amplifier. The detailed operation of this circuit can be described precisely using conventional semiconductor electronics terminology. The voltage measured at that location, relative to the common or poda lead of the differential amplifier, is described by a quiescent value. This quiescent value is equal to the collector supply voltage minus the nominal 20 pA current times the impedance of the collector supply. As the illumination rises, the output current actually decreases. The result is that the output voltage rises due to the decrease in output current. The circuit is said to hyperpolarize in the presence of illumination.

4.7.2 Transduction MOVE

The transduction function within a photoreceptor is performed by a liquid crystalline material coated onto the external surface of a protein substrate, known as opsin. The liquid crystalline material consists of one of four

chromophores with an overall sensitivity to light with a wavelength of between roughly 300 nm. and 675 nm. Each chromophore is sensitive to a region of about 100 nm. within this range. The chromophores are retinoids derived from Vitamin A. However, they are not retinal or retinol. Whereas both retinal and retinol contain a single polar atom in a conjugated carbon chain, the chromophores contain two polar atoms in a conjugated carbon chain. The optical performance of the compounds is significantly different.

Both retinal and retinol exhibit an absorption spectra related to the length of the conjugated carbon chain they are based on. The peak of this absorption spectra is located at almost precisely 500 nm. The absorption coefficient of these materials is not very high. The absorption spectra of these materials is isotropic in dilute solution.

The chromophores of the visual process are different. They exhibit a higher absorption coefficient based on the quantum resonance occurring between the two polar atoms. This resonance absorption is only exhibited when the material is in the liquid crystalline state. The spectral peak is not related to the total length of the conjugated carbon chain. It is only related to the length of the conjugated chain, including the polar atoms as termini, between the two polar atoms. Because of the "slow wave structure" found in the liquid crystal, the spectral response of these materials is highly anisotropic. Peak absorption is achieved when the incident light is parallel to the optical axis of the individual molecules. This optical axis is essentially parallel to the mechanical axis of these all-trans molecules. Because of the "slow wave structure," the liquid crystal is most sensitive to a wavelength approximately 250 times longer than the physical length of the molecule.

In the case of chordates, the liquid crystalline material of the chromophores is formed on the surface of the disk substrates with the optical axis of the chromophore perpendicular to the surface of the disk. In this configuration, the liquid crystal exhibits a very high absorption coefficient for light passing along the axis of the disk stack. It exhibits essentially no absorption to light passing perpendicular to the stack.

The above situation explains a problem in many laboratory experiments. The spectral absorption measured by micro-reflectometry along the mechanical axis of the OS will exhibit the anisotropic resonance absorption spectrum of one of the four chromophores. The peak will occur at either 342, 437, 523 or 625 nm. for animals at a body temperature of 98.6 Fahrenheit. The spectral absorption measured using an optical beam passing perpendicular to the mechanical axis of an OS will always exhibit the isotropic (non-resonant) absorption spectrum of the underlying conjugated carbon chain. In this case that chain shows a peak at 500 nm. regardless of which chromophore is actually present. This peak is not exclusive to retinal or retinol. It is characteristic of any simple conjugated carbon chain terminated with at least one polar atom.

Figure 12.9.2-1 illustrates the quantum mechanical model of the transduction process for a specific chromophore to transfer the energy of an incident photon to the dendrite of the IS for further manipulation. The terminology is discussed in detail in Appendix A. Only the highlights will be discussed below.

4.7.2.1 Quiescent operation MOVE

Under quiescent conditions, in the absence of illumination, all of the electrons associated with the liquid crystalline chromophore on the disks are located in the quantum mechanical ground state labeled **n** in the left half of the drawing. There are no excited electrons, "excitons," in the **Π*** band. No signal is generated within the OS or the dendritic structure of the IS. The transducer material is in quantum mechanical contact with the dendrites of the IS. Note the interface between the bands of the liquid crystal on the left and the liquid crystalline semiconductor device on the right need not overlap. The energy is transferred by a quantum mechanical process, not a conductive one. Note also the horizontal scale change between the two sides of the diagram.

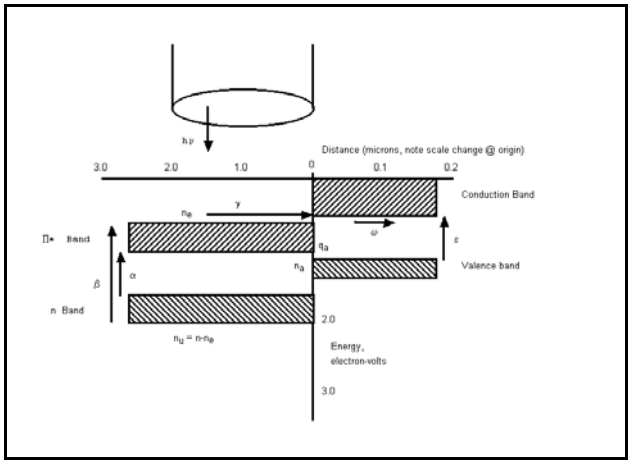

Figure 12.9.2-1 The quantum mechanical interface between a specific liquid crystalline chromophore and the associated liquid crystalline semiconductor device of the dendritic structure. See text for terminology.

4.7.2.2 Operation with illumination MOVE

Upon illumination by radiation of proper wavelength, each incoming photon with an energy greater than that indicated by **α** and less than that indicated by **β** will cause an electron to be excited from the ground state, **n**, into the **Π*** band of the liquid crystalline transducer. These excitons appear at a location directly above where the photon was absorbed. This can be anywhere in the 2.0 micron diameter of the crystalline structure shown. These excitons

will travel to the quantum junction with the translation circuitry of the photoreceptor cell by one of several means. The important point is that there travel velocity is finite and the resulting ensemble of excited electrons exhibits a finite delay time between excitation and arrival at the boundary where excitation can occur.

The lifetime of excitons in the Π^* band is very long relative to events associated with vision, i.e., the chromophores are not known to fluoresce under physiological conditions.

Upon arrival at the boundary, the excitons are prepared to give up their energy if there is a quantum mechanical opportunity to do so. This opportunity is provided by the input structure of the dendrites. Under normal conditions, each exciton will give up its energy and be de-excited back to the ground state, **n**, in exchange for a free electron (or hole) being released within the junction of the first Activa of the dendritic structure. [xxx actually in the base region of the Activa]

At any given time the absorption coefficient of the liquid crystal associated with a given disk (or possibly a surface of the disk if the coating is fractured along the disk edge), is proportional to the number of unexcited electrons in the **n** band given by $\mathbf{n_u = n - n_e}$

4.7.2.3 Transient operation MOVE

The transient performance of the transducer is quite straight forward. However, it does include a state variable. Upon the application of illumination, the absorption coefficient is directly proportional to the number of unexcited electrons in the **n** band. If the photoreceptor has been in the dark for some time, all of the available electrons are in the **n** band and $\mathbf{n_u = n.}$ If however, the photoreceptor was recently illuminated, it is possible some of the excited electrons have not yet been de-excited. In that case, the number of available electrons is $\mathbf{n_u = n - n_e}$. Once a photon is absorbed, an exciton appears in the $\mathbf{\Pi^*}$ band within less than a microsecond. The travel time to the boundary is appreciably longer and is a function of how many excitons are in the band. Once at the boundary, de-excitation occurs in less than a microsecond under physiological conditions. The result is that the "attack" transient response of the transducer to illumination, the time to generate excitons in the $\mathbf{\Pi^*}$ band, has a short time constant and the "decay" transient response, the time to clear the $\mathbf{\Pi^*}$ band, has a much longer time constant. However, *these are not the time constants of interest in vision.*

In vision, the time constants of interest are related to the boundary situation. The attack time constant related to vision is a function of the travel time between the creation of an exciton and its arrival at the boundary, ready for de-excitation. This time constant is a function of the illumination level. The decay time constant is related to how long it takes to clear the $\mathbf{\Pi^*}$ band of excitons after the illumination ceases. Normally, this time constant is independent of the prior illumination level. The entire equation of the transient response of the transducer/translation process is given in the Photoexcitation/De-excitation Equation, (P/D) given in Appendix A. The attack time constant of the combination is quite variable, extending from less than one millisecond for high illumination to greater than one-half second for very low illumination. The decay time constant is nearly constant at a given temperature. For humans, its value is 0.525 seconds. These are only two of the time constants important in vision. They are essentially independent of any metabolic conditions occurring in conjunction with the active circuitry of the eye.

4.7.3 Translation and initial amplification MOVE

To understand the initial translation and amplification occurring in the photoreceptor cell, it is necessary to understand the entire electronic configuration of the cell. Important optimizations have been made that are not obvious without such comprehension. First, it must be understood that the circuitry is based on a current, not a voltage. Second, there are normally nine dendrites in human which are arranged in the furrows along the sides of the disk stack. Third, each dendrite is in quantum mechanical contact with each disk it passes, essentially all of the disks of its associated OS. Fourth, each dendrite can collect free electrons generated at each disk/dendrite interface. Fifth, the free electrons collected by all of the dendrites are passed through the ciliary collar and summed at the common output terminal of all of the Activas within each dendrite of the dendritic structure. Sixth, the common output terminal of the dendritic structure is connected to a second amplifier within the IS proper and, through the photoreceptor cell wall at the poda, with the fluid matrix surrounding the photoreceptor cell. This second amplifier develops the output signal current delivered to the axon of the cell.

Figure 12.9.3-1 illustrates the electronic circuitry of the photoreceptor cell. The left side of the schematic is descriptive of one dendrite. The current from all of the dendrites pass through the ciliary collar and joined to the

output amplifier as described above. For simplicity in further description, all of the "first amplifiers" and individual dendrite leads will be replaced by a single equivalent amplifier that will be called the adaptation amplifier. Thus a single adaptation amplifier is connected to a single output amplifier. More will be said later about the multiple impedances and power sources shown.

4.7.3.1 Quiescent operation MOVE

The overall photoreceptor circuit is arranged as a differential pair, a common circuit in man-made analog circuits. One of the principal features of such a circuit is the constant current through the lead including the dendritic power source. Note also the fact that the base lead to the Activa on the left is not connected electrically to any other potential. The junction associated with this Activa receives all of its excitation quantum mechanically from the transducer. This feature is common in man-made photo-transistors.

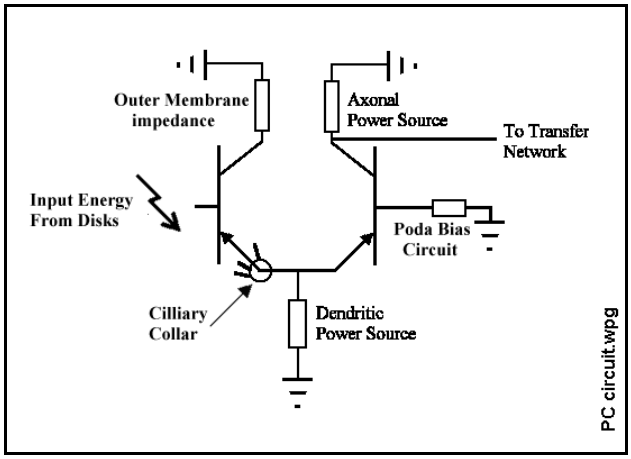

Figure 12.9.3-1 The fundamental circuit of the photoreceptor cell showing the adaptation amplifier (left) and the output amplifier (right). See text for details.

In the absence of illumination, no excitation is received from the transducer. No free electrons are created in the adaptation amplifier junction and no current flows between the emitter and collector of the Activa. The result is that any current flowing through the dendritic power source lead is determined by the characteristics of the dendritic power source and the poda bias circuit. Both of these elements are related to the external membrane of the photoreceptor cell. However, they are in contact with different electrolytes outside of the membrane and possibly inside the membrane as will be discussed later. These elements are optimized in the case of human to cause a nominal twenty picoamperes (20 pA) to flow in the collector of the output amplifier. This current passes through the axonal power source. The voltage at the collector is seen to be equal to the potential generated by the axonal power source minus the voltage drop associated with the current passing through the axonal power source. This voltage is normally called the membrane resting potential in the biological literature. However, it is not a characteristic of the membrane. It is more properly called the output amplifier collector potential or the axon conduit potential. It is the potential of the fluid inside the conduit connected to the pedicle (or spherule) of the axon. It is always less than the membrane potential except under output amplifier cutoff conditions.

It should be noted that no metallic conductors are used in the visual system, or the nervous system, of animals. All of the currents are carried by electrolytic conductors consisting of conduits filled with fluid. The conduits are generally described as microtubules or groups of microtubules.

4.7.5 Transmission from the distribution Activa to the pedicle MOVE

The transmission of the signal along the axon of a photoreceptor is not significantly different from that of any other analog neuron. This subject will be addressed in detail in Section **XXX** where the secondary aspects of the problem are most important. Recently, Hsu, et. al[50]. have explored this subject. However, they used an overly simple cable model (so common in biophysical studies of the neural system over the years) and employed computerized models (the NeuronC simulator) that have not been validated from a theoretical perspective. Their cable model is limited to resistors and capacitors using "compartmental modeling" which appears to mean lumped constant conditions. They treat both the inner segment and axon as linear devices with the illumination causing a change in a resistance. This work does not support their assumptions or conclusions.

A more accurate model treats the axon as a conventional coaxial cable with an intrinsic capacitance and intrinsic inductance per unit length. The serial resistance is negligibly small and the shunt conductance is also negligibly small for the conditions of interest in vision.

---

[50]Hsu, A. Tsukamoto, Y. Smith, R. & Sterling, P. (1998) Functional architecture of primate cone and rod axons. Vision Res. vol. 38, pp. 2539-2549

4.7.6 The output transfer network MOVE

With most laboratory work involving measurement of the voltage at or near the axon of the photoreceptor, it is useful to have an expression for that voltage in terms of the signal current and ultimately the input illumination. Computing the measured voltage from the signal current is not straight forward. The neural circuits are DC coupled. The impedance of the node formed at the junction of the output amplifier collector, the axon power source and the input to the next neuron is complex. The output impedance of the amplifier can be considered ohmic but it is very high, theoretically infinite. The impedance presented by the axon power source is essentially a perfect diode.

The impedance looking toward the gap junction is a major surprise. Analysis of this structure from a semiconductor physics perspective leads to the inevitable conclusion that if biased properly, it is an active electronic device, an Activa, in its own right. Operating in a common base (or poda) configuration, it provides a nearly perfect (lossless) current transmission path between the presynaptic axoplasm and the post synaptic dendroplasm. Based on this discovery, it is the input impedance of the gap junction itself that contributes to the effective impedance of the axonal node, not the input impedance of the dendrite of the post synaptic neuron (which is similar).

The effective impedance of the output node of the photoreceptor is that of the two diodes in parallel, the axon power supply diode and the gap junction input diode, both of which are forward biased. Under small signal conditions, this impedance can be considered a constant. However, signals at this point are usually large under both normal operation and laboratory conditions and the actual diode impedance characteristic must be used. This is the cause of the logarithmic rise in output voltage at this node in response to linear current increases through the photoreceptor cell.

4.7.6.1 The fundamental transfer network, the gap junction MOVE

The fundamental morphology involved is shown in **Figure 12.9.5-1**.**[xxx lower right part of bipolar with diffusion.wpg]** The resulting fundamental situation schematic, a further expansion of the signal carrying circuit in **Section 4.7.3.1**, is illustrated in **Figure 12.9.5-1**. The current signal delivered to the input of the next neural stage is determined by the characteristics of the axon supply of the photoreceptor cell and the power supplies available to the Activa comprising the gap junction. These power supplies are provided by the "soup" found in the vicinity of the gap junction, as also illustrated in the morphological view. The solutions within the axon and dendrite as well as those in the surrounding medium are all important in determining both the static and dynamic operating characteristics of the gap junction.

4.7.6.2 An alternate transfer network MOVE

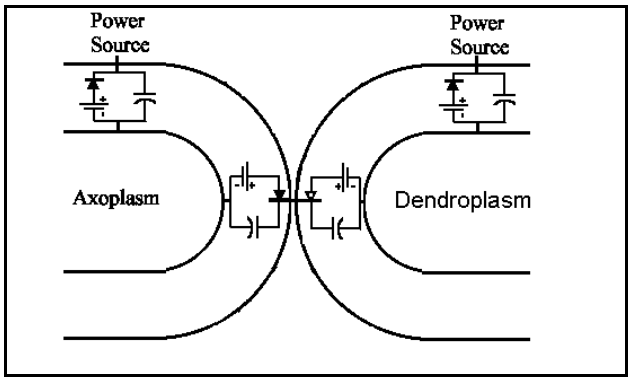

Figure 12.9.5-1 The fundamental gap junction between two cells. A signal current enters from the left. An equal signal current exits from the right due to "transistor action" in the gap area.

There are many cases where one photoreceptor cell feeds signals to a large number of signal processing cells of the neural laminate. Whether this is performed using a multitude of gap junctions in parallel or through other means must be determined by further experimentation. Since simple gap junctions appear to involve common base circuits, they do not achieve any current gain. It is reasonable to anticipate some of the photoreceptor axon terminals contain additional signal processing elements. This would likely involve an additional Activa configured in a common emitter configuration capable of achieving current gain. This stage would then feed multiple following stages and avoid signal to noise problems in cases where a finite output current was divided among a large number of following stages. It is likely that considerations such as these account for the difference in size between the terminations of photoreceptor cells, the spherules and pedicles. The use of a single active device to achieve current gain will cause an inversion of the signal polarity. The presence of this type of circuit could account for the occasional report in the literature of a positive going output signal from a photoreceptor cell with increasing illumination.

4.7.7.1 Measured photoreceptor currents and voltages MOVE

The statements in the above summary require support. Fortunately, such data is available.

Figure 12.9.5-2 provides the results of the suction pipette technique developed by Baylor, et. al[51]. using the suction pipette as a Faraday Cage enclosing a portion of a photoreceptor cell. The procedure involves the isolation of a single in-vivo PC by sucking it into a Faraday cage. All of the current emanating from the PC along that part of the cell enclosed by the Faraday cage is collected and measured.

The current profile is quite similar to the voltage profile measured earlier by Penn & Hagins[52] in bulk retinal membranes. This profile suggests that the IPM is a resistive medium but the simple electrical model developed by Hagins for the photoreceptor cell is too simple[53]. A more comprehensive model will be provided later in this work.

Both Baylor, et. al. and Penn & Hagins employed transverse illumination in their early experiments. Thus, their data does not reflect the operational (anisotropic) spectral sensitivity of the photoreceptors to axial light. Later Baylor work has employed axial illumination.

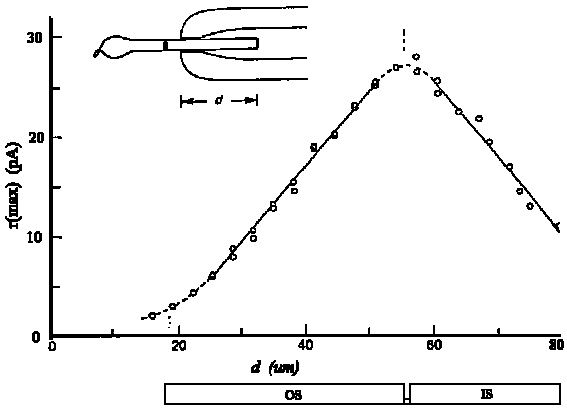

Figure 12.9.5-2 Current captured by a Faraday Cage surrounding the Outer Segment and Inner Segment of a photoreceptor cell as a function of position. Ordinate is response to a diffuse 20 msec 500 nm flash delivering 64 photons per square microns, a saturating light. Abscissa is distance from electrode tip to distal tip of outer segment (see Inset). The cell was expelled and drawn in twice, and most points are averages of two measurements. During the experiment, the response at the optimal position (d=58 microns) decayed from 26.8 to 22.4 pA and all points have been scaled to give 26.8 pA at this position. Curve fitted by eye. This cell was completely isolated from the retina. From Baylor, Lamb & Yau (1979).

[51]Baylor, D. Lamb, T. & Yau, K.-W. (1979) The membrane current of single rod outer segments. J. Physiol. vol. 288, pp. 589-611

[52]Penn, R. & Hagins, W. (1969) Signal transmission along retinal rods and the origin of the electroretinographic a-wave. Nature, vol. 223, pp. 201-205

[53]Hagins, W. (1965) Electrical signs of information flow in photoreceptors. In Symposia on Quantitative Biology, vol. XXX Long Island, NY: Cold Spring Harbor Laboratory

TABLE OF CONTENTS 1/30/02

Chapter 12 List of Figures 4/30/17

AUTHOR INDEX (active)
(Have not learned to use two separate concordances yet)
(Now must use two separate runs and freeze content of list after each run)
(program files/corel .....corel user files\authors)

SUBJECT INDEX (using advanced indexing option)